Geometric renormalization unravels self-similarity of the multiscale human connectome

Muhua Zheng,[1,2] Antoine Allard,[3,4] Patric Hagmann,[5]
Yasser Alemán-Gómez,[5,6,7] and M. Ángeles Serrano[1,2,8]

[1]*Departament de Física de la Matèria Condensada, Universitat de Barcelona, Martí i Franquès 1, E-08028 Barcelona, Spain*

[2]*Universitat de Barcelona Institute of Complex Systems (UBICS), Universitat de Barcelona, Barcelona, Spain*

[3]*Département de physique, de génie physique et d'optique, Université Laval, Québec , Canada G1V 0A6*

[4]*Centre interdisciplinaire de modélisation mathématique, Université Laval, Québec, Canada G1V 0A6*

[5]*Department of Radiology, Centre Hospitalier Universitaire Vaudois (CHUV) and University of Lausanne (UNIL), Lausanne, Switzerland*

[6]*Center for Psychiatric Neuroscience, Department of Psychiatry, Centre Hospitalier Universitaire Vaudois (CHUV) and University of Lausanne (UNIL), Prilly, Switzerland*

[7]*Medical Image Analysis Laboratory (MIAL), Centre d'Imagerie BioMédicale (CIBM), Lausanne, Switzerland*

[8]*ICREA, Passeig Lluís Companys 23, E-08010 Barcelona, Spain*

(Dated: June 27, 2020)

www.pnas.org/cgi/doi/10.1073/pnas.1922248117

CONTENTS

I. RESULTS FOR UL DATASET

A. Parcellation and distribution of areas

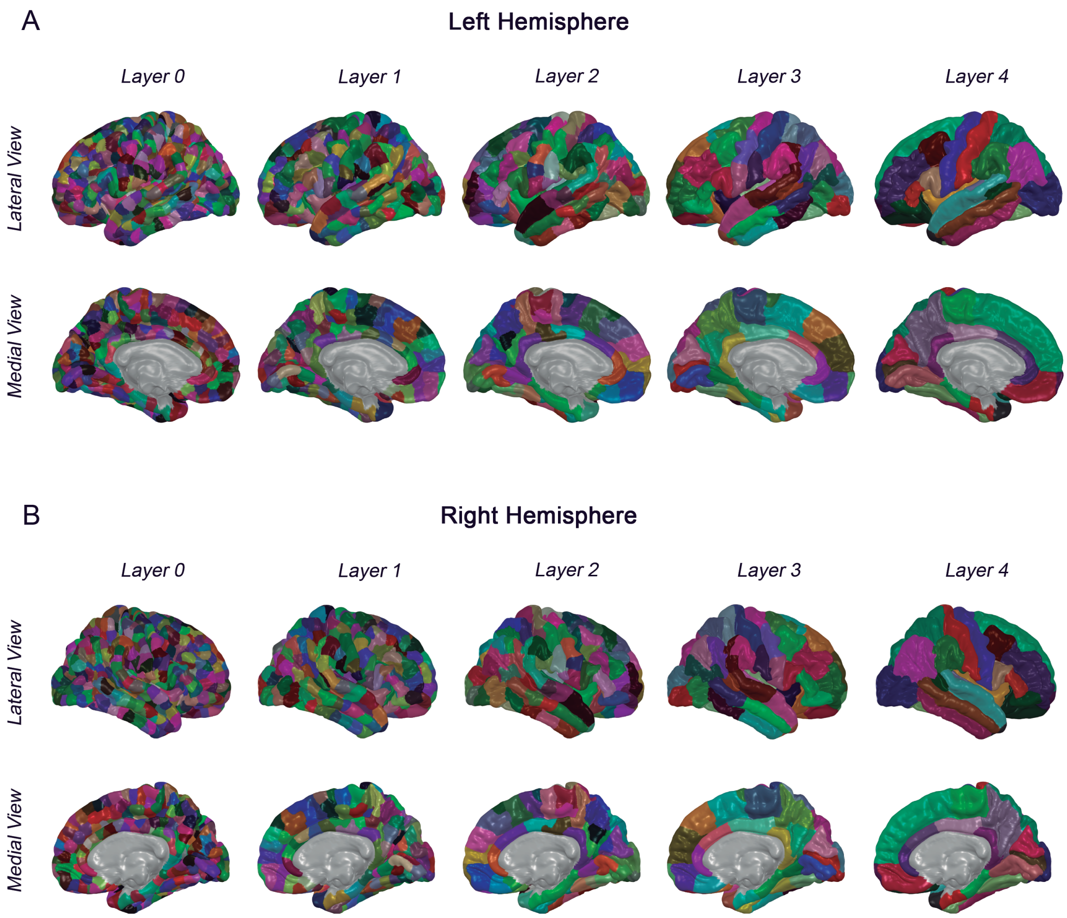

FIG. S1. **Lateral and medial views of the multi-scale cortical parcellation.**

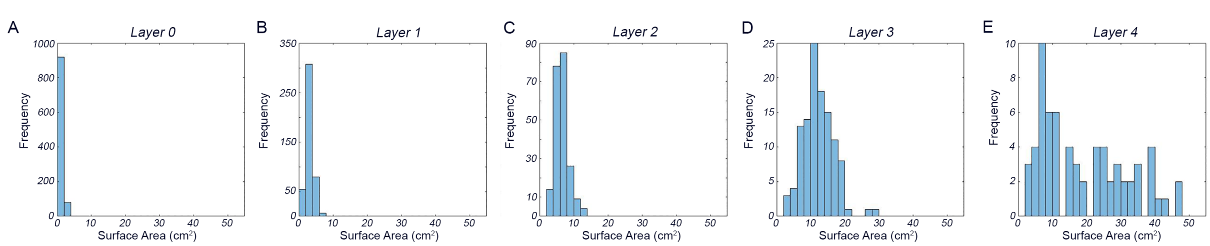

FIG. S2. **Histograms of surface areas of regions at each connectome scale.**

B. Average fiber length at different resolutions

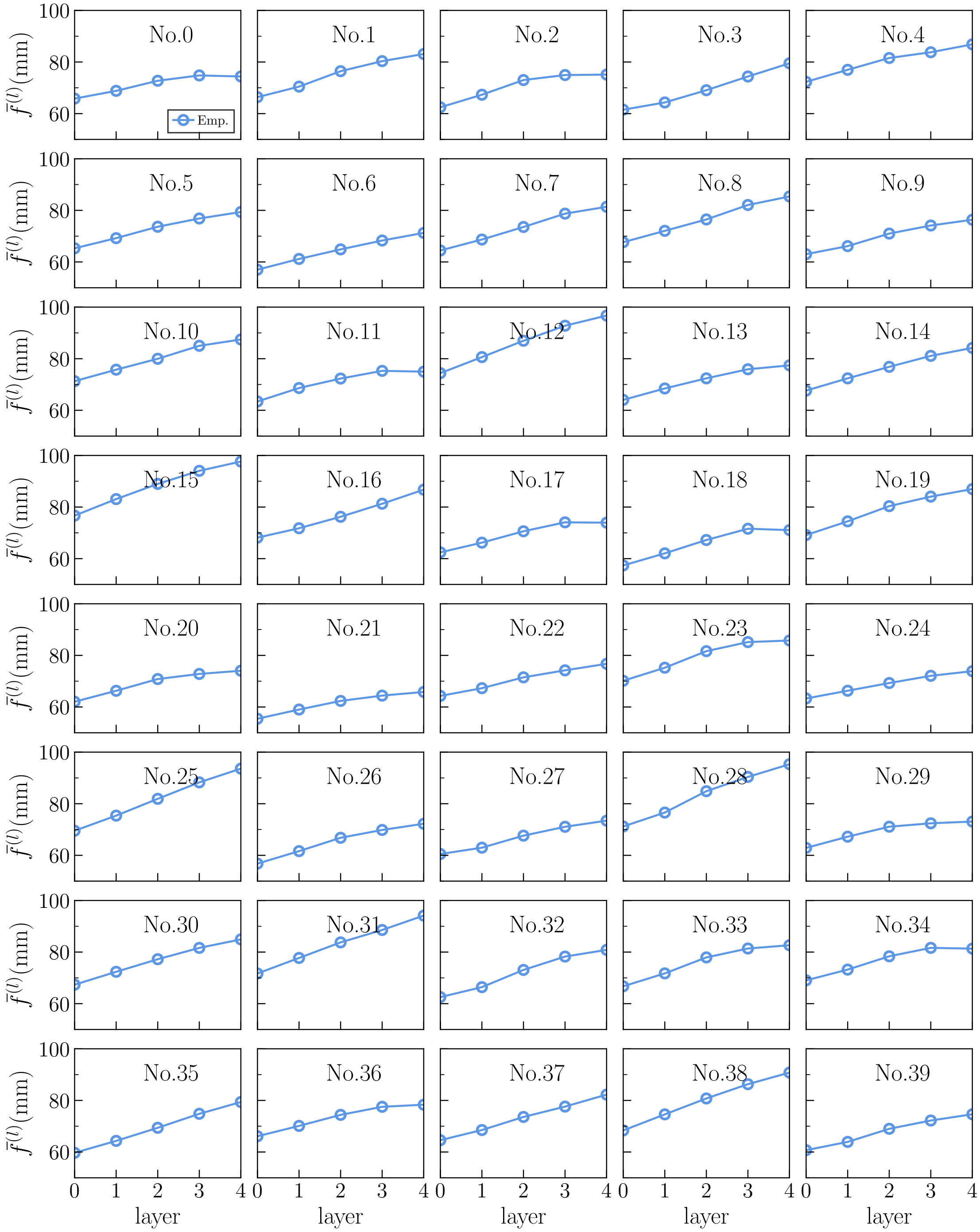

FIG. S3. Average fiber length $\bar{f}^{(l)}$(mm) for each subject in UL dataset.

C. MH connectomes vs GR flows for all subjects

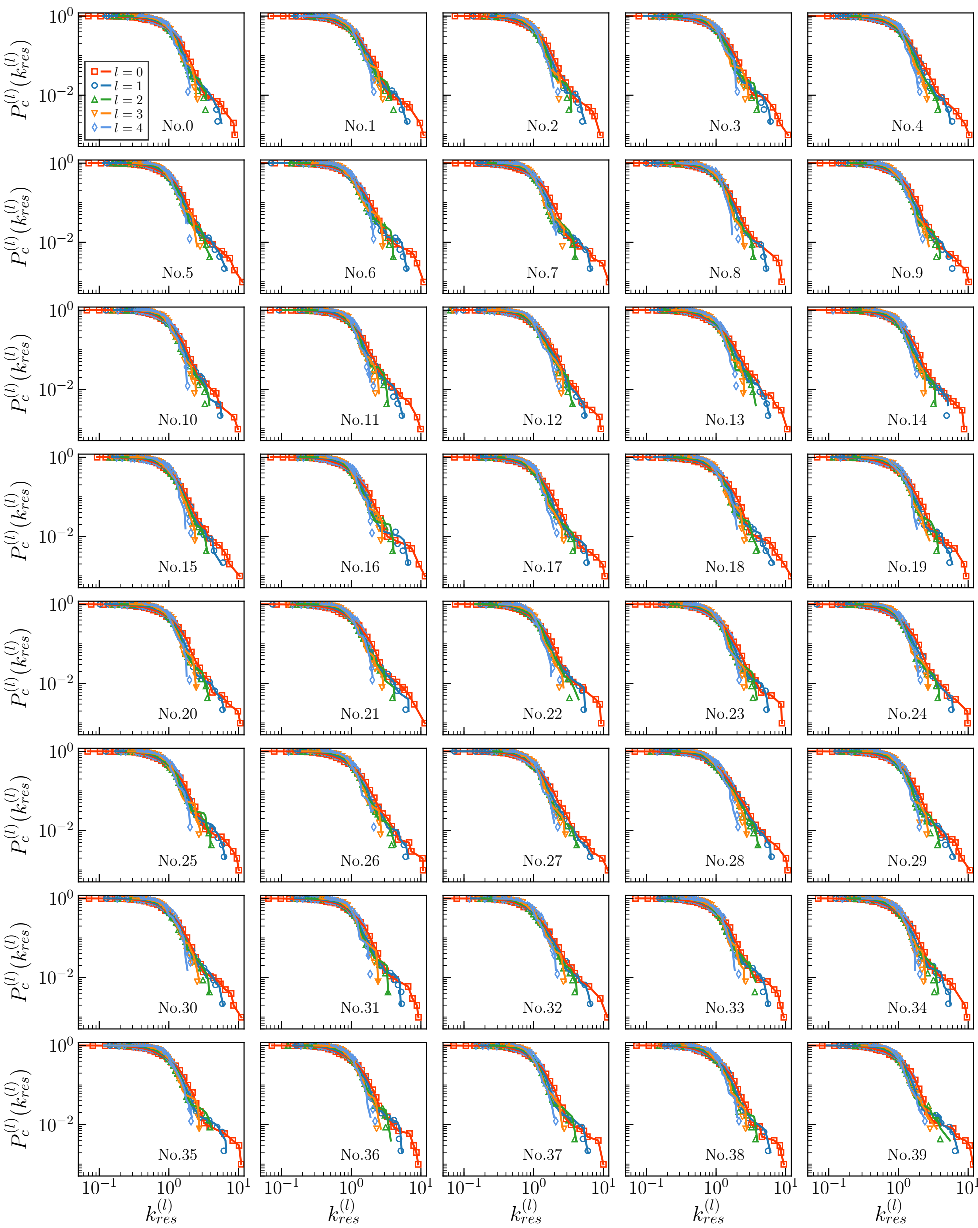

FIG. S4. Complementary cumulative degree distribution $P_c^{(l)}(k_{res}^{(l)})$ of rescaled degrees $k_{res}^{(l)}$ for different layers l in each subject as compared to the multiscale GR unfolding, where the symbols correspond to the empirical multiscale connectome and the line to the GR flow.

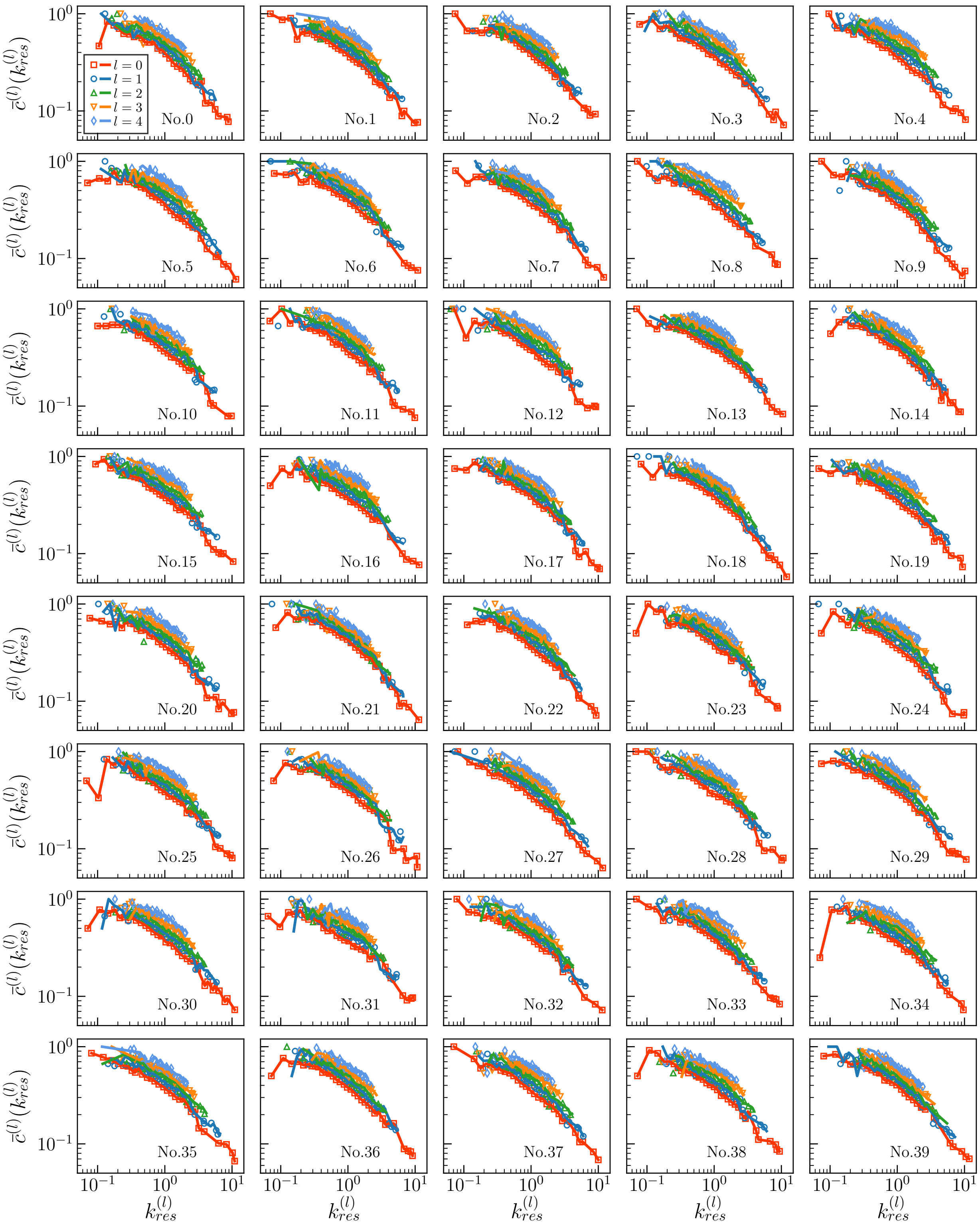

FIG. S5. The degree-dependent clustering coefficient $\bar{c}^{(l)}(k_{res}^{(l)})$ of rescaled degrees $k_{res}^{(l)}$ for different layers l in each subject as compared to the multiscale GR shell, where the symbols correspond to the empirical multiscale connectome and the line to the GR flow.

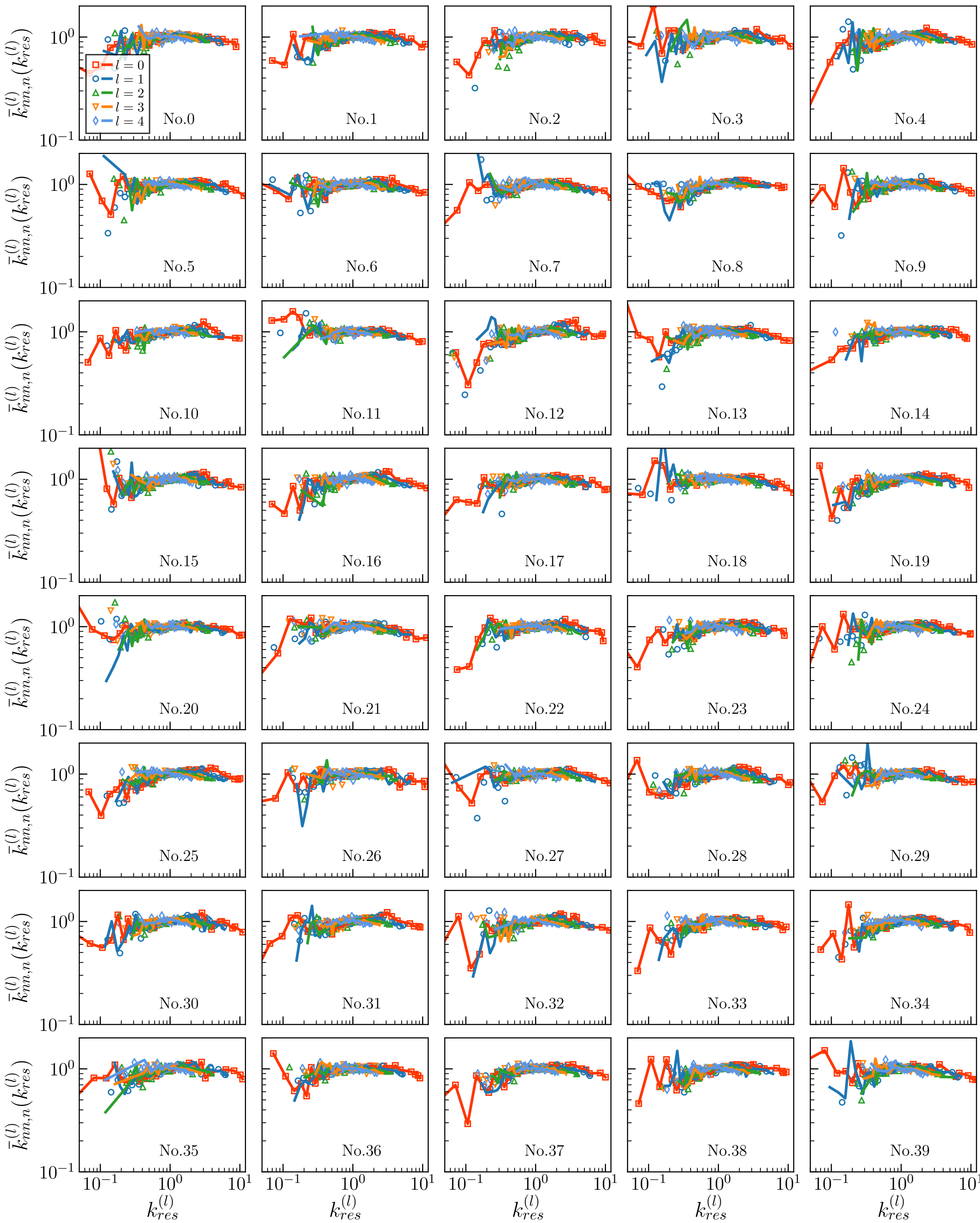

FIG. S6. Normalized average nearest-neighbour degree $\bar{k}^{(l)}_{nn,n}(k^{(l)}_{res}) = \bar{k}^{(l)}_{nn}(k^{(l)}_{res})\langle k^{(l)}\rangle/\langle (k^{(l)})^2\rangle$ versus rescaled degrees $k^{(l)}_{res}$ for different layers l in each subject as compared to the multiscale GR unfolding, where the symbols correspond to the empirical multiscale connectome and the line to the GR flow.

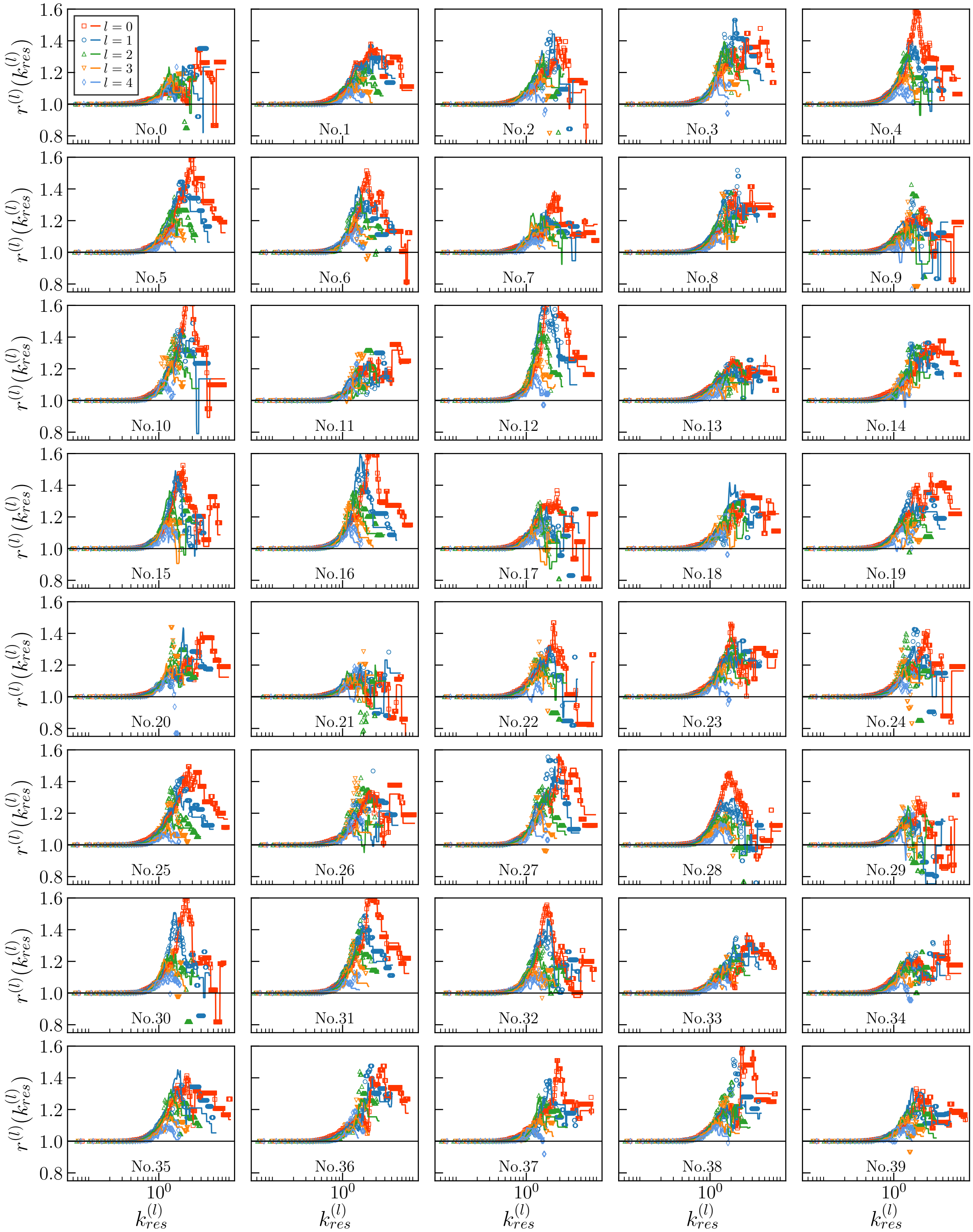

FIG. S7. Rich club coefficient $r^{(l)}(k_{res}^{(l)})$ versus rescaled degrees $k_{res}^{(l)}$ for different layers l in each subject as compared to the multiscale GR unfolding, where the symbols correspond to the empirical multiscale connectome and the line to the GR flow. The two largest hubs in subjects 2 and 21 are disconnected, giving two outlier values 0.

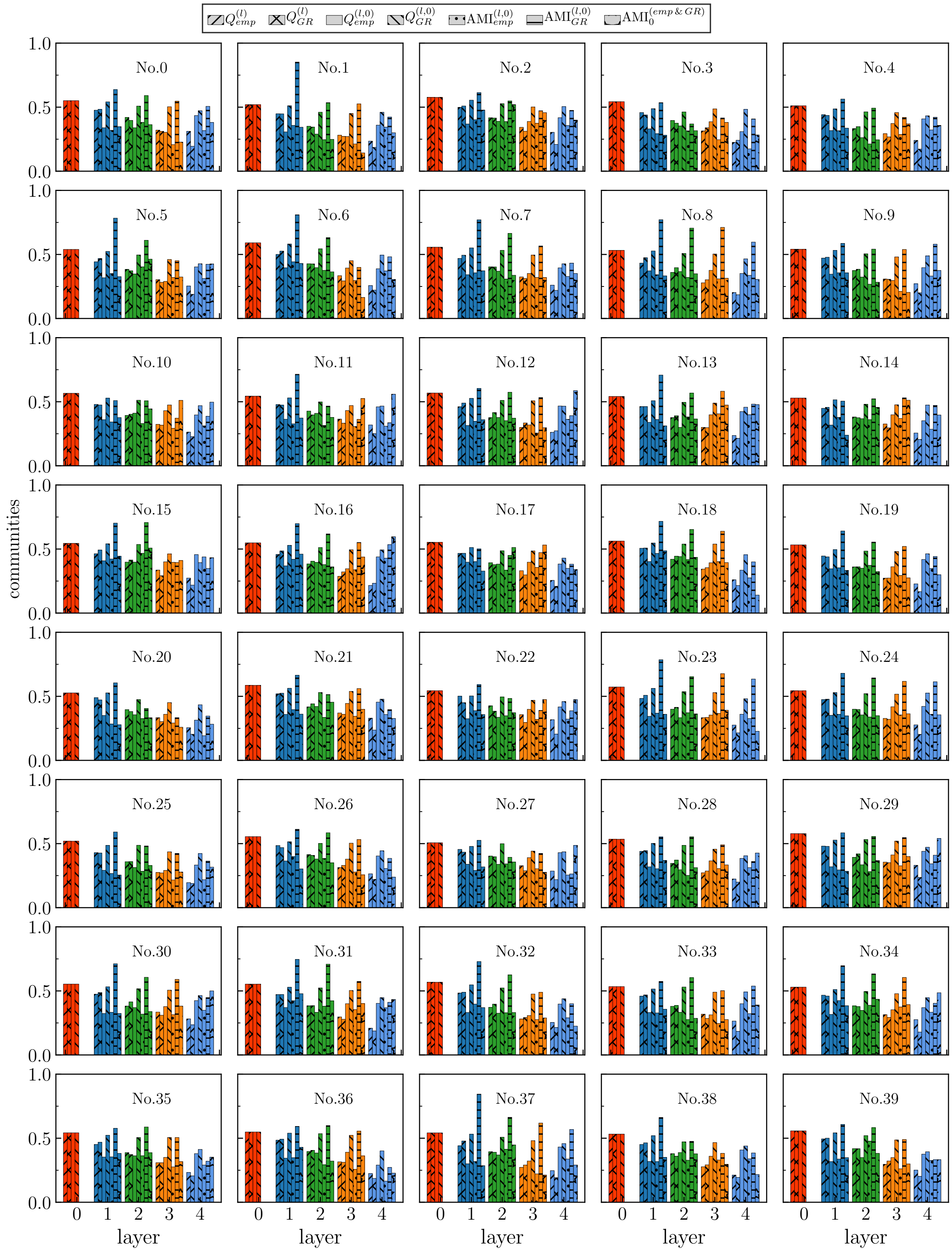

FIG. S8. Community structure of the empirical multiscale connectomes and the GR unfolding.

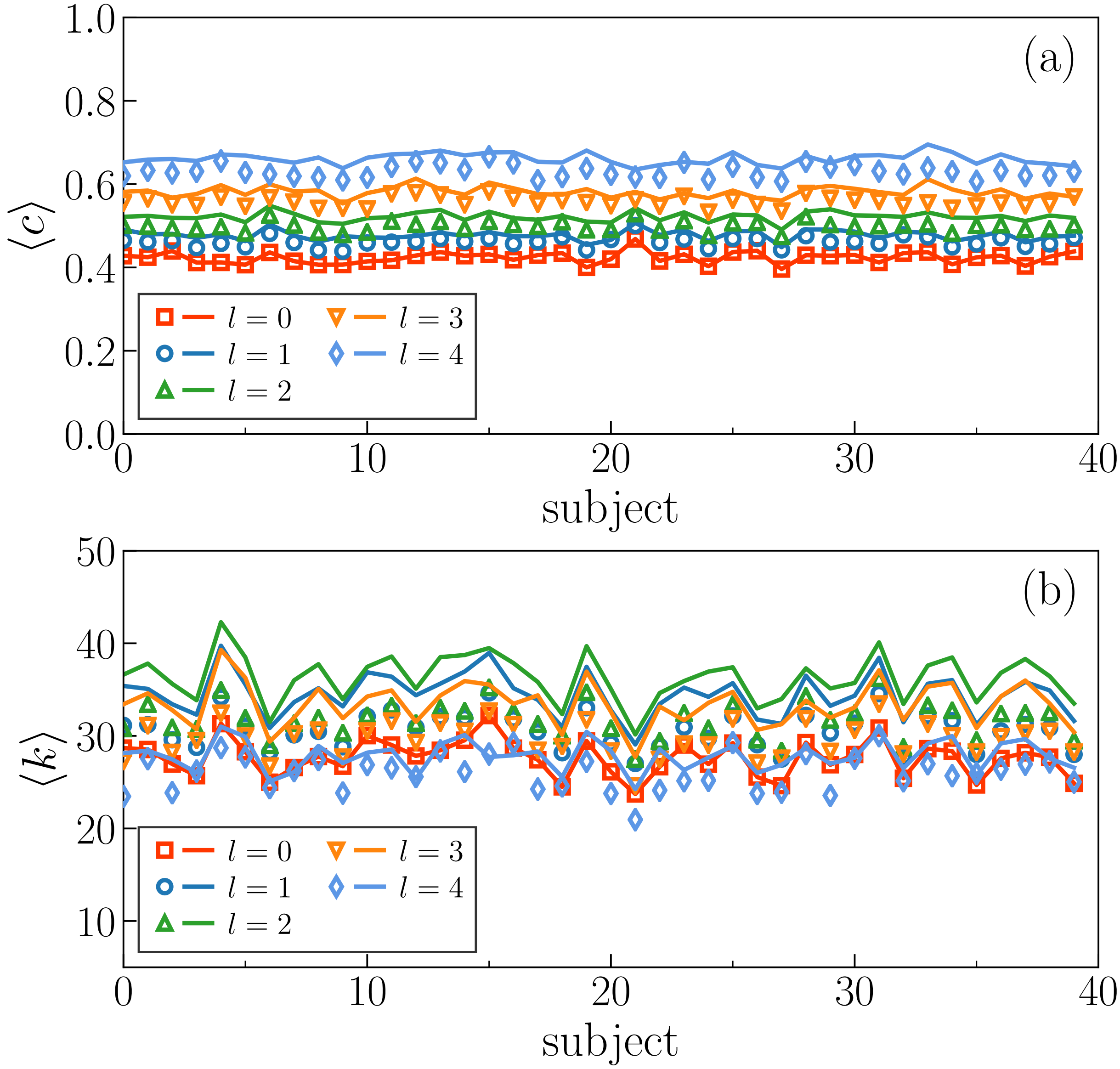

FIG. S9. Average clustering coefficient and mean degree for all the layers in each subject as compared to the multiscale GR unfolding, where the symbols correspond to the empirical multiscale connectome and the lines to the GR flow.

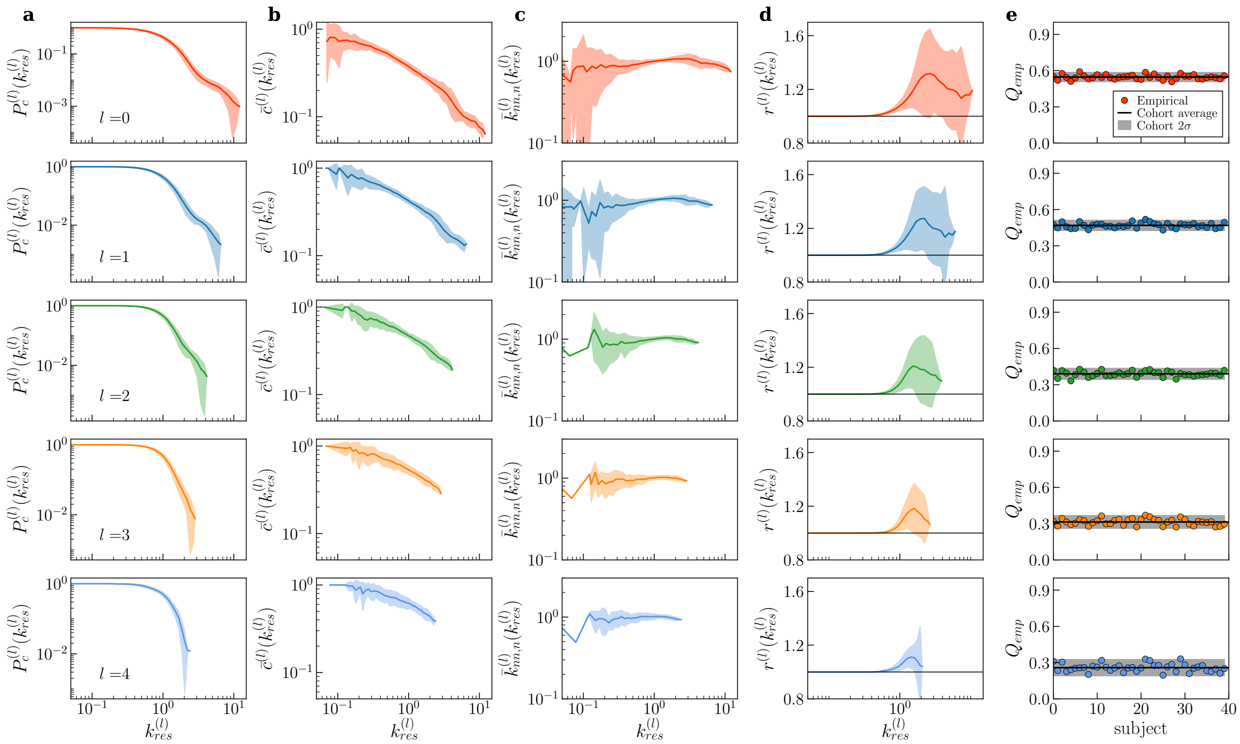

FIG. S10. **Network properties across 40 subjects for all layers in the UL dataset.** Each column shows the complementary cumulative degree distribution, degree-dependent clustering coefficient, degree-degree correlations, rich club coefficient and modularity. The degrees have been rescaled by the internal average degree of the corresponding layer $k_{res}^{(l)} = k^{(l)}/\langle k^{(l)} \rangle$. The solid lines show the corresponding average values across 40 subjects in the cohort and the shadows indicate 2σ deviations.

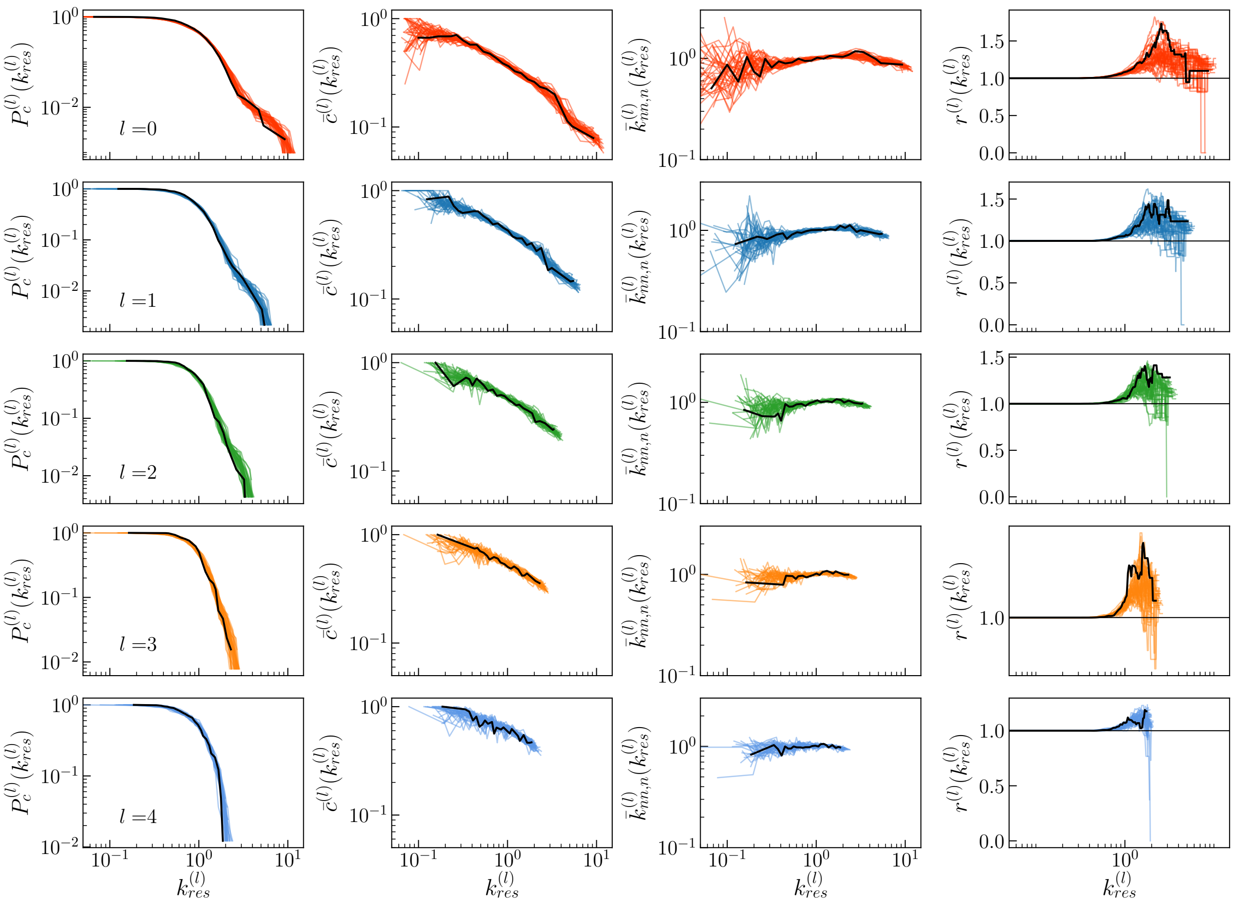

FIG. S11. **Subject No. 10 is a typical subject in the UL dataset.** Each column shows the complementary cumulative degree distribution, degree dependent clustering coefficient, degree-degree correlations and rich club coefficient. The degrees have been rescaled by the internal average degree of the corresponding layer $k_{res}^{(l)} = k^{(l)}/\langle k^{(l)}\rangle$. Different lines correspond to different subject in each cohort. The results for subject No. 10 have been highlighted in black color.

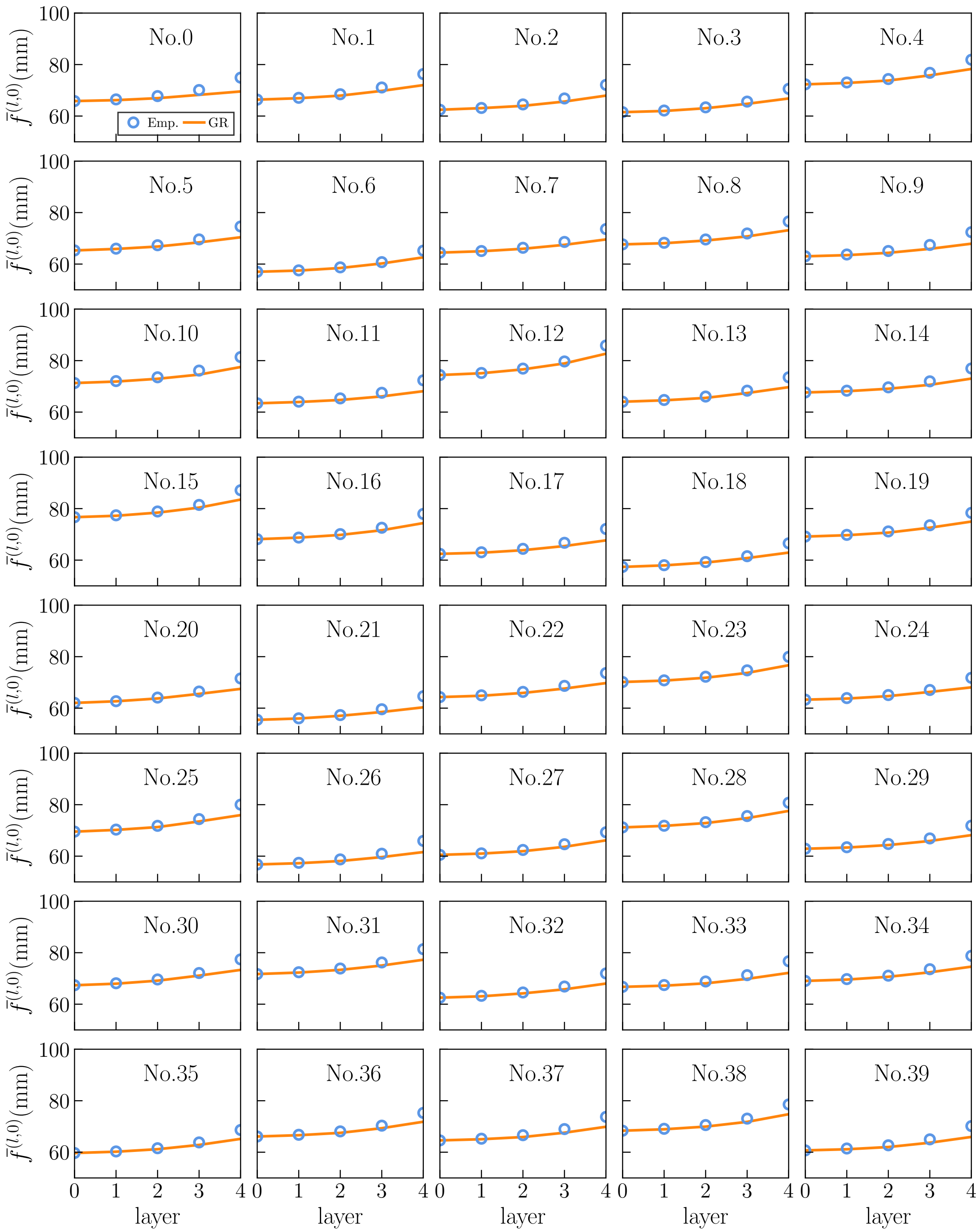

FIG. S12. Average fiber length $\bar{f}^{(l,0)}$ in layer 0 of links outside supernodes in layer l, where supernodes are defined by the anatomical coarse-graining in the empirical curve (symbols) or the similarity coarse-graining in the GR case (lines).

D. Behavior of the connection probabilities

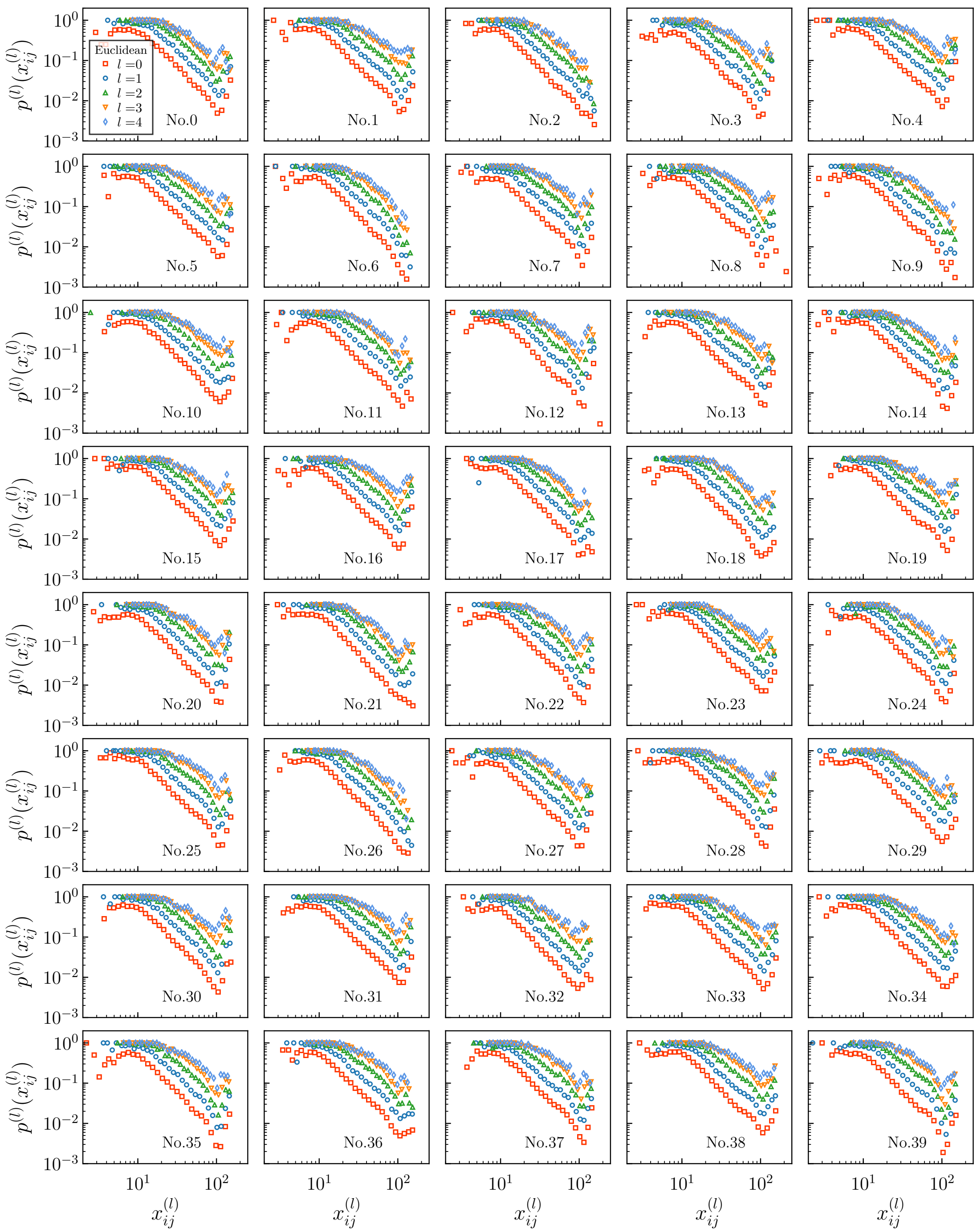

FIG. S13. Empirical connection probabilities $p^{(l)}(x_{ij}^{(l)})$ for each subject in the Euclidean space. The whole range of Euclidean distances x_{ij} is binned, and for each bin the ratio of the number of connected connectome pairs to the total number of connectome pairs falling within this bin is shown.

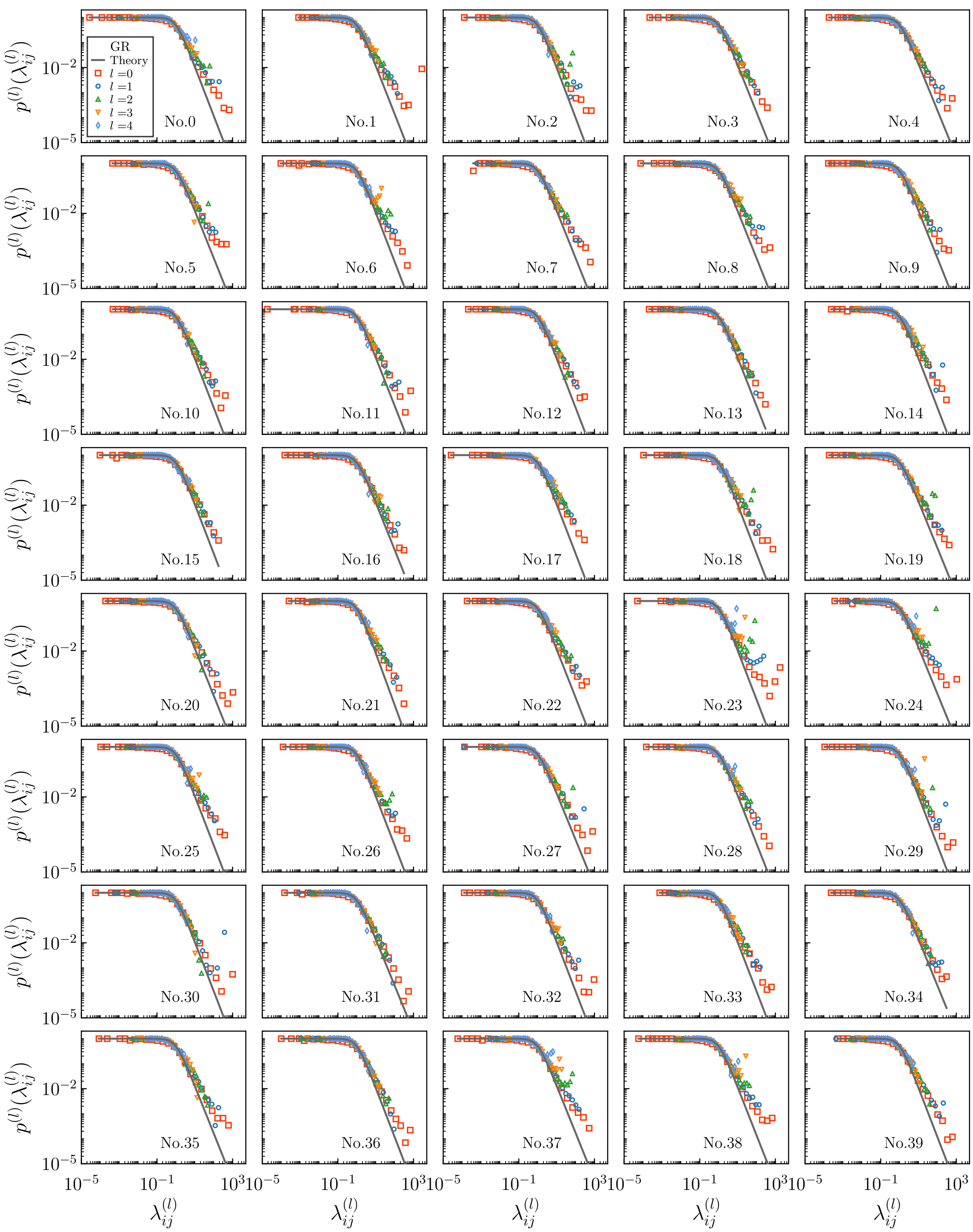

FIG. S14. Empirical versus theoretical connection probability $p^{(l)}(\lambda_{ij}^{(l)})$ within a given range of $\lambda_{ij}^{(l)}$ in GR shell for each subject. Open symbols are the connection probability of GR networks within a given range of $\lambda_{ij}^{(l)}$ and the gray lines shows the theoretical curves.

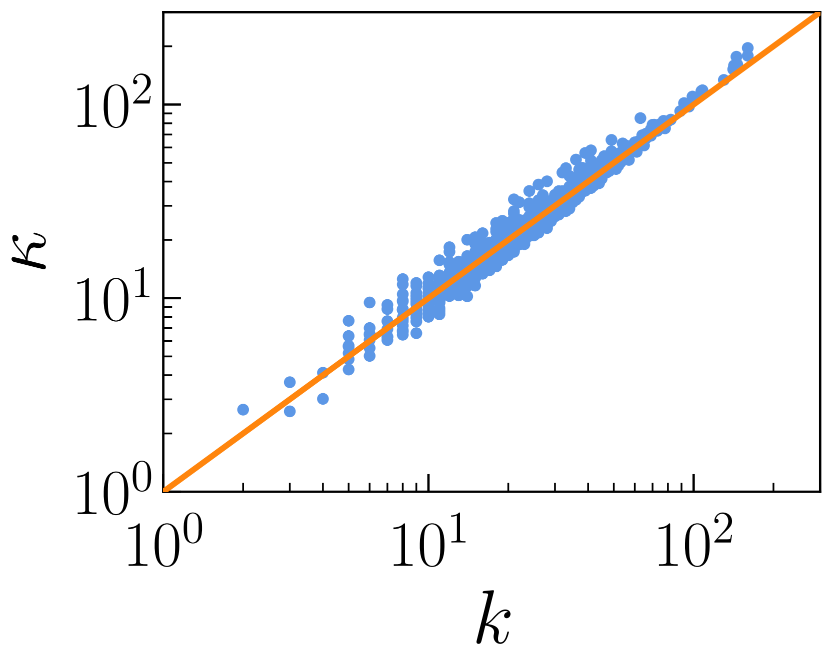

FIG. S15. **Hidden degrees κ versus observed degree k of highest resolution layer in subject No. 10.**

E. Navigability on the independent MH connectome layers and GR shell

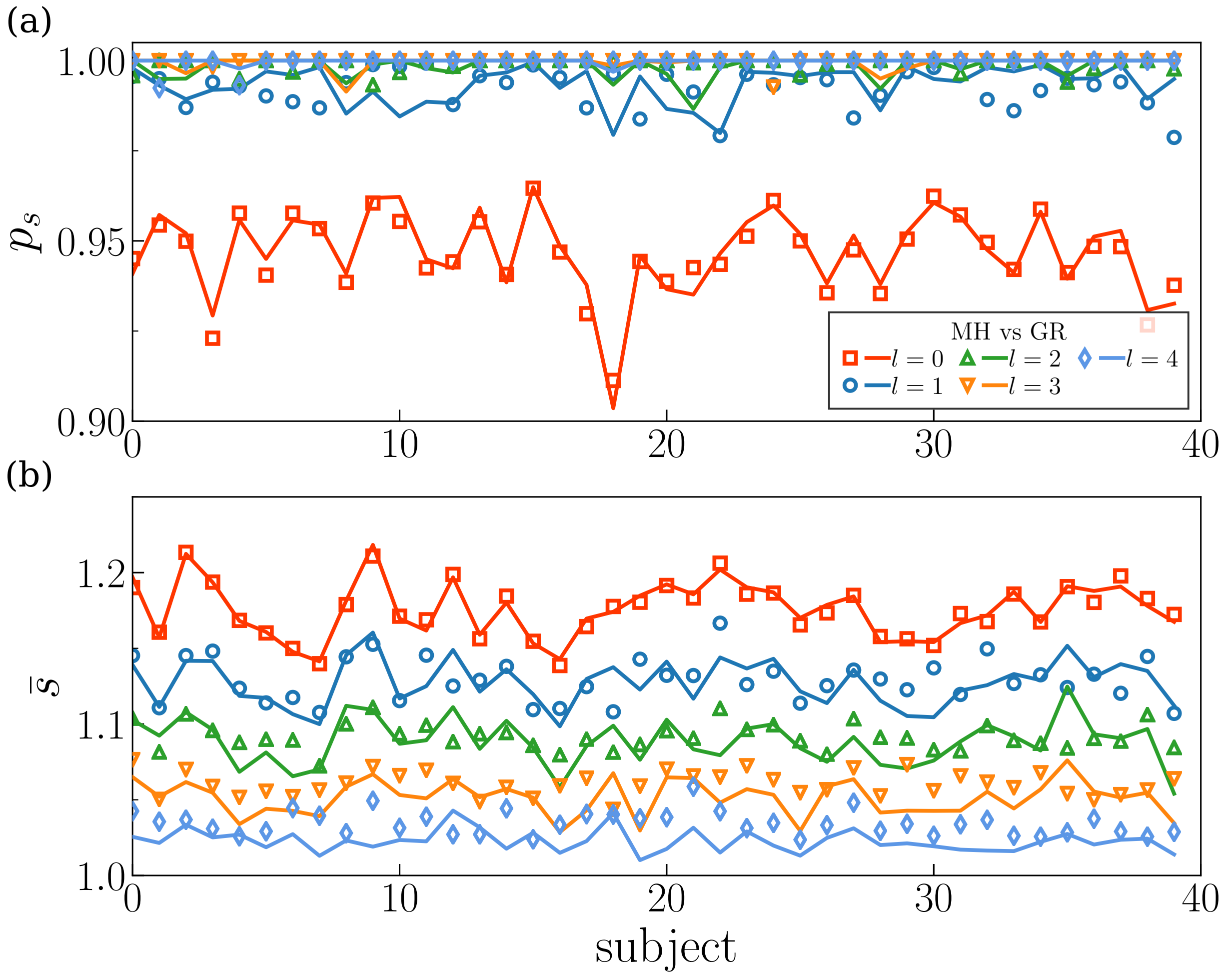

FIG. S16. **Navigability in the hyperbolic space on the independent MH connectome layers and GR shell.** open symbols correspond to the independent hyperbolic embeddings of the MH connectome layers and the solid lines to the GR shell.

F. Multiscale navigation protocol.

In this section, we study the performance of the multiscale GR protocol[1] in the GR shell of the 40 MH connectomes. Notice that when a packet can get stuck into a loop in single layer greedy routing, the multiscale navigation protocol can find alternative paths by taking advantage of the increased efficiency of greedy forwarding in the coarse-grained layers. When node i needs to send a packet to a destination node j, node i performs a virtual greedy forwarding step in the highest possible layer to find which supernode should be next in the greedy path. Based on this, node i then forwards the packet to its physical neighbour in the real network, which guarantees that it will eventually reach such supernode. The full details of this process is described as follows.

To guarantee navigation inside supernodes, we require an extra condition in the renormalization process and only consider blocks of connected consecutive nodes (a single node can be left alone forming a supernode by itself) to produce the GR shell. Notice that the new requirement does not alter the self-similarity of the renormalized networks forming the multiscale shell nor the congruency with the hidden metric space [1].

With respect to standard greedy routing in single layered networks, the multiscale navigation protocol requires adding the following information about the supernodes and their neighbors.

(i) The coordinates $(r_i^{(l)}, \theta_i^{(l)})$ of node i in every layer l.

(ii) For each node i, she should know her (super)neighbours list and their coordinates in each layer.

(iii) Let SuperN(i, l) be the supernode to which i belongs in layer l. Supposed that SuperN(i, l) contains (super)nodes $\{i, i_1, i_2 \ldots\}$ and SuperN(k, l) has (super)nodes $\{k, k_1, k_2 \ldots\}$ in layer l. If SuperN(i, l) is connected to SuperN(k, l), there is at least one edge between (super)nodes $\{i, i_1, i_2 \ldots\}$ and $\{k, k_1, k_2 \ldots\}$ in layer l, and the connected (super)nodes of $\{i, i_1, i_2 \ldots\}$ and $\{k, k_1, k_2 \ldots\}$ are called "gateway'. So, for every superneighbour of node SuperN(i, l) in layer l, node i knows which (super)node or (super)nodes in layer $l-1$ are gateways reaching it.

(iv) If SuperN$(i, l-1)$ is a gateway reaching some supernode s, at least one of its (super)neighbours in layer $l-1$ belongs to s; node i knows which.

This information allows us to navigate the network as follows. If node i wants to send a packet to a destination node j, node i should know j's coordinates in all L layers $(r_i^{(l)}, \theta_i^{(l)})$ and then node i will first check if it is connected to j; in that case, the decision is clear. If it is not, it will performs a virtual greedy forwarding step in the highest possible layer to find which supernode should be next in the greedy path. The detailed steps are provided as following:

1. Find the highest layer l_{max} in which SuperN(i, l_{max}) and SuperN(j, l_{max}) still have different coordinates. Set $l = l_{max}$.

2. Perform a standard step of greedy routing in layer l: find the closest neighbour of SuperN(i, l) to SuperN(j, l). This is the current target SuperT(l).

3. While $l > 0$, look into layer $l - 1$:

   Set $l = l - 1$.

   If SuperN(i, l) is a gateway connecting to some (super)node within SuperT$(l+1)$, node i sets as new current target SuperT(l) its (super)neighbour belonging to SuperT$(l+1)$ closest to SuperN(j, l). Else node i sets as new target SuperT(l) the gateway in SuperN$(i, l+1)$ connecting to SuperT$(l+1)$ (its (super)neighbour belonging to SuperN$(i, l+1)$).

4. In layer $l = 0$, SuperT(0) belongs to the real network and she is a neighbour of i, so node i forwards the message to SuperT(0).

Fig. S17 (a) shows the gain in success rate as the number of renormalized layers used in the multiscale navigation process is increased, for the representative subject in the cohort. Interestingly, the navigability properties of every GR brain representation are very similar. For all subjects, the success rate increases significantly with the number of navigated layers in the shell, in fact it becomes very close to 100% with the inclusion of just two renormalized layers (Fig. S17 (c)), and this improvement comes at the expense of only a mild increase of the stretch of successful paths (Fig. S17 (b) and (d)).

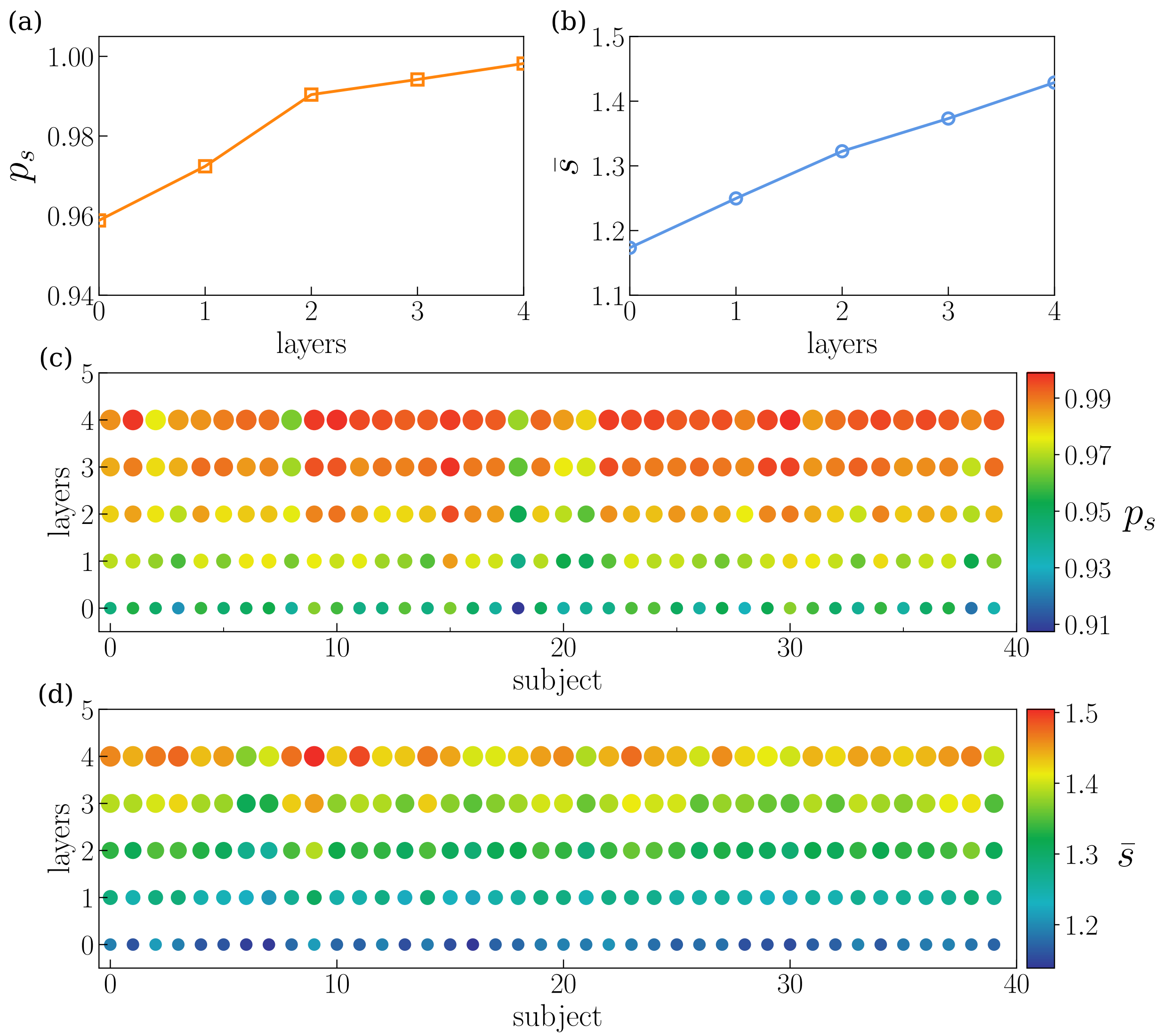

FIG. S17. **Performance of the GR multiscale navigation protocol in the GR shells of the human connectomes.** (a) Success rate p_s and (b) average stretch $\bar{s}$ as a function of the number of GR shell layers used in the routing process for subject No. 10, computed for 10^4 randomly selected pairs of nodes in layer $l = 0$. (c) and (d) The same for the 40 subjects in the cohort. The colors of the dots represent the magnitude of the corresponding property and their sizes are proportional to the number of layers used in the routing process.

G. Network properties of null models

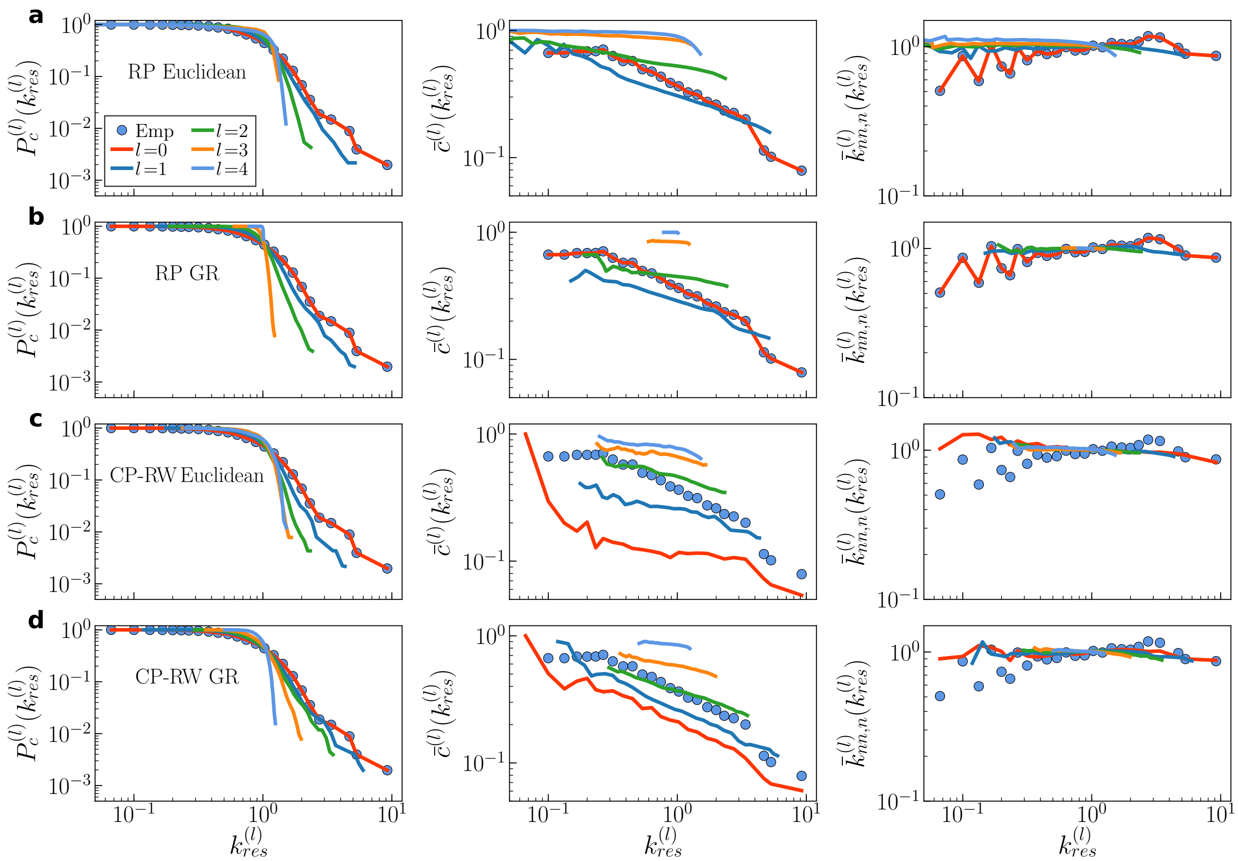

FIG. S18. **Loss the self-similarity in null networks**. Each column shows complementary cumulative degree distribution $P_c^{(l)}(k_{res}^{(l)})$, degree-dependent clustering coefficient $\bar{c}^{(l)}(k_{res}^{(l)})$, and degree-degree correlations $\bar{k}_{nn,n}^{(l)}(k_{res}^{(l)})$.

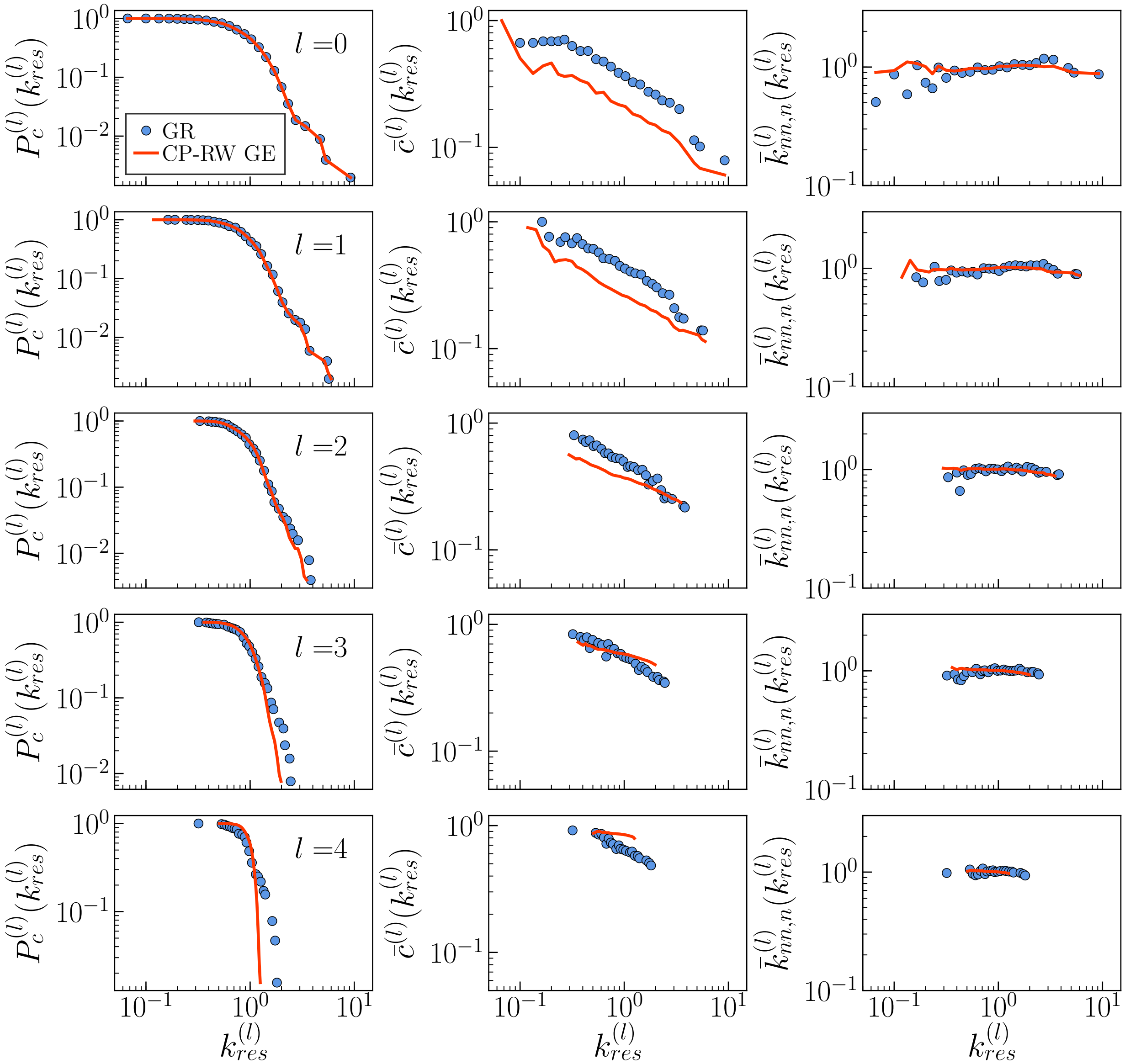

FIG. S19. **Comparision the network properties between standard GR and CP-RW GE model.** Each column shows complementary cumulative distribution $P_c^{(l)}(k_{res}^{(l)})$, degree dependent clustering coefficient $\bar{c}^{(l)}(k_{res}^{(l)})$, and degree-degree correlations $\bar{k}_{nn,n}^{(l)}(k_{res}^{(l)})$. We found that the self-similarity was still preserved to some extents in layer 0 to 2.

II. CROSS-VALIDATING RESULTS IN THE HCP DATASET

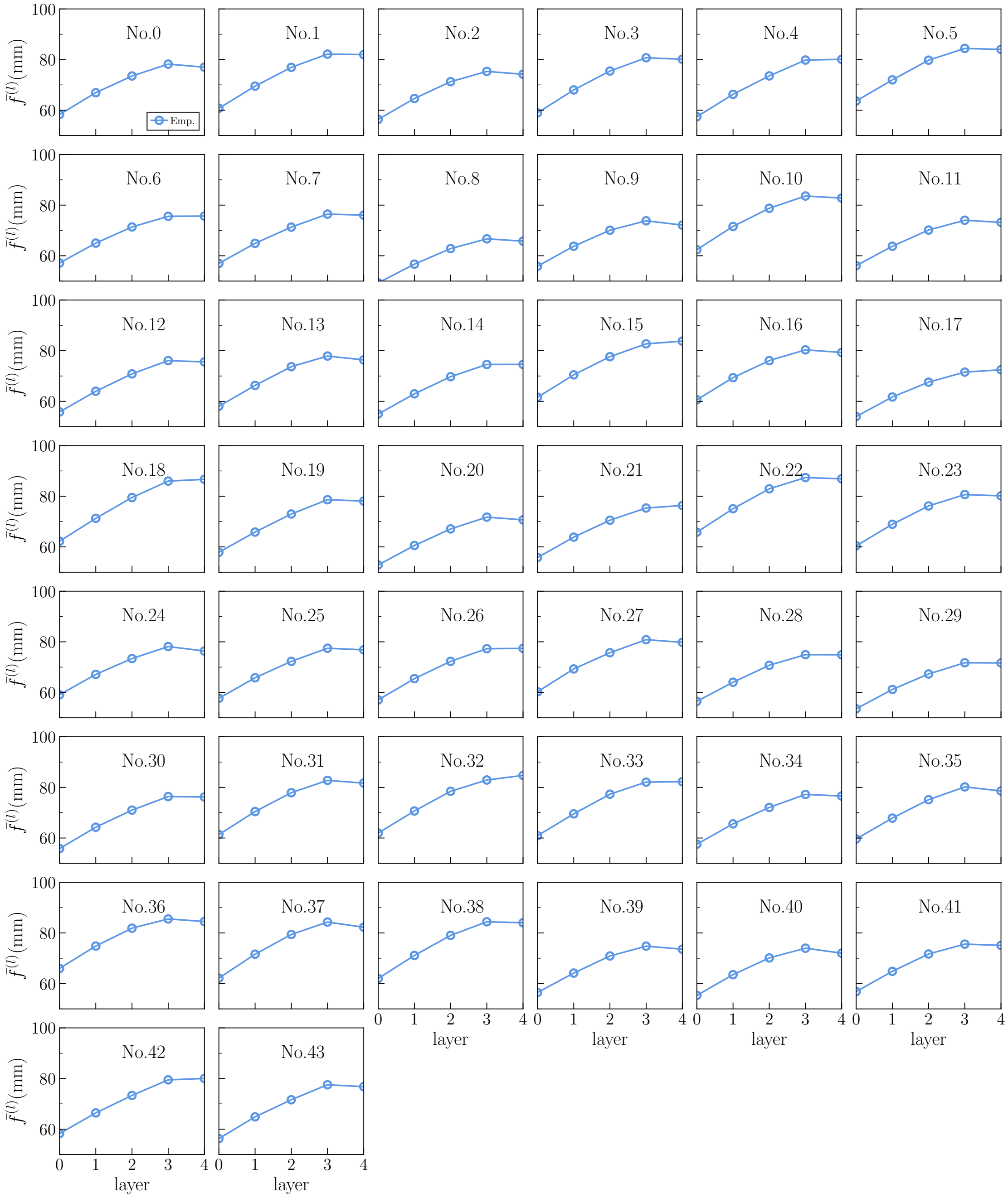

FIG. S20. Average fiber length $\bar{f}^{(l)}$ for each subject in HCP dataset.

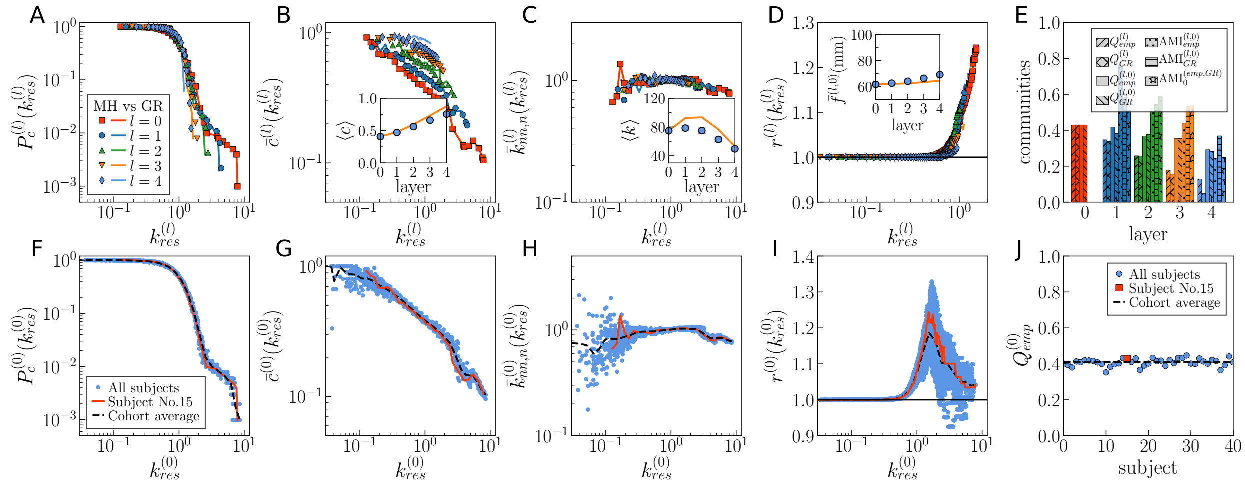

FIG. S21. **Self-similarity of the MH connectome at different resolutions**. (*A*-*E*) Results for HCP subject No. 15. Filled symbols correspond to the empirical MH connectome and the lines to the GR shell. (*A*) Complementary cumulative degree distribution $P_c^{(l)}(k_{res}^{(l)})$. (*B*) Degree dependent clustering coefficient $\bar{c}^{(l)}(k_{res}^{(l)})$. Inset: flow of the average clustering coefficient $\langle c \rangle$. (*C*) Degree-degree correlations $\bar{k}_{nn,n}^{(l)}(k_{res}^{(l)})$. Inset: flow of the average degree $\langle k \rangle$. (*D*) Rich club coefficient $r^{(l)}(k_{res}^{(l)})$ for low and intermediate values of the rescaled threshold degrees. Inset: average fiber length $\bar{f}^{(l,0)}$ in layer 0 of links outside supernodes in layer l, where supernodes are defined by the anatomical coarse-graining in the empirical curve or the similarity coarse-graining in the GR case. In the three insets in (*B*)-(*D*), error bars show the ± 2 standard error interval around the mean; when not visible the bars are within symbol size. (*E*) Community structure of the multiscale connectomes. $Q^{(l)}$ is the modularity in layer l, $Q^{(l,0)}$ is the modularity that the community structure of layer l induces in layer 0, and $\mathrm{AMI}^{(l)}$ is the adjusted mutual information between the latter and the community partition directly detected in layer 0 (see Materials and Methods). The subindices $\{emp, GR\}$ indicate the empirical MH connectomes and the GR shell, respectively. $\mathrm{AMI}_0^{(emp,GR)}$ is the adjusted mutual information between topological communities in the empirical MH connectomes at each layer and the GR flow measured in their projection over layer 0. (*F*-*J*) Variability of topological properties in the HCP dataset. Blue symbols correspond to the properties of layer 0 in all subjects. The red line correspond to HCP subject No. 10. The black dashed line represents the average value across the 44 subjects in the cohort. In the plots, degrees have been rescaled by the average degree of the corresponding layer $k_{res}^{(l)} = k^{(l)}/\langle k^{(l)} \rangle$.

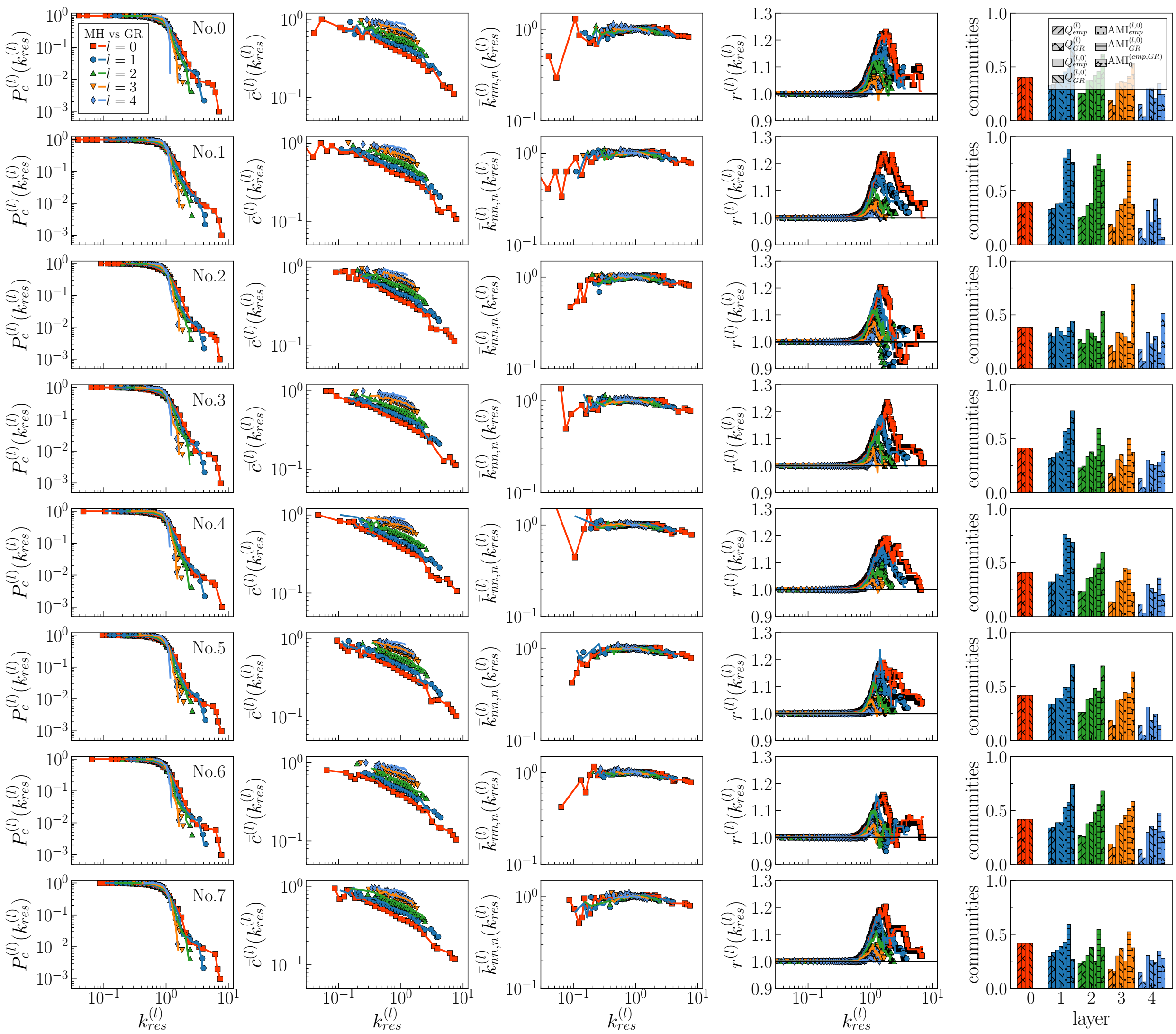

FIG. S22. **Self-similarity of the MH connectome at different resolutions**. We show results for subject No. 0-7 in HCP dataset. Filled symbols correspond to the empirical MH connectome and the lines to the GR shell. Each column shows complementary cumulative distribution $P_c^{(l)}(k_{res}^{(l)})$, degree dependent clustering coefficient $\bar{c}^{(l)}(k_{res}^{(l)})$, degree-degree correlations $\bar{k}_{nn,n}^{(l)}(k_{res}^{(l)})$, rich club coefficient $r^{(l)}(k_{res}^{(l)})$, and community structure of the multiscale connectomes.

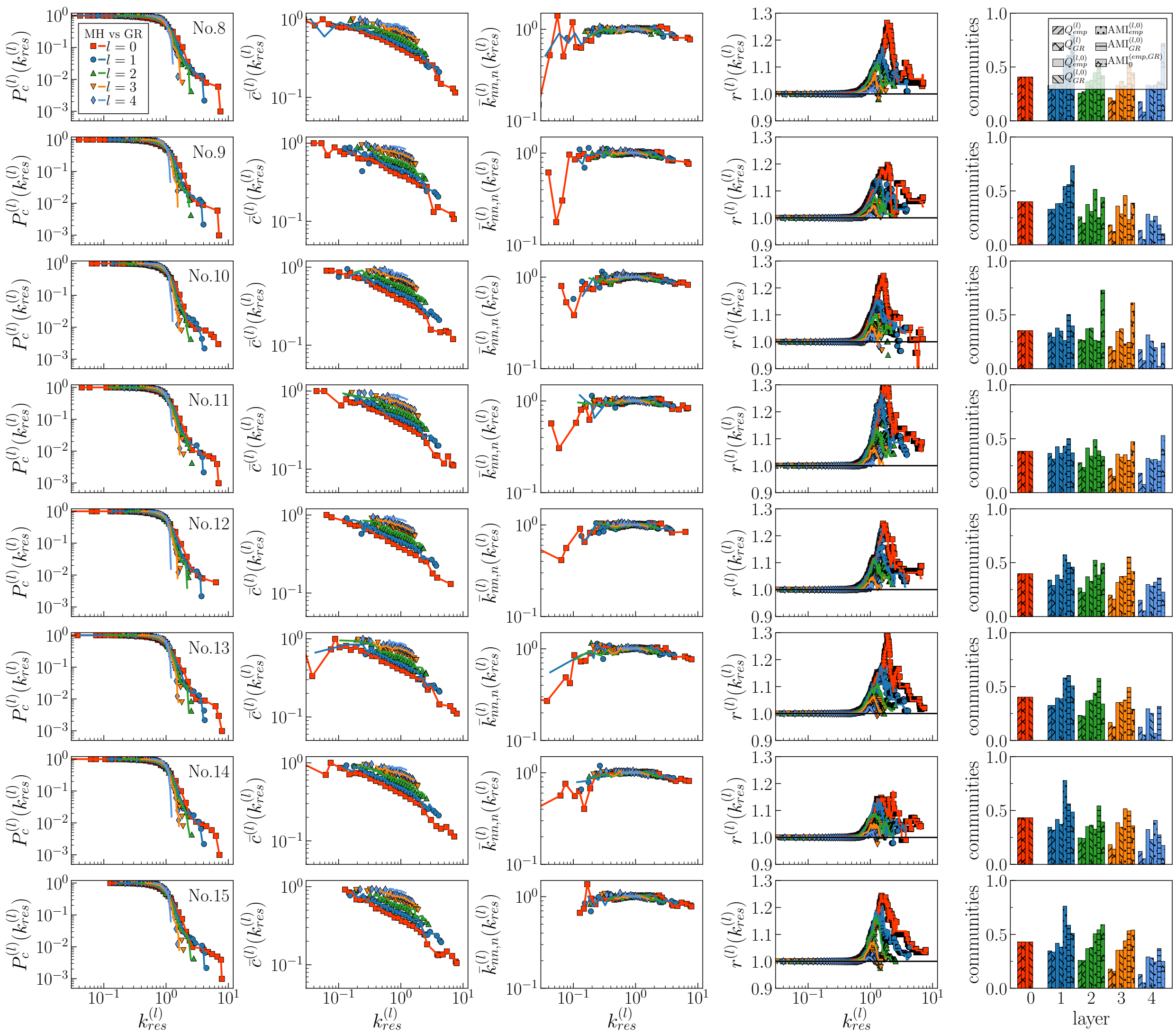

FIG. S23. **Self-similarity of the MH connectome at different resolutions**. We show results for subject No. 8-15 in HCP dataset. Filled symbols correspond to the empirical MH connectome and the lines to the GR shell. Each column shows complementary cumulative distribution $P_c^{(l)}(k_{res}^{(l)})$, degree dependent clustering coefficient $\bar{c}^{(l)}(k_{res}^{(l)})$, degree-degree correlations $\bar{k}_{nn,n}^{(l)}(k_{res}^{(l)})$, rich club coefficient $r^{(l)}(k_{res}^{(l)})$, and community structure of the multiscale connectomes.

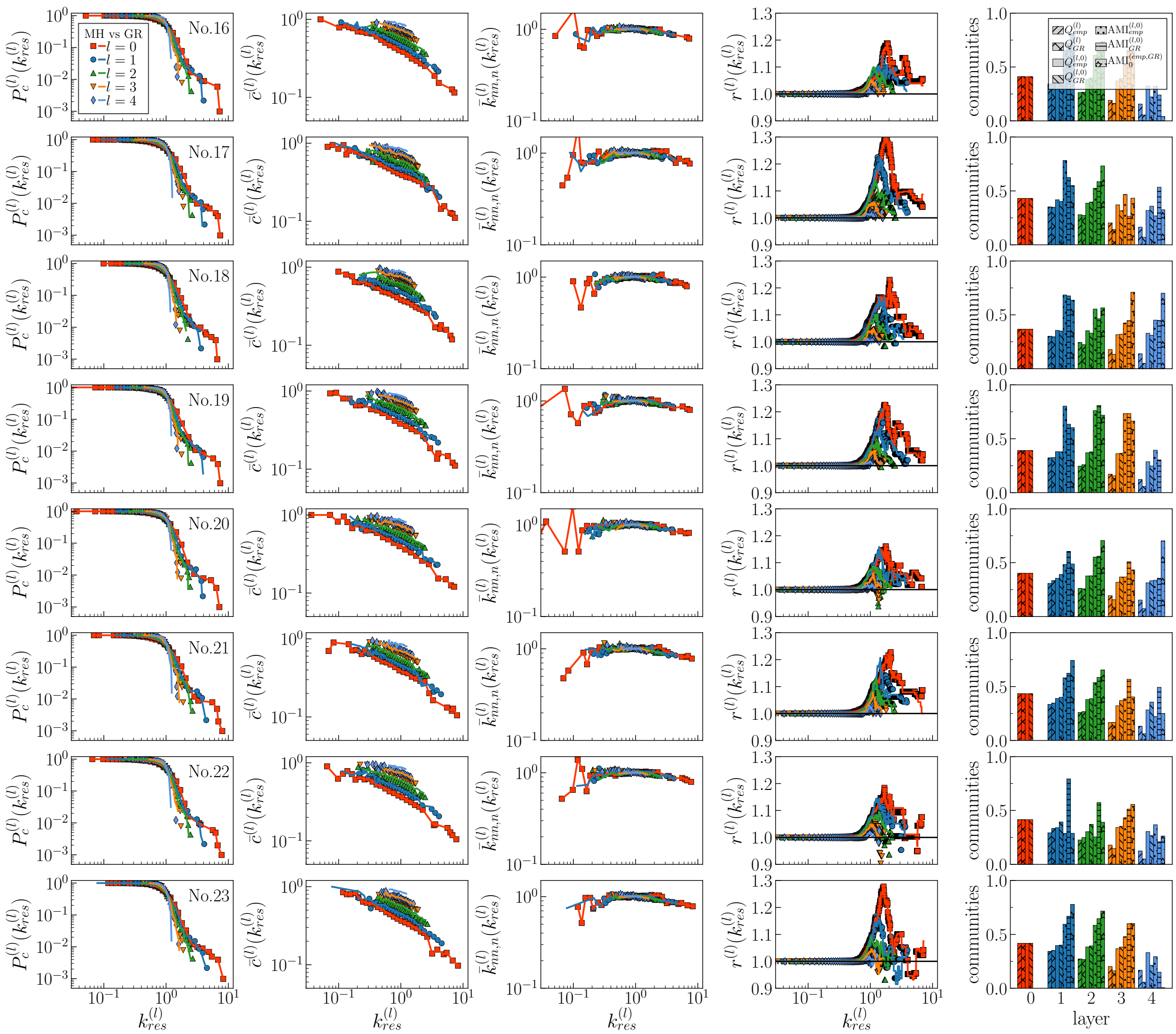

FIG. S24. **Self-similarity of the MH connectome at different resolutions**. We show results for subject No. 16-23 in HCP dataset. Filled symbols correspond to the empirical MH connectome and the lines to the GR shell. Each column shows complementary cumulative distribution $P_c^{(l)}(k_{res}^{(l)})$, degree dependent clustering coefficient $\bar{c}^{(l)}(k_{res}^{(l)})$, degree-degree correlations $\bar{k}_{nn,n}^{(l)}(k_{res}^{(l)})$, rich club coefficient $r^{(l)}(k_{res}^{(l)})$, and community structure of the multiscale connectomes.

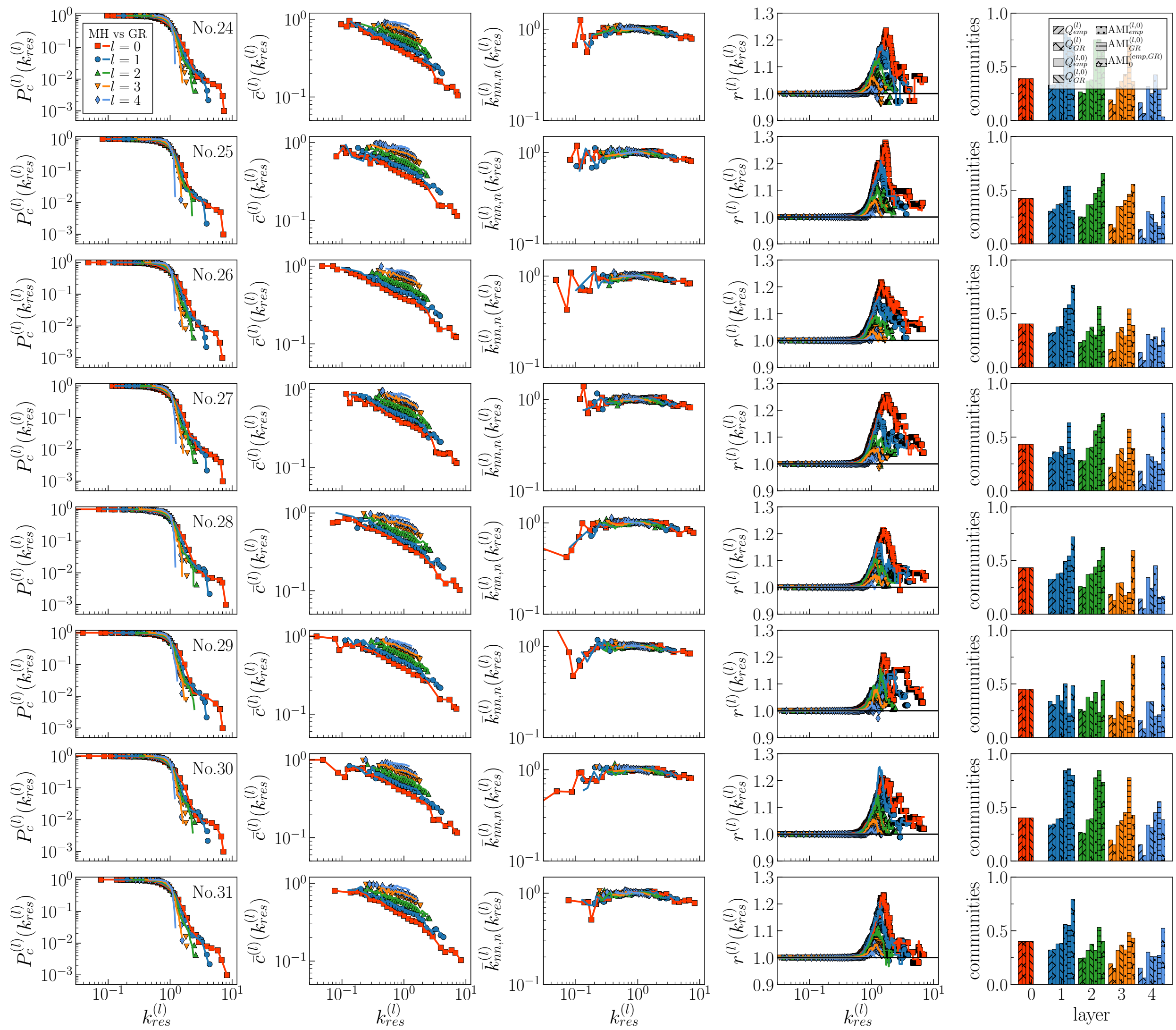

FIG. S25. **Self-similarity of the MH connectome at different resolutions**. We show results for subject No. 14-31 in HCP dataset. Filled symbols correspond to the empirical MH connectome and the lines to the GR shell. Each column shows complementary cumulative distribution $P_c^{(l)}(k_{res}^{(l)})$, degree dependent clustering coefficient $\bar{c}^{(l)}(k_{res}^{(l)})$, degree-degree correlations $\bar{k}_{nn,n}^{(l)}(k_{res}^{(l)})$, rich club coefficient $r^{(l)}(k_{res}^{(l)})$, and community structure of the multiscale connectomes.

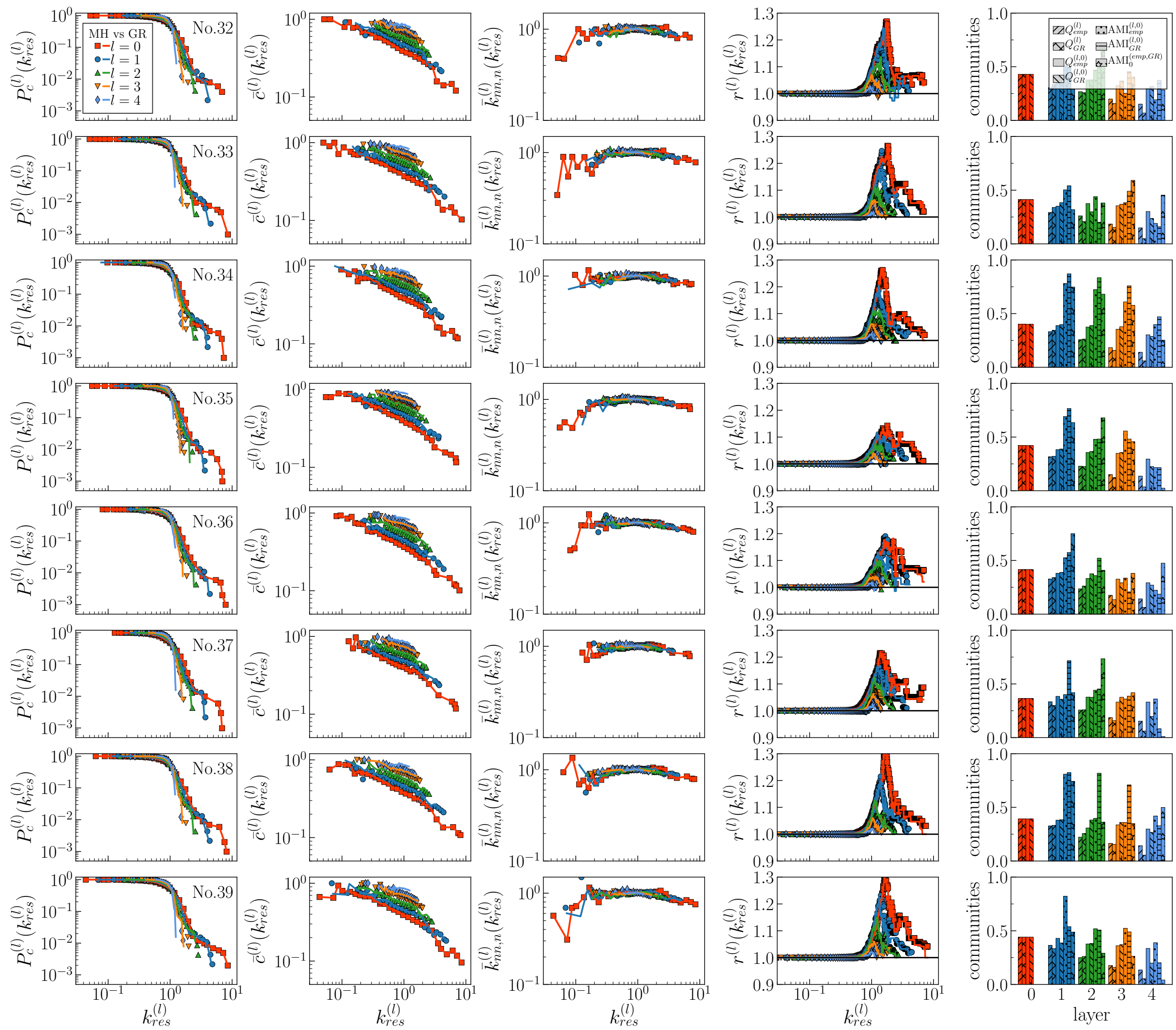

FIG. S26. **Self-similarity of the MH connectome at different resolutions**. We show results for subject No. 32-39 in HCP dataset. Filled symbols correspond to the empirical MH connectome and the lines to the GR shell. Each column shows complementary cumulative distribution $P_c^{(l)}(k_{res}^{(l)})$, degree dependent clustering coefficient $\bar{c}^{(l)}(k_{res}^{(l)})$, degree-degree correlations $\bar{k}_{nn,n}^{(l)}(k_{res}^{(l)})$, rich club coefficient $r^{(l)}(k_{res}^{(l)})$, and community structure of the multiscale connectomes.

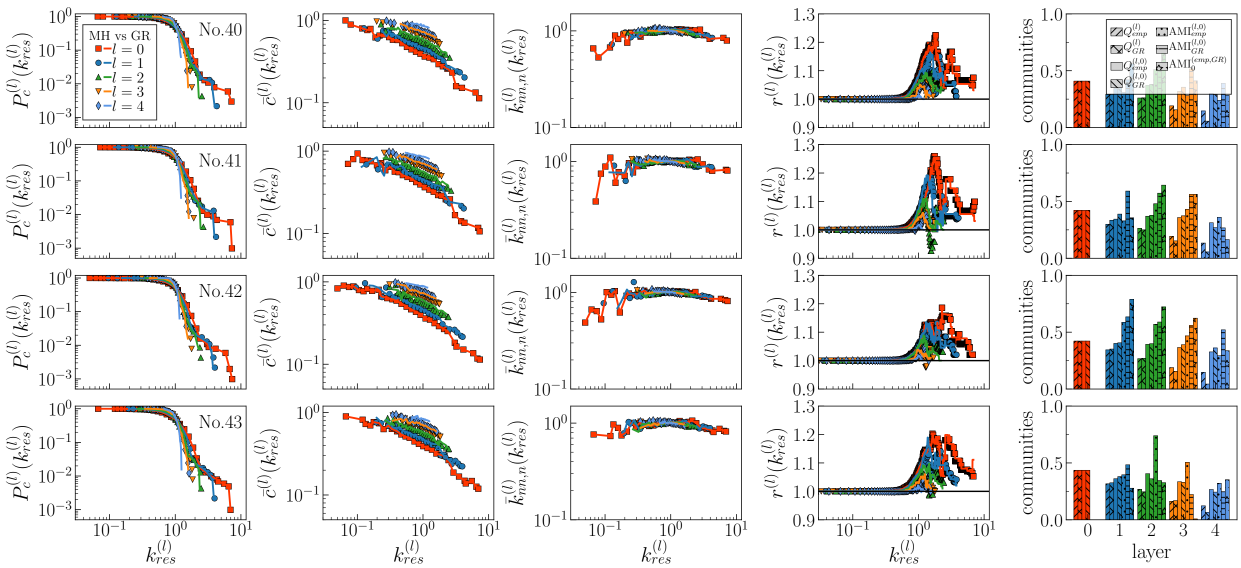

FIG. S27. **Self-similarity of the MH connectome at different resolutions**. We show results for subject No. 40-43 in HCP dataset. Filled symbols correspond to the empirical MH connectome and the lines to the GR shell. Each column shows complementary cumulative distribution $P_c^{(l)}(k_{res}^{(l)})$, degree dependent clustering coefficient $\bar{c}^{(l)}(k_{res}^{(l)})$, degree-degree correlations $\bar{k}_{nn,n}^{(l)}(k_{res}^{(l)})$, rich club coefficient $r^{(l)}(k_{res}^{(l)})$, and community structure of the multiscale connectomes.

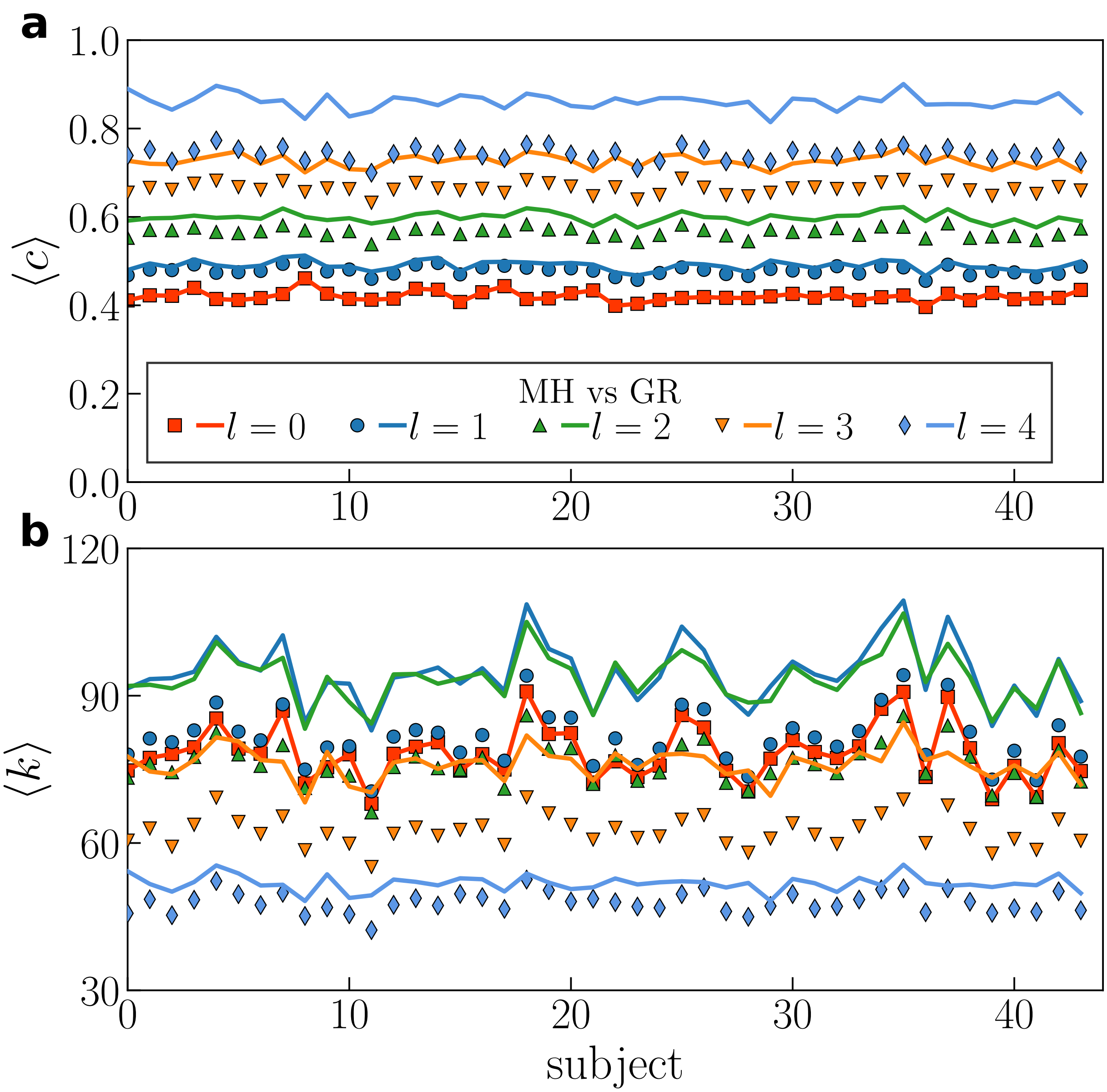

FIG. S28. Average clustering coefficient (a) and mean degree (b) for all the layers in each subject as compared to the multiscale GR unfolding, where the symbols correspond to the empirical multiscale connectome and the lines to the GR flow.

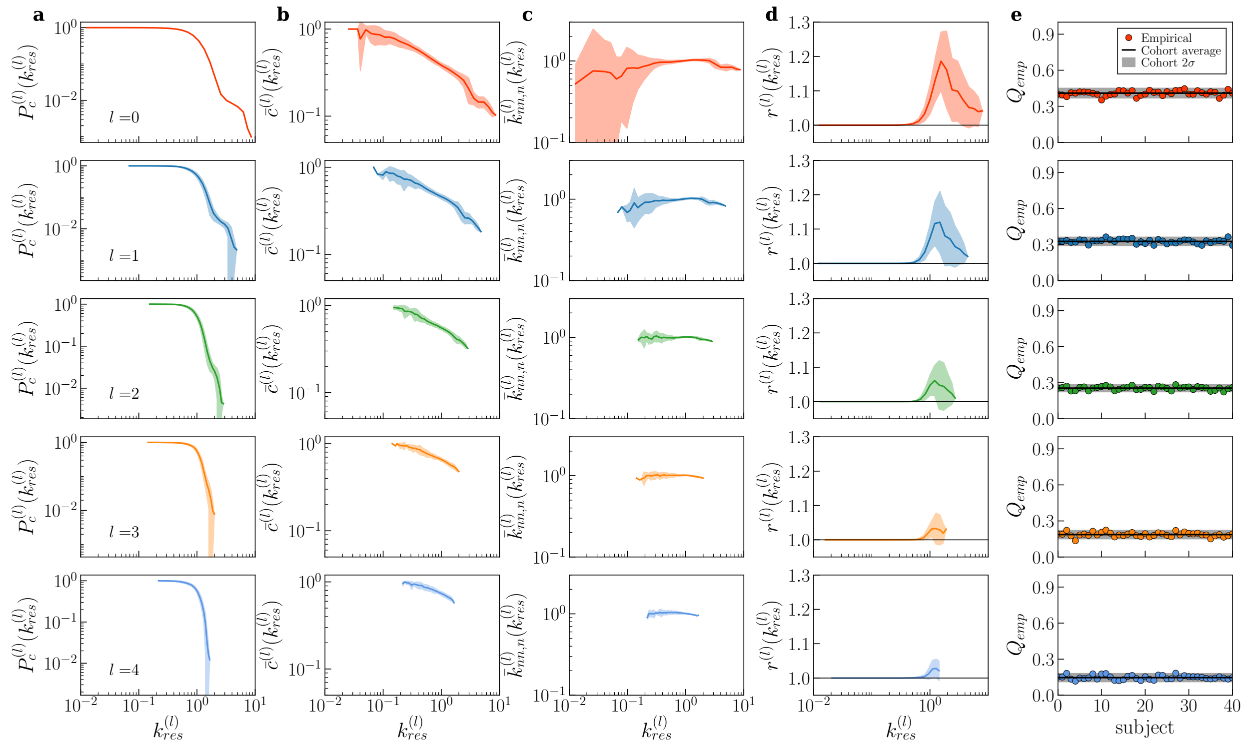

FIG. S29. **Network properties across 44 subjects for all layers in the HCP dataset.** Each column shows the complementary cumulative degree distribution, degree-dependent clustering coefficient, degree-degree correlations, rich club coefficient and modularity. The degrees have been rescaled by the internal average degree of the corresponding layer $k_{res}^{(l)} = k^{(l)}/\langle k^{(l)} \rangle$. The solid lines show the corresponding average values across 44 subjects in the cohort and the shadows indicate 2σ deviations.

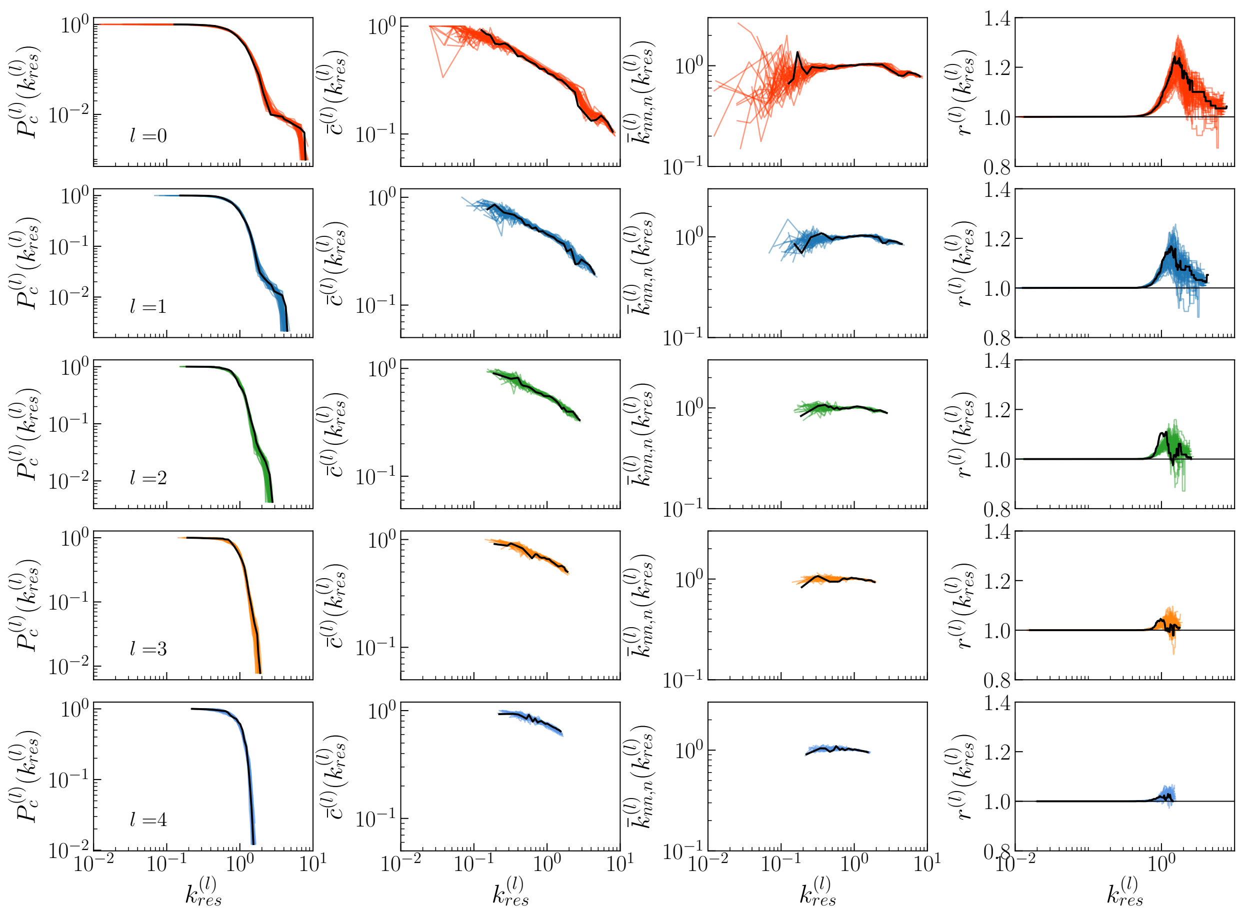

FIG. S30. **Subject No. 15 is a typical subject in HCP dataset.** Each column shows the complementary cumulative degree distribution, degree dependent clustering coefficient, degree-degree correlations and rich club coefficient. The degrees have been rescaled by the internal average degree of the corresponding layer $k_{res}^{(l)} = k^{(l)}/\langle k^{(l)}\rangle$. Different lines correspond to different subject in each cohort. The results for subject No. 15 have been highlighted in black color.

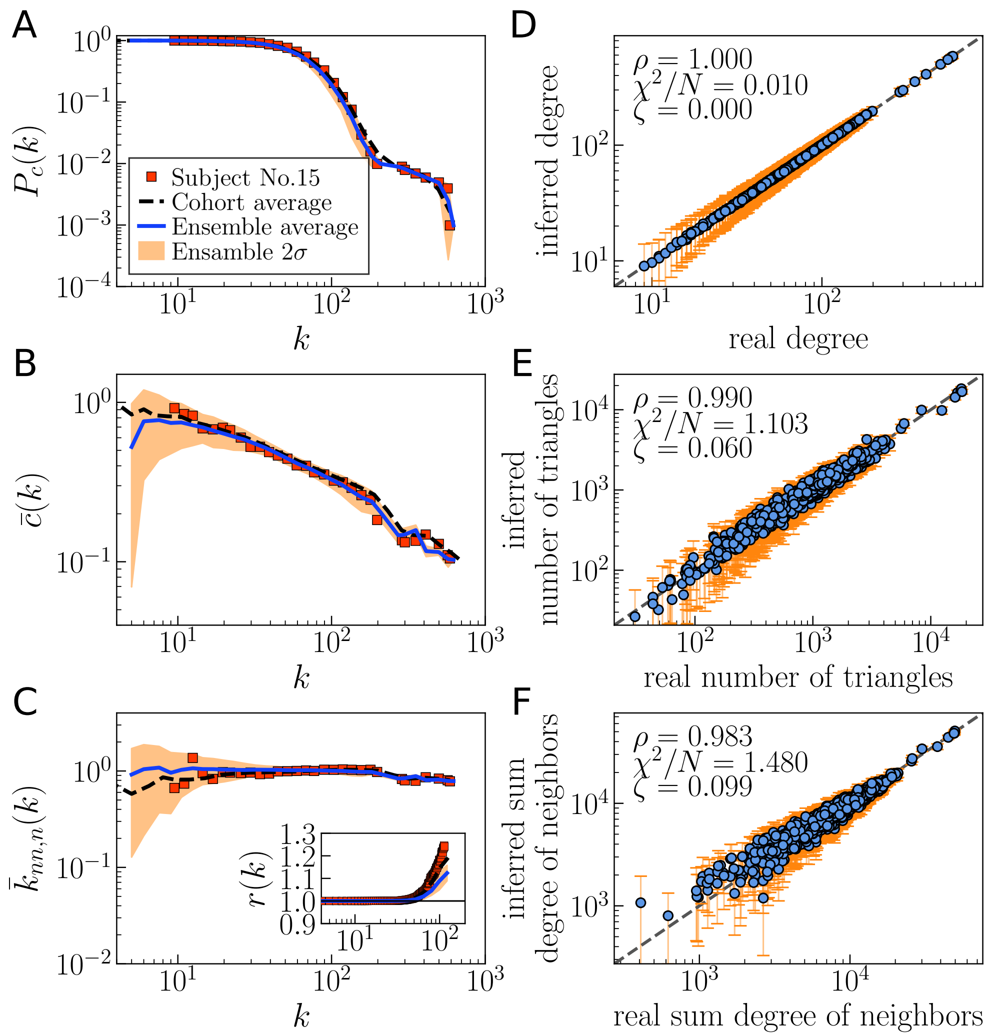

FIG. S31. **Network properties of $l = 0$ as compared to model predictions for HCP subject No. 15**. (A) Complementary cumulative degree distribution, (B) custering spectrum, (C) average nearest neighbors degree, and (C)-inset rich club coefficient. Red symbols correspond to subject No. 15, and black dashed lines to the group average across the 44 subjects in the sample. Blue lines correspond to the ensemble average over 100 synthetic networks generated with the $\mathbb{S}^1$ model using the coordinates and parameters inferred by Mercator [2], and the orange regions to the 2σ confidence interval around the expected value. (D)-(F) Comparison of predictions in our model (average over the ensemble of 100 synthetic networks) with real values for (D) degrees, (E) number of triangles, and (F) sum of degrees of neighbors. Error bars show the 2σ confidence interval around the expected values. Statistical tests for the goodness of fit — Pearson correlation coefficient ρ, χ^2 test is normalized by the number of nodes, and ζ score— are reported in each graph.

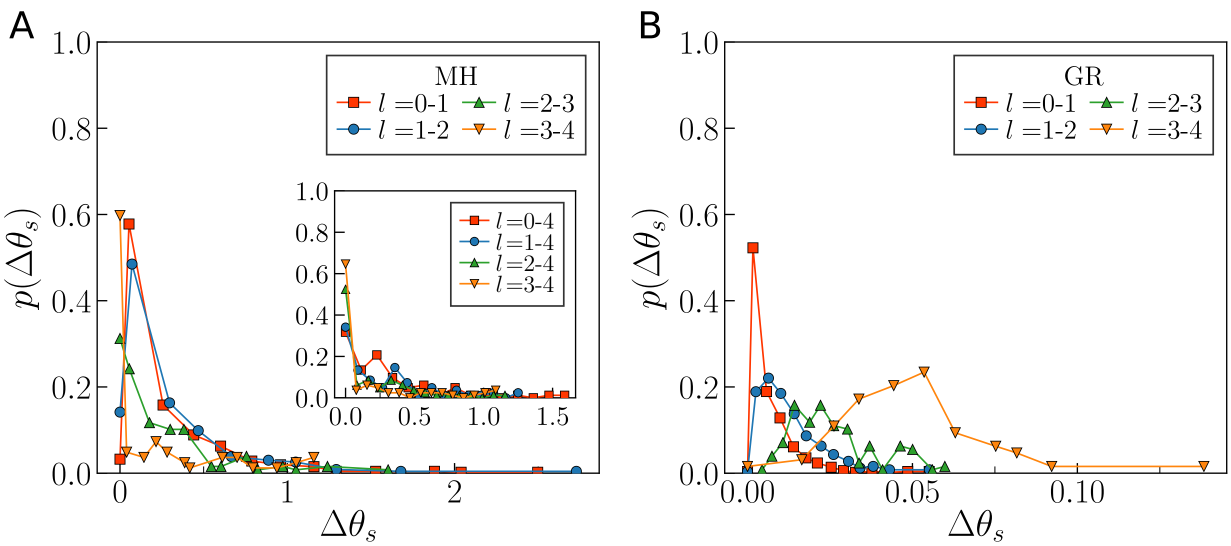

FIG. S32. Results for HCP subject No. 15. (*A*) and (*B*). Distribution $p(\Delta\theta_s)$ of average angular separation between subnodes of coarse-grained nodes from one layer to the next in MH and GR, respectively. The inset in (*A*) shows the distribution $p(\Delta\theta_s)$ from layer l to 4 in MH.

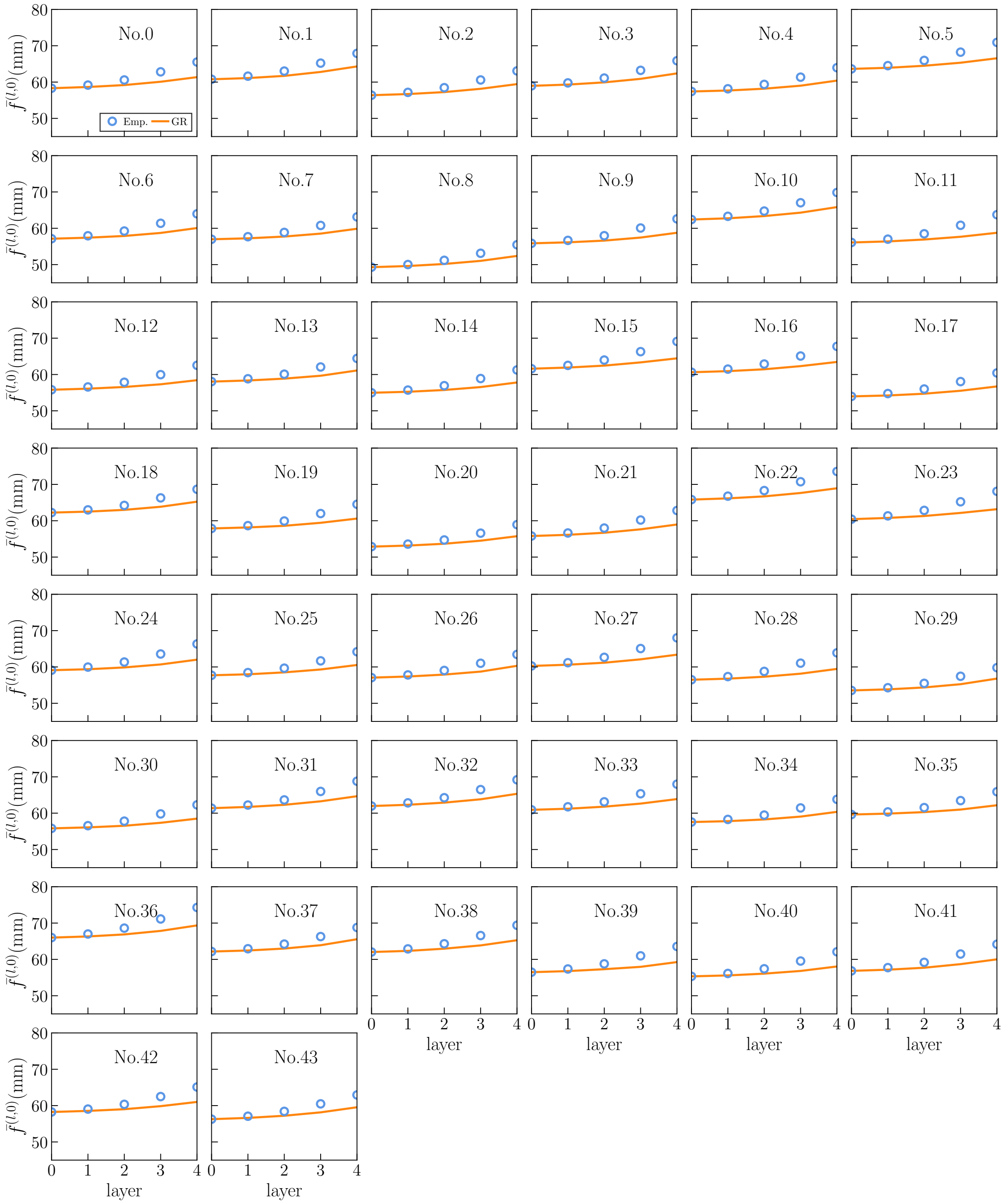

FIG. S33. Average fiber length $\bar{f}^{(l,0)}$ in layer 0 of links outside supernodes in layer l, where supernodes are defined by the anatomical coarse-graining in the empirical curve (symbols) or the similarity coarse-graining in the GR case (lines).

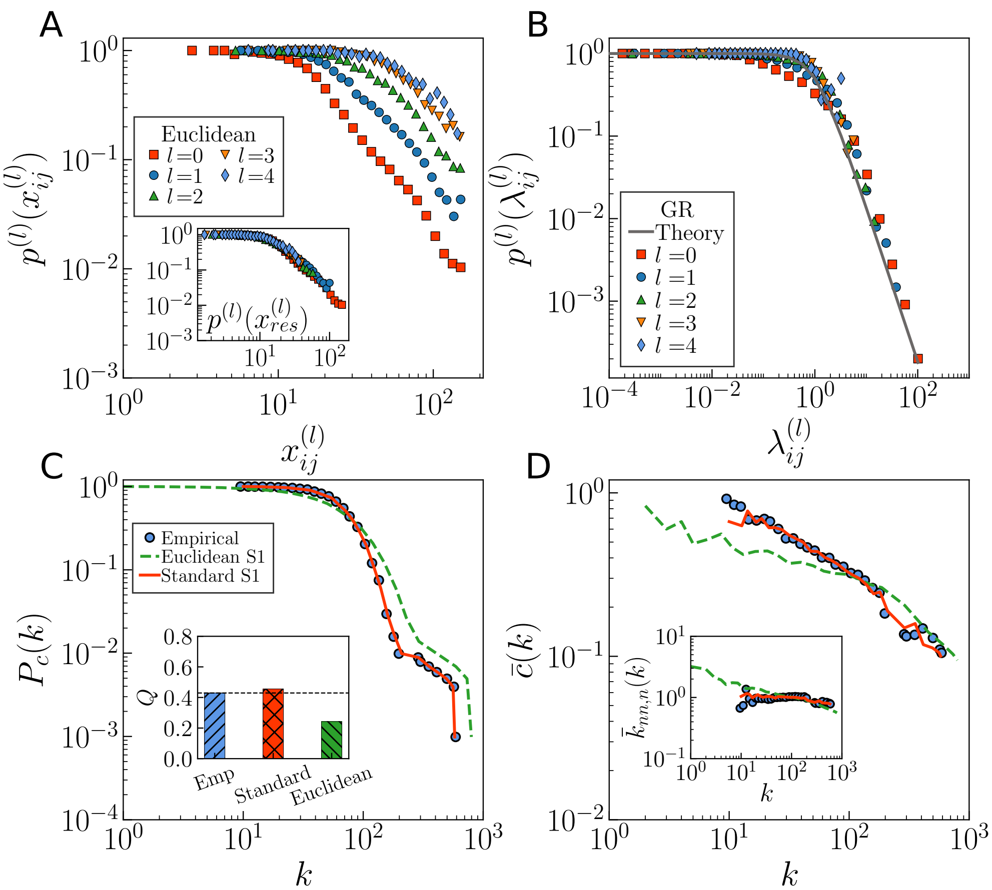

FIG. S34. **Empirical vs theoretical probability of connection.** Results for HCP subject No. 15. (*A*) Empirical connection probabilities $p^{(l)}(x_{ij}^{(l)})$ in Euclidean space. Euclidean distances x_{ij} are binned, and for each bin the ratio of the number of connected node pairs to the total number of pairs falling within the bin is shown. Inset shows the empirical connection probabilities $p^{(l)}(x_{res}^{(l)})$ as a function of rescale distances $x_{res}^{(l)} = x^{(l)}/a^{(l)}$ in the MH connectome, where the $a^{(l)} = [1.0, 1.5, 2.6, 3.8, 4.0]$ for different layer l. (*B*) Empirical versus theoretical connection probability $p^{(l)}(\lambda_{ij}^{(l)})$ in the GR shell as a function of hyperbolic distance $\lambda_{ij}^{(l)}$. (*C*) Complementary cumulative degree distribution $P_c(k)$. Modularity Q, as measured by the Louvain method, is shown in the inset. (*D*)Degree dependent clustering coefficient $\bar{c}(k)$. Inset: degree-degree correlations $\bar{k}_{nn,n}(k)$. The filled symbols correspond to the empirical connectome of Subject No. 15. Green dashed lines are generated using the $\mathbb{S}^1$ model with Euclidean distances($\beta = 2.31, \mu = 0.0030$), and red lines correspond to the standard $\mathbb{S}^1$ model ($\beta = 1.87, \mu = 0.0039$).

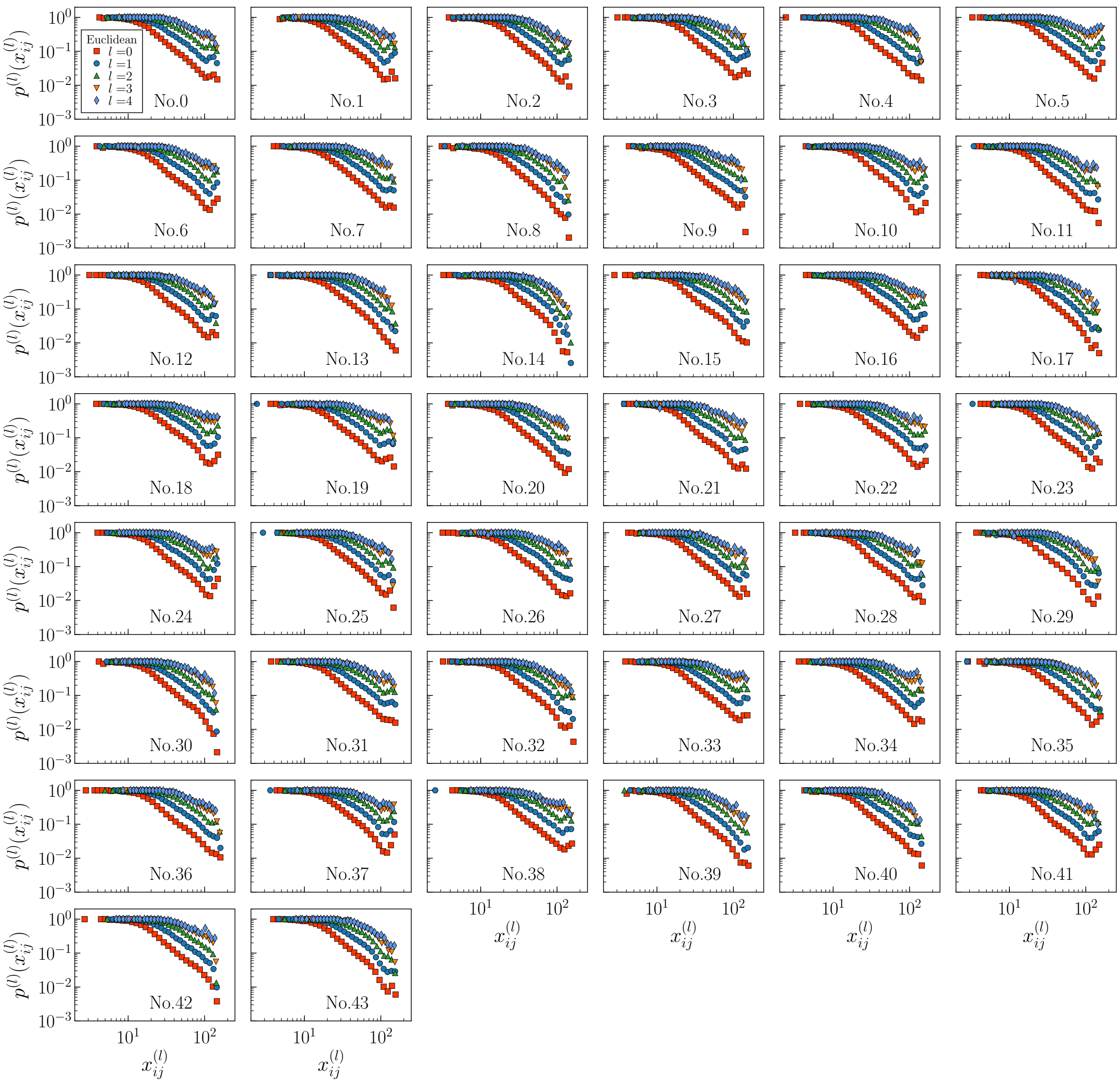

FIG. S35. Empirical connection probabilities $p^{(l)}(x_{ij}^{(l)})$ for each subject in HCP dataset. The whole range of Euclidean distances x_{ij} is binned, and for each bin the ratio of the number of connected connectome pairs to the total number of connectome pairs falling within this bin is shown.

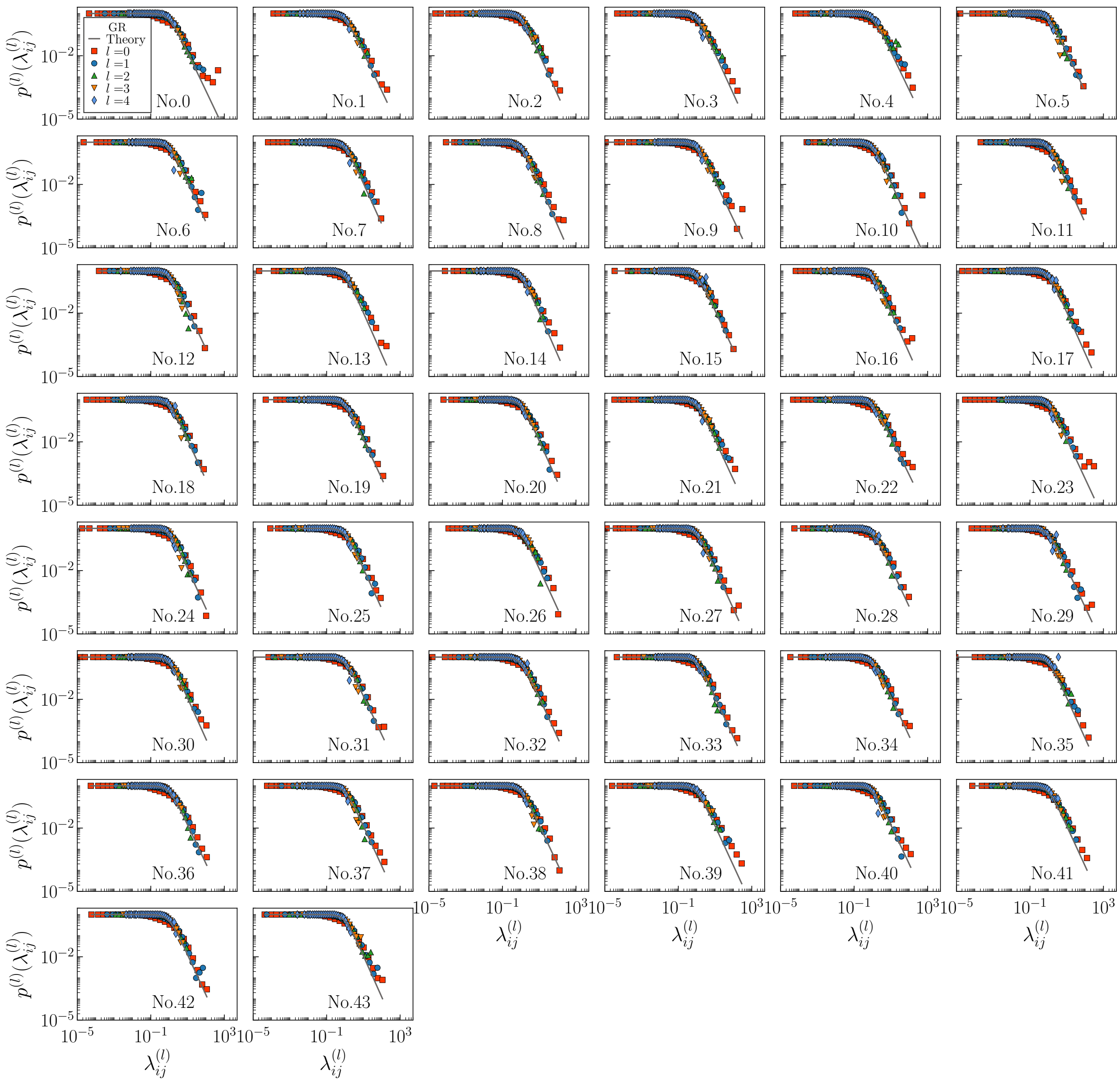

FIG. S36. Empirical versus theoretical connection probability $p^{(l)}(\lambda_{ij}^{(l)})$ within a given range of $\lambda_{ij}^{(l)}$ on GR shell for each subject in HCP dataset. Symbols are the connection probability of GR networks within a given range of $\lambda_{ij}^{(l)}$ and the gray lines shows the theoretical curves.

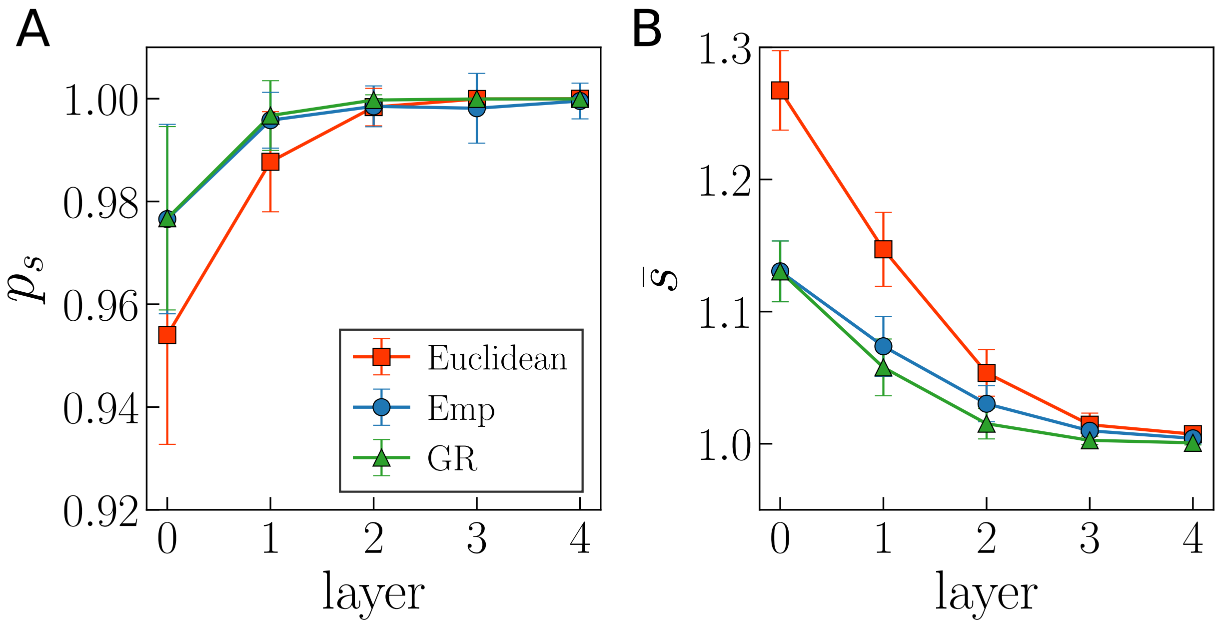

FIG. S37. **Navigability of MH and GR maps at different resolutions.** (A) average success rate (B) and average stretch for all HCP subjects. The error bars show the 2σ confidence interval around the expected values.

III. COMPARISON OF SIMILARITY DISTANCES WITH EUCLIDEAN DISTANCES AND HOMOPHILY

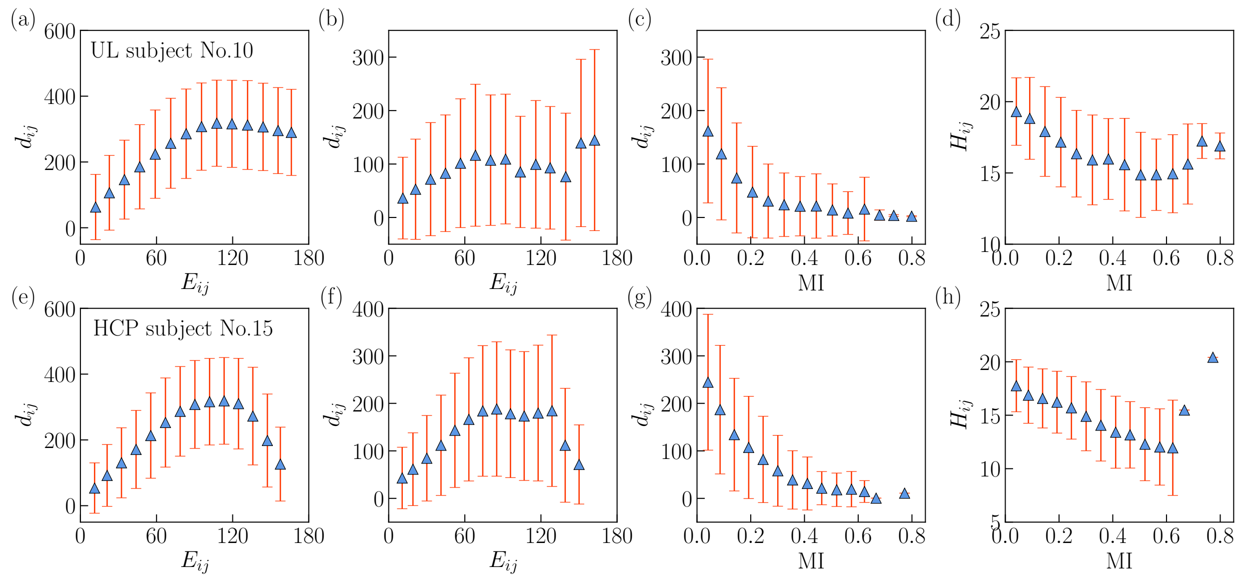

FIG. S38. **Similarity distance vs Euclidean distance and homophily.** (a)-(d) show results for subject No. 10 in the UL dataset and (e)-(h) for subject No. 15 in the HCP dataset. (a) and (e), Similarity distance ($d_{ij} = R\Delta\theta_{ij}$) vs Euclidean distance (E_{ij}) for all pairs of nodes in the connectome. (b) and (f), Similarity distance(d_{ij}) vs Euclidean(E_{ij}) for connected pairs of nodes. (c) and (g), similarity distance (d_{ij}) vs matching index (MI). (d) and (h) hyperbolic distance (H_{ij}) vs matching index (MI). The matching index is a normalized measure of overlap in two nodes' neighborhoods (ratio between the number of common neighbors and the total number of neighbors of the two discounting the pair), as defined in Ref. [3]. In each plot, we show a binned statistic with 15 equal-width bins. Each symbol shows the mean value in the bin and error bar indicates 1 standard deviation around the average value.

IV. STATISTICS FOR SUBJECTS IN THE UL AND THE HCP DATASETS

TABLE S1. Overview of the 40 connectomes in the UL dataeset. The number of nodes (N), the number of links (L), the density of links ($\rho_l = 2L/N(N-1)$), its average degree ($\langle k \rangle = 2L/N$), the average local clustering coefficient ($\langle c \rangle$), the average fiber length ($f^{(l)}$ (mm)), and corresponding ± 1 standard error interval around the mean (SEM), the assortativity coefficient (r_c), the modularity (Q), the number of the communities (Nc), and the hyperbolic embedding parameter β and μ.

Subject	Layer	N	L	ρ_l	$\langle k \rangle \pm$ SEM	$\langle c \rangle \pm$ SEM	$f^{(l)} \pm$ SEM	r_c	Q	N_c	β	μ
No. 0	0	1009	14470	0.03	28.68±0.669	0.43±0.005	65.82±43.675	-0.016	0.55	5	1.96	0.011
	1	461	7177	0.07	31.14±0.825	0.47±0.006	68.82±44.082	0.005	0.48	5	2.22	0.011
	2	233	3586	0.13	30.78±0.937	0.50±0.008	72.74±45.021	0.031	0.42	5	2.41	0.012
	3	128	1744	0.21	27.25±1.031	0.56±0.012	74.80±46.285	0.040	0.32	3	2.63	0.014
	4	82	962	0.29	23.46±1.102	0.62±0.016	74.39±47.996	0.021	0.31	3	3.08	0.018
No. 1	0	1010	14406	0.03	28.53±0.729	0.42±0.005	66.38±44.958	-0.003	0.52	5	1.93	0.011
	1	461	7195	0.07	31.21±0.944	0.46±0.006	70.46±45.278	0.003	0.45	6	2.11	0.011
	2	233	3893	0.14	33.42±1.158	0.50±0.008	76.44±46.113	-0.012	0.35	3	2.26	0.011
	3	128	1992	0.25	31.12±1.257	0.57±0.010	80.33±47.629	-0.039	0.28	3	2.48	0.012
	4	82	1129	0.34	27.54±1.328	0.63±0.013	83.11±50.287	-0.080	0.23	4	2.78	0.015
No. 2	0	1014	13671	0.03	26.96±0.638	0.44±0.005	62.45±42.759	0.008	0.58	6	2.00	0.012
	1	462	6833	0.06	29.58±0.812	0.46±0.006	67.32±43.889	0.027	0.50	5	2.19	0.012
	2	233	3599	0.13	30.89±0.954	0.49±0.008	73.01±45.070	0.056	0.42	4	2.41	0.012
	3	128	1806	0.22	28.22±1.031	0.55±0.011	74.95±45.415	0.043	0.34	4	2.63	0.014
	4	82	978	0.29	23.85±1.131	0.63±0.015	75.12±47.046	-0.035	0.30	3	3.23	0.018
No. 3	0	1011	12991	0.03	25.70±0.648	0.41±0.005	61.51±43.188	0.003	0.54	7	1.89	0.012
	1	462	6642	0.06	28.75±0.842	0.45±0.006	64.32±43.813	0.029	0.46	4	2.08	0.011
	2	233	3581	0.13	30.74±1.016	0.49±0.008	69.07±45.923	0.046	0.40	5	2.26	0.012
	3	128	1888	0.23	29.50±1.135	0.55±0.011	74.38±49.242	0.049	0.31	3	2.48	0.013
	4	82	1074	0.32	26.20±1.302	0.63±0.015	79.49±53.949	0.005	0.23	2	2.78	0.015
No. 4	0	1014	15879	0.03	31.32±0.778	0.41±0.005	72.32±50.544	0.014	0.51	6	1.85	0.009
	1	462	7896	0.07	34.18±0.999	0.46±0.006	76.98±52.410	0.036	0.44	4	2.08	0.010
	2	233	4069	0.15	34.93±1.165	0.50±0.008	81.56±53.710	0.057	0.33	4	2.26	0.010
	3	128	2077	0.26	32.45±1.254	0.57±0.010	83.79±54.812	0.042	0.29	3	2.63	0.012
	4	82	1177	0.35	28.71±1.408	0.66±0.013	86.85±58.033	-0.027	0.24	3	2.93	0.014
No. 5	0	1014	14340	0.03	28.28±0.698	0.41±0.005	65.30±42.579	-0.013	0.54	5	1.89	0.011
	1	462	7175	0.07	31.06±0.900	0.45±0.006	69.23±43.346	-0.003	0.44	5	2.11	0.011
	2	233	3719	0.14	31.92±1.043	0.48±0.007	73.64±43.925	0.008	0.38	4	2.22	0.011
	3	128	1919	0.24	29.98±1.141	0.55±0.009	76.85±45.317	0.004	0.30	4	2.48	0.013
	4	82	1137	0.34	27.73±1.260	0.63±0.012	79.36±47.597	-0.021	0.25	3	2.78	0.014
No. 6	0	1013	12660	0.02	25.00±0.653	0.44±0.005	57.01±38.389	-0.012	0.59	6	1.96	0.013
	1	462	6519	0.06	28.22±0.865	0.48±0.007	61.16±39.025	-0.006	0.50	5	2.26	0.013
	2	233	3375	0.12	28.97±1.009	0.53±0.009	64.87±39.810	-0.014	0.43	4	2.52	0.013
	3	128	1712	0.21	26.75±1.080	0.57±0.012	68.31±41.896	-0.014	0.33	3	2.78	0.015
	4	82	1000	0.30	24.39±1.196	0.62±0.015	71.27±45.710	-0.017	0.26	4	3.00	0.017
No. 7	0	1014	13474	0.03	26.58±0.702	0.42±0.005	64.45±43.876	-0.023	0.56	6	1.89	0.011
	1	462	6955	0.07	30.11±0.902	0.46±0.006	68.69±45.530	-0.012	0.47	4	2.11	0.011
	2	233	3651	0.14	31.34±1.019	0.50±0.007	73.55±47.353	-0.006	0.40	3	2.41	0.012
	3	128	1934	0.24	30.22±1.079	0.56±0.010	78.72±50.132	0.000	0.32	4	2.63	0.013
	4	82	1076	0.32	26.24±1.201	0.62±0.014	81.38±53.156	-0.041	0.26	3	2.86	0.015

Subject	Layer	N	L	ρ_l	$\langle k\rangle \pm$ SEM	$\langle c\rangle \pm$ SEM	$f^{(l)} \pm$ SEM	r_c	Q	N_c	β	μ
No. 8	0	1002	13910	0.03	27.76±0.652	0.41±0.005	67.65±45.004	0.017	0.53	5	1.89	0.011
	1	462	7041	0.07	30.48±0.845	0.44±0.007	72.07±46.547	0.051	0.43	4	2.04	0.011
	2	233	3723	0.14	31.96±1.053	0.49±0.008	76.47±47.376	0.067	0.36	4	2.19	0.011
	3	128	1960	0.24	30.62±1.177	0.54±0.010	82.08±50.685	0.056	0.28	3	2.41	0.012
	4	82	1124	0.34	27.41±1.317	0.62±0.013	85.38±54.262	0.005	0.20	4	2.48	0.014
No. 9	0	1010	13496	0.03	26.72±0.632	0.41±0.005	63.02±41.763	-0.007	0.54	5	1.89	0.011
	1	462	6658	0.06	28.82±0.802	0.44±0.006	66.13±42.236	0.000	0.47	4	2.08	0.011
	2	233	3532	0.13	30.32±0.938	0.48±0.008	71.00±43.525	0.010	0.37	3	2.26	0.012
	3	128	1774	0.22	27.72±1.022	0.54±0.011	74.12±45.548	0.004	0.31	3	2.56	0.014
	4	82	977	0.29	23.83±1.147	0.61±0.016	76.36±47.999	-0.052	0.27	4	2.78	0.017
No. 10	0	1014	15222	0.03	30.02±0.675	0.41±0.005	71.29±48.238	0.004	0.57	6	1.96	0.010
	1	462	7414	0.07	32.10±0.855	0.46±0.006	75.74±49.299	0.019	0.48	4	2.19	0.011
	2	233	3754	0.14	32.22±0.943	0.49±0.008	79.97±50.254	0.043	0.39	4	2.34	0.011
	3	128	1954	0.24	30.53±1.037	0.54±0.010	85.00±52.882	0.060	0.32	3	2.60	0.013
	4	82	1102	0.33	26.88±1.213	0.62±0.013	87.45±57.162	0.015	0.26	3	2.78	0.015
No. 11	0	1013	14695	0.03	29.01±0.702	0.42±0.005	63.42±42.951	-0.030	0.54	6	1.93	0.011
	1	462	7577	0.07	32.80±0.891	0.46±0.007	68.64±44.197	-0.021	0.48	4	2.19	0.011
	2	233	3872	0.14	33.24±1.000	0.51±0.009	72.30±44.861	-0.010	0.43	3	2.48	0.011
	3	128	2023	0.25	31.61±1.053	0.58±0.011	75.29±46.142	0.013	0.36	3	2.93	0.013
	4	82	1088	0.33	26.54±1.146	0.64±0.015	74.97±47.933	0.002	0.32	3	3.45	0.016
No. 12	0	1001	13933	0.03	27.84±0.663	0.43±0.005	74.40±57.807	0.044	0.57	7	1.96	0.011
	1	460	7112	0.07	30.92±0.870	0.46±0.006	80.62±60.153	0.080	0.46	5	2.19	0.011
	2	233	3655	0.14	31.37±1.031	0.50±0.008	86.96±62.239	0.081	0.38	4	2.34	0.012
	3	128	1875	0.23	29.30±1.174	0.58±0.011	92.78±66.547	0.071	0.30	3	2.78	0.014
	4	82	1049	0.32	25.59±1.368	0.65±0.014	96.71±71.598	-0.014	0.26	3	3.08	0.016
No. 13	0	1013	14409	0.03	28.45±0.771	0.44±0.005	64.03±43.296	-0.011	0.54	6	1.93	0.011
	1	462	7409	0.07	32.07±0.994	0.47±0.006	68.46±43.863	0.002	0.46	4	2.11	0.010
	2	233	3845	0.14	33.00±1.143	0.51±0.008	72.39±43.825	0.009	0.38	5	2.34	0.011
	3	128	2009	0.25	31.39±1.275	0.57±0.010	75.90±45.009	-0.027	0.30	4	2.63	0.012
	4	82	1163	0.35	28.37±1.400	0.65±0.014	77.41±46.731	-0.087	0.24	4	2.78	0.014
No. 14	0	1013	14959	0.03	29.53±0.713	0.43±0.005	67.63±45.728	0.001	0.53	5	1.96	0.011
	1	462	7382	0.07	31.96±0.890	0.46±0.007	72.39±47.018	0.011	0.45	4	2.19	0.011
	2	233	3808	0.14	32.69±1.025	0.49±0.008	76.85±47.985	0.013	0.38	3	2.34	0.011
	3	128	1952	0.24	30.50±1.104	0.55±0.010	81.09±50.685	0.027	0.33	3	2.63	0.013
	4	82	1071	0.32	26.12±1.264	0.63±0.014	84.18±54.978	0.014	0.26	3	3.08	0.016
No. 15	0	1007	16208	0.03	32.19±0.749	0.43±0.005	76.68±53.253	0.001	0.54	5	1.96	0.010
	1	462	8003	0.08	34.65±0.966	0.47±0.006	83.08±55.373	0.022	0.46	3	2.19	0.010
	2	233	4102	0.15	35.21±1.119	0.51±0.008	88.97±57.472	0.043	0.40	4	2.41	0.011
	3	128	2092	0.26	32.69±1.202	0.58±0.011	94.04±60.183	0.037	0.34	3	2.78	0.012
	4	82	1150	0.35	28.05±1.384	0.67±0.014	97.63±65.524	-0.025	0.27	3	3.26	0.015
No. 16	0	1014	14539	0.03	28.68±0.738	0.42±0.005	68.14±46.715	-0.004	0.55	5	1.89	0.010
	1	462	7352	0.07	31.83±0.958	0.46±0.006	71.78±47.023	0.004	0.46	4	2.11	0.011
	2	233	3801	0.14	32.63±1.124	0.50±0.008	76.22±48.008	0.014	0.38	3	2.34	0.011
	3	128	1999	0.25	31.23±1.259	0.57±0.010	81.28±50.587	0.029	0.29	3	2.48	0.012
	4	82	1198	0.36	29.22±1.448	0.65±0.012	86.73±55.434	0.015	0.22	3	2.78	0.014
No. 17	0	1014	13901	0.03	27.42±0.683	0.43±0.005	62.44±43.569	-0.011	0.55	6	1.96	0.011
	1	462	7030	0.07	30.43±0.861	0.46±0.006	66.20±43.898	-0.005	0.47	4	2.19	0.011
	2	233	3642	0.13	31.26±0.987	0.50±0.009	70.61±44.926	0.001	0.39	3	2.34	0.012
	3	128	1821	0.22	28.45±1.061	0.55±0.011	74.07±46.623	0.017	0.33	3	2.63	0.014
	4	82	994	0.30	24.24±1.166	0.61±0.015	73.95±47.219	-0.015	0.26	4	2.78	0.017
No. 18	0	1014	12418	0.02	24.49±0.653	0.43±0.005	57.36±40.798	-0.029	0.56	5	1.96	0.013
	1	462	6510	0.06	28.18±0.837	0.47±0.007	62.05±41.924	-0.024	0.51	4	2.22	0.012
	2	233	3497	0.13	30.02±0.969	0.51±0.008	67.22±42.933	-0.014	0.42	3	2.48	0.013
	3	128	1847	0.23	28.86±1.052	0.56±0.011	71.59±44.098	-0.025	0.34	4	2.78	0.014
	4	82	1008	0.30	24.59±1.140	0.62±0.015	71.06±45.854	-0.044	0.26	2	3.08	0.017

Subject	Layer	N	L	ρ_l	$\langle k \rangle \pm$ SEM	$\langle c \rangle \pm$ SEM	$f^{(l)} \pm$ SEM	r_c	Q	N_c	β	μ
No. 19	0	1011	14883	0.03	29.44±0.708	0.40±0.005	69.15±46.830	0.017	0.53	6	1.85	0.010
	1	462	7633	0.07	33.04±0.932	0.44±0.007	74.46±49.017	0.033	0.45	4	2.04	0.010
	2	233	4042	0.15	34.70±1.130	0.49±0.008	80.35±51.407	0.034	0.36	4	2.22	0.010
	3	128	2032	0.25	31.75±1.246	0.56±0.010	84.05±54.276	0.033	0.27	3	2.48	0.012
	4	82	1117	0.34	27.24±1.412	0.64±0.013	86.97±58.517	-0.000	0.23	3	2.48	0.014
No. 20	0	1011	13201	0.03	26.11±0.654	0.42±0.005	62.04±42.881	-0.013	0.53	5	1.89	0.011
	1	462	6749	0.06	29.22±0.852	0.47±0.007	66.28±43.375	-0.008	0.49	4	2.19	0.012
	2	233	3589	0.13	30.81±0.967	0.49±0.008	70.82±44.369	0.020	0.40	4	2.34	0.012
	3	128	1816	0.22	28.38±1.037	0.55±0.012	72.81±44.735	0.021	0.33	4	2.63	0.014
	4	82	975	0.29	23.78±1.170	0.62±0.016	74.04±46.391	0.002	0.26	2	2.93	0.017
No. 21	0	1012	12004	0.02	23.72±0.636	0.47±0.006	55.45±38.946	-0.044	0.59	6	2.08	0.014
	1	462	6241	0.06	27.02±0.806	0.50±0.007	59.01±38.968	-0.022	0.52	6	2.37	0.014
	2	233	3200	0.12	27.47±0.923	0.53±0.009	62.35±39.676	-0.020	0.42	3	2.63	0.014
	3	128	1576	0.19	24.62±0.967	0.56±0.013	64.41±41.296	0.008	0.37	3	2.78	0.016
	4	82	859	0.26	20.95±1.068	0.62±0.017	65.83±43.853	0.022	0.33	3	3.04	0.020
No. 22	0	1014	13519	0.03	26.66±0.657	0.42±0.005	64.29±44.784	-0.013	0.54	6	1.93	0.011
	1	462	6669	0.06	28.87±0.819	0.46±0.006	67.28±45.278	0.002	0.50	5	2.17	0.012
	2	233	3429	0.13	29.43±0.941	0.49±0.008	71.49±45.832	0.015	0.43	4	2.34	0.012
	3	128	1758	0.22	27.47±0.982	0.55±0.011	74.21±47.045	0.023	0.36	3	2.63	0.014
	4	82	989	0.30	24.12±1.079	0.62±0.014	76.73±49.833	-0.028	0.32	3	3.15	0.017
No. 23	0	1014	14709	0.03	29.01±0.701	0.43±0.005	70.15±50.763	0.006	0.57	5	1.96	0.011
	1	462	7147	0.07	30.94±0.887	0.47±0.006	75.22±52.027	0.017	0.48	4	2.19	0.011
	2	233	3783	0.14	32.47±1.059	0.51±0.008	81.64±53.650	0.036	0.40	4	2.41	0.011
	3	128	1864	0.23	29.12±1.148	0.57±0.012	85.15±56.933	0.022	0.33	4	2.71	0.014
	4	82	1031	0.31	25.15±1.288	0.65±0.015	85.76±59.914	-0.047	0.28	3	3.23	0.017
No. 24	0	1014	13661	0.03	26.94±0.660	0.40±0.005	63.30±40.449	-0.005	0.54	5	1.85	0.011
	1	462	6868	0.06	29.73±0.849	0.45±0.006	66.30±40.190	0.009	0.47	4	2.08	0.011
	2	233	3587	0.13	30.79±0.970	0.48±0.008	69.28±40.086	0.031	0.40	4	2.22	0.011
	3	128	1858	0.23	29.03±1.072	0.53±0.010	72.08±42.551	0.029	0.33	3	2.41	0.013
	4	82	1033	0.31	25.20±1.216	0.61±0.014	73.88±45.514	-0.036	0.28	3	2.78	0.016
No. 25	0	1013	14802	0.03	29.22±0.737	0.44±0.005	69.53±50.198	0.015	0.52	6	1.96	0.011
	1	462	7428	0.07	32.16±0.979	0.47±0.006	75.38±52.684	0.012	0.43	5	2.15	0.011
	2	233	3893	0.14	33.42±1.185	0.51±0.008	81.90±55.150	-0.002	0.36	5	2.26	0.011
	3	128	2039	0.25	31.86±1.297	0.56±0.011	88.28±59.237	-0.010	0.27	4	2.48	0.012
	4	82	1200	0.36	29.27±1.422	0.64±0.014	93.61±63.824	-0.050	0.20	3	2.63	0.013
No. 26	0	1013	12942	0.03	25.55±0.673	0.44±0.005	56.78±40.265	-0.020	0.55	5	1.96	0.012
	1	462	6709	0.06	29.04±0.857	0.47±0.007	61.63±41.598	0.000	0.49	5	2.19	0.012
	2	233	3445	0.13	29.57±0.995	0.51±0.009	66.80±43.586	0.009	0.41	4	2.41	0.013
	3	128	1732	0.21	27.06±1.056	0.55±0.012	69.83±46.121	0.004	0.31	3	2.63	0.014
	4	82	975	0.29	23.78±1.176	0.62±0.015	72.24±50.272	-0.008	0.26	3	2.93	0.017
No. 27	0	1014	12483	0.02	24.62±0.619	0.40±0.005	60.51±41.126	-0.004	0.51	5	1.85	0.012
	1	462	6352	0.06	27.50±0.798	0.44±0.006	62.96±41.281	0.009	0.46	4	2.08	0.012
	2	233	3308	0.12	28.39±0.946	0.47±0.008	67.63±42.449	0.018	0.40	5	2.22	0.012
	3	128	1766	0.22	27.59±1.051	0.54±0.011	71.06±44.524	0.034	0.33	4	2.48	0.014
	4	82	981	0.30	23.93±1.179	0.61±0.015	73.43±47.249	-0.021	0.29	3	2.78	0.017
No. 28	0	1012	14812	0.03	29.27±0.774	0.43±0.005	71.18±52.646	0.000	0.53	6	1.93	0.010
	1	462	7440	0.07	32.21±1.024	0.48±0.007	76.57±54.983	-0.001	0.44	5	2.19	0.011
	2	233	3995	0.15	34.29±1.243	0.52±0.009	84.86±59.155	-0.012	0.35	4	2.34	0.011
	3	128	2039	0.25	31.86±1.333	0.58±0.012	90.38±61.600	-0.026	0.27	3	2.56	0.012
	4	82	1151	0.35	28.07±1.442	0.65±0.015	95.31±65.566	-0.039	0.22	3	2.78	0.014
No. 29	0	1012	13601	0.03	26.88±0.670	0.43±0.005	62.88±41.839	-0.016	0.58	6	1.96	0.012
	1	462	6998	0.07	30.29±0.852	0.46±0.006	67.22±42.522	-0.010	0.48	4	2.19	0.011
	2	233	3694	0.14	31.71±0.952	0.50±0.008	71.09±42.622	-0.000	0.39	3	2.41	0.012
	3	128	1813	0.22	28.33±1.011	0.57±0.011	72.42±43.307	0.021	0.36	3	2.78	0.014
	4	82	966	0.29	23.56±1.116	0.64±0.016	73.09±45.577	-0.002	0.33	3	3.38	0.018

Subject	Layer	N	L	ρ_l	$\langle k \rangle \pm$ SEM	$\langle c \rangle \pm$ SEM	$f^{(l)} \pm$ SEM	r_c	Q	N_c	β	μ
No. 30	0	1013	14177	0.03	27.99±0.711	0.43±0.005	67.36±47.975	-0.008	0.55	5	1.96	0.011
	1	462	7246	0.07	31.37±0.911	0.46±0.006	72.35±49.696	0.022	0.47	5	2.15	0.011
	2	233	3778	0.14	32.43±1.067	0.50±0.008	77.23±50.352	0.016	0.38	3	2.32	0.011
	3	128	1960	0.24	30.62±1.130	0.56±0.011	81.62±52.396	0.028	0.33	3	2.63	0.013
	4	82	1131	0.34	27.59±1.287	0.65±0.014	84.91±56.072	-0.004	0.28	3	3.08	0.015
No. 31	0	1014	15641	0.03	30.85±0.760	0.41±0.005	71.71±51.033	0.014	0.55	6	1.85	0.009
	1	462	7983	0.07	34.56±0.994	0.46±0.006	77.72±54.036	0.026	0.47	4	2.11	0.010
	2	233	4220	0.16	36.22±1.132	0.50±0.007	83.75±57.298	0.051	0.38	4	2.34	0.010
	3	128	2141	0.26	33.45±1.216	0.56±0.010	88.56±59.873	0.032	0.30	3	2.56	0.011
	4	82	1231	0.37	30.02±1.386	0.63±0.012	94.13±65.808	0.002	0.21	3	2.48	0.013
No. 32	0	1013	12875	0.03	25.42±0.673	0.43±0.005	62.54±46.293	-0.001	0.57	6	1.96	0.012
	1	462	6409	0.06	27.74±0.867	0.48±0.007	66.40±47.918	0.009	0.48	6	2.22	0.013
	2	233	3351	0.12	28.76±1.052	0.50±0.009	73.08±51.161	0.034	0.37	4	2.26	0.012
	3	128	1795	0.22	28.05±1.174	0.55±0.011	78.25±53.290	0.028	0.28	4	2.41	0.013
	4	82	1031	0.31	25.15±1.271	0.62±0.015	80.85±55.859	0.005	0.25	3	2.78	0.016
No. 33	0	1014	14510	0.03	28.62±0.714	0.44±0.005	66.73±46.049	-0.008	0.53	5	1.96	0.011
	1	462	7427	0.07	32.15±0.929	0.47±0.007	71.73±46.530	0.002	0.46	4	2.19	0.011
	2	233	3876	0.14	33.27±1.066	0.50±0.008	77.93±47.755	0.009	0.38	3	2.34	0.011
	3	128	2004	0.25	31.31±1.138	0.56±0.010	81.38±49.065	0.016	0.32	3	2.63	0.012
	4	82	1106	0.33	26.98±1.292	0.64±0.015	82.64±51.067	-0.043	0.26	3	3.08	0.015
No. 34	0	1012	14344	0.03	28.35±0.706	0.41±0.005	69.04±45.713	-0.001	0.53	5	1.85	0.010
	1	461	7292	0.07	31.64±0.904	0.45±0.006	73.20±45.988	0.020	0.47	5	2.04	0.010
	2	233	3814	0.14	32.74±1.025	0.48±0.007	78.36±47.041	0.035	0.38	4	2.19	0.011
	3	128	1921	0.24	30.02±1.047	0.54±0.011	81.64±48.906	0.024	0.31	4	2.56	0.013
	4	82	1053	0.32	25.68±1.197	0.63±0.015	81.33±50.079	-0.015	0.28	3	3.08	0.016
No. 35	0	1009	12460	0.02	24.70±0.665	0.42±0.005	59.69±41.052	-0.001	0.54	6	1.89	0.012
	1	462	6467	0.06	28.00±0.867	0.46±0.006	64.31±42.744	0.012	0.45	5	2.11	0.012
	2	233	3439	0.13	29.52±1.035	0.50±0.008	69.39±43.860	0.012	0.39	5	2.34	0.012
	3	128	1808	0.22	28.25±1.136	0.55±0.010	74.81±46.898	0.015	0.31	3	2.48	0.013
	4	82	1064	0.32	25.95±1.276	0.61±0.014	79.37±50.431	-0.040	0.23	3	2.48	0.015
No. 36	0	1014	13978	0.03	27.57±0.693	0.43±0.005	66.11±45.586	-0.011	0.55	6	1.96	0.011
	1	462	7053	0.07	30.53±0.891	0.47±0.007	70.12±46.290	-0.006	0.49	4	2.19	0.011
	2	233	3775	0.14	32.40±1.052	0.50±0.008	74.40±46.276	-0.004	0.40	3	2.34	0.011
	3	128	1915	0.24	29.92±1.157	0.55±0.011	77.52±48.562	0.009	0.32	3	2.48	0.013
	4	82	1083	0.33	26.41±1.288	0.63±0.015	78.34±51.617	-0.034	0.22	2	2.93	0.016
No. 37	0	1014	14282	0.03	28.17±0.693	0.40±0.005	64.59±43.099	-0.004	0.54	5	1.88	0.011
	1	462	7216	0.07	31.24±0.898	0.45±0.006	68.52±43.720	-0.006	0.44	4	2.11	0.011
	2	233	3783	0.14	32.47±1.036	0.49±0.008	73.59±44.947	-0.009	0.39	4	2.30	0.011
	3	128	1940	0.24	30.31±1.132	0.55±0.010	77.60±47.272	-0.024	0.27	3	2.52	0.013
	4	82	1105	0.33	26.95±1.282	0.62±0.013	82.25±52.116	-0.044	0.25	3	2.71	0.015
No. 38	0	1011	14001	0.03	27.70±0.679	0.43±0.005	68.35±47.067	0.025	0.53	6	1.93	0.011
	1	462	7129	0.07	30.86±0.909	0.46±0.006	74.59±49.171	0.040	0.45	5	2.08	0.011
	2	233	3788	0.14	32.52±1.086	0.49±0.008	80.76±51.217	0.045	0.38	4	2.26	0.011
	3	128	1952	0.24	30.50±1.235	0.55±0.010	86.29±54.329	0.033	0.28	4	2.34	0.012
	4	82	1115	0.34	27.20±1.378	0.62±0.012	90.79±59.115	-0.019	0.21	4	2.48	0.014
No. 39	0	1013	12599	0.02	24.87±0.695	0.44±0.005	60.71±40.883	-0.031	0.56	5	1.96	0.013
	1	462	6468	0.06	28.00±0.902	0.47±0.007	63.92±40.596	-0.028	0.49	5	2.19	0.012
	2	233	3433	0.13	29.47±1.053	0.50±0.008	68.99±41.314	-0.027	0.42	5	2.34	0.012
	3	128	1808	0.22	28.25±1.162	0.57±0.011	72.21±42.214	-0.027	0.30	3	2.71	0.014
	4	82	1026	0.31	25.02±1.262	0.63±0.015	74.63±44.861	-0.075	0.25	3	2.93	0.016

TABLE S2. Overview of the 44 connectomes in the HCP dataeset. The number of nodes (N), the number of links (L), the density of links ($\rho_l = 2L/N(N-1)$), its average degree ($\langle k \rangle = 2L/N$), the average local clustering coefficient ($\langle c \rangle$), the average fiber length ($f^{(l)}$ (mm)), and corresponding ±1 standard error interval around the mean (SEM), the assortativity coefficient (r_c), the modularity (Q), the number of the communities (Nc), and the hyperbolic embedding parameter β and μ.

Subject	Layer	N	L	ρ_l	$\langle k \rangle \pm$ SEM	$\langle c \rangle \pm$ SEM	$f^{(l)} \pm$ SEM	r_c	Q	N_c	β	μ
No. 0	0	1014	37910	0.07	74.77±1.509	0.41±0.004	58.31±43.175	-0.021	0.40	5	1.83	0.004
	1	462	18024	0.17	78.03±1.758	0.47±0.004	66.92±44.813	-0.005	0.33	3	2.02	0.004
	2	233	8540	0.32	73.30±1.765	0.55±0.006	73.51±45.896	-0.016	0.25	3	2.19	0.005
	3	128	3871	0.48	60.48±1.617	0.65±0.007	78.20±47.528	-0.052	0.19	3	3.02	0.007
	4	82	1873	0.56	45.68±1.591	0.74±0.010	77.00±49.433	-0.098	0.15	2	3.58	0.010
No. 1	0	1014	39210	0.08	77.34±1.661	0.42±0.004	60.77±44.773	-0.036	0.39	3	1.83	0.004
	1	462	18776	0.18	81.28±1.910	0.48±0.005	69.51±45.948	-0.035	0.33	3	2.00	0.004
	2	233	8875	0.33	76.18±1.851	0.57±0.006	76.93±47.307	-0.041	0.26	3	2.37	0.005
	3	128	4029	0.50	62.95±1.608	0.67±0.006	82.16±48.826	-0.047	0.19	2	2.67	0.006
	4	82	1990	0.60	48.54±1.531	0.75±0.008	81.97±50.412	-0.090	0.15	2	3.61	0.009
No. 2	0	1014	39609	0.08	78.12±1.539	0.42±0.004	56.38±40.686	-0.028	0.38	4	1.92	0.004
	1	462	18603	0.17	80.53±1.754	0.48±0.005	64.62±41.902	-0.025	0.33	3	2.16	0.004
	2	233	8671	0.32	74.43±1.710	0.57±0.005	71.26±43.164	-0.023	0.27	3	2.54	0.005
	3	128	3791	0.47	59.23±1.545	0.66±0.007	75.33±44.626	-0.036	0.22	2	3.60	0.007
	4	82	1857	0.56	45.29±1.419	0.73±0.009	74.19±45.822	-0.073	0.18	2	3.82	0.010
No. 3	0	1014	40309	0.08	79.50±1.711	0.44±0.004	58.96±43.097	-0.041	0.41	4	1.91	0.004
	1	462	19158	0.18	82.94±1.965	0.49±0.005	68.01±44.740	-0.041	0.32	3	2.02	0.004
	2	233	9033	0.33	77.54±1.903	0.58±0.006	75.47±46.003	-0.054	0.23	3	2.39	0.005
	3	128	4078	0.50	63.72±1.660	0.68±0.007	80.71±48.110	-0.062	0.18	2	2.92	0.006
	4	82	1986	0.60	48.44±1.512	0.75±0.009	80.13±49.525	-0.097	0.13	2	3.70	0.009
No. 4	0	1014	43276	0.08	85.36±1.687	0.41±0.004	57.41±41.454	-0.040	0.41	4	1.81	0.003
	1	462	20470	0.19	88.61±1.886	0.47±0.004	66.27±43.139	-0.033	0.32	4	1.97	0.004
	2	233	9609	0.36	82.48±1.812	0.57±0.005	73.54±44.661	-0.043	0.23	3	2.37	0.004
	3	128	4431	0.55	69.23±1.575	0.68±0.005	79.81±46.430	-0.042	0.14	3	3.08	0.006
	4	82	2142	0.64	52.24±1.520	0.77±0.006	80.09±48.261	-0.065	0.12	2	3.20	0.008
No. 5	0	1014	40165	0.08	79.22±1.546	0.41±0.004	63.63±45.504	-0.032	0.42	4	1.85	0.004
	1	462	19100	0.18	82.68±1.769	0.47±0.005	71.98±46.051	-0.032	0.34	3	2.06	0.004
	2	233	9093	0.34	78.05±1.721	0.56±0.005	79.75±47.253	-0.041	0.26	3	2.52	0.005
	3	128	4114	0.51	64.28±1.550	0.67±0.006	84.40±48.945	-0.059	0.18	3	3.13	0.007
	4	82	2033	0.61	49.59±1.454	0.75±0.008	84.01±51.240	-0.095	0.14	2	4.31	0.009
No. 6	0	1014	39638	0.08	78.18±1.571	0.42±0.004	57.13±41.277	-0.042	0.42	4	1.89	0.004
	1	462	18692	0.18	80.92±1.784	0.48±0.005	65.01±42.186	-0.042	0.34	3	2.10	0.004
	2	233	8821	0.33	75.72±1.749	0.57±0.006	71.37±43.120	-0.048	0.27	3	2.53	0.005
	3	128	3958	0.49	61.84±1.562	0.66±0.007	75.59±44.708	-0.054	0.19	3	2.84	0.007
	4	82	1942	0.58	47.37±1.481	0.74±0.009	75.67±46.882	-0.094	0.14	3	2.81	0.008
No. 7	0	1014	44089	0.09	86.96±1.696	0.43±0.004	56.98±39.373	-0.033	0.42	4	1.94	0.004
	1	462	20383	0.19	88.24±1.900	0.49±0.004	64.92±40.040	-0.020	0.29	3	2.14	0.004
	2	233	9312	0.34	79.93±1.822	0.58±0.005	71.32±40.703	-0.023	0.23	2	2.45	0.005
	3	128	4186	0.52	65.41±1.598	0.68±0.006	76.46±42.401	-0.049	0.18	2	3.00	0.006
	4	82	2044	0.62	49.85±1.474	0.76±0.008	76.05±44.288	-0.094	0.14	2	3.33	0.009
No. 8	0	1014	36557	0.07	72.10±1.633	0.46±0.005	49.29±35.917	-0.044	0.41	4	1.97	0.004
	1	462	17316	0.16	74.96±1.831	0.50±0.005	56.69±37.010	-0.042	0.33	3	2.18	0.005
	2	233	8296	0.31	71.21±1.772	0.57±0.006	62.83±37.979	-0.036	0.26	3	2.49	0.005
	3	128	3746	0.46	58.53±1.570	0.66±0.007	66.68±39.094	-0.037	0.21	2	2.84	0.007
	4	82	1851	0.56	45.15±1.475	0.73±0.009	65.79±40.188	-0.062	0.18	2	3.41	0.010

Subject	Layer	N	L	ρ_l	$\langle k \rangle \pm$ SEM	$\langle c \rangle \pm$ SEM	$f^{(l)} \pm$ SEM	r_c	Q	N_c	β	μ
	0	1014	38249	0.07	75.44±1.613	0.43±0.004	55.86±40.591	-0.045	0.40	4	1.83	0.004
	1	462	18352	0.17	79.45±1.858	0.48±0.005	63.77±41.589	-0.043	0.33	3	2.03	0.004
No. 9	2	233	8702	0.32	74.70±1.850	0.56±0.006	70.08±42.715	-0.045	0.26	3	2.19	0.005
	3	128	3960	0.49	61.88±1.712	0.66±0.007	73.82±44.027	-0.061	0.18	3	2.48	0.006
	4	82	1922	0.58	46.88±1.625	0.75±0.009	72.11±43.995	-0.105	0.13	2	2.84	0.009
	0	1014	39578	0.08	78.06±1.493	0.41±0.004	62.41±43.797	-0.024	0.35	3	1.90	0.004
	1	462	18410	0.17	79.70±1.721	0.48±0.005	71.58±45.113	-0.022	0.33	3	2.19	0.004
No. 10	2	233	8589	0.32	73.73±1.694	0.57±0.006	78.76±46.197	-0.022	0.27	3	2.48	0.005
	3	128	3831	0.47	59.86±1.552	0.66±0.007	83.60±47.906	-0.033	0.21	3	3.23	0.007
	4	82	1865	0.56	45.49±1.430	0.73±0.009	82.79±50.090	-0.080	0.18	2	3.51	0.010
	0	1013	34436	0.07	67.99±1.343	0.41±0.004	56.10±41.192	-0.025	0.38	4	1.90	0.004
	1	462	16289	0.15	70.52±1.542	0.46±0.004	63.75±42.384	-0.015	0.36	4	2.12	0.005
No. 11	2	233	7718	0.29	66.25±1.546	0.54±0.006	70.16±43.299	-0.017	0.28	4	2.36	0.006
	3	128	3527	0.43	55.11±1.433	0.63±0.007	74.03±44.312	-0.036	0.22	3	2.80	0.007
	4	82	1733	0.52	42.27±1.412	0.70±0.009	73.19±45.508	-0.067	0.18	2	3.03	0.010
	0	1014	39631	0.08	78.17±1.541	0.42±0.004	55.80±40.787	-0.029	0.40	4	1.84	0.004
	1	462	18863	0.18	81.66±1.741	0.47±0.004	63.98±42.180	-0.013	0.34	3	2.00	0.004
No. 12	2	233	8793	0.33	75.48±1.749	0.56±0.006	70.85±43.667	-0.023	0.27	3	2.46	0.005
	3	128	3960	0.49	61.88±1.583	0.66±0.007	76.09±45.451	-0.043	0.20	2	2.99	0.007
	4	82	1944	0.59	47.41±1.516	0.74±0.009	75.56±46.732	-0.090	0.15	2	2.99	0.009
	0	1014	40358	0.08	79.60±1.692	0.44±0.004	58.05±40.581	-0.044	0.40	4	1.97	0.004
	1	462	19173	0.18	83.00±1.886	0.49±0.005	66.29±41.941	-0.042	0.32	4	2.13	0.004
No. 13	2	233	9043	0.33	77.62±1.846	0.57±0.006	73.68±43.391	-0.042	0.23	3	2.56	0.005
	3	128	4042	0.50	63.16±1.714	0.68±0.007	77.88±44.575	-0.037	0.17	3	2.64	0.006
	4	82	1999	0.60	48.76±1.592	0.76±0.008	76.36±45.471	-0.076	0.12	2	3.58	0.009
	0	1014	40821	0.08	80.51±1.583	0.44±0.004	54.98±38.809	-0.040	0.43	4	1.98	0.004
	1	462	19050	0.18	82.47±1.788	0.50±0.005	62.97±40.035	-0.043	0.35	4	2.19	0.004
No. 14	2	233	8767	0.32	75.25±1.749	0.57±0.006	69.72±41.571	-0.042	0.25	3	2.59	0.005
	3	128	3934	0.48	61.47±1.583	0.66±0.007	74.57±43.268	-0.060	0.18	3	3.18	0.007
	4	82	1938	0.58	47.27±1.521	0.74±0.009	74.58±45.075	-0.100	0.12	3	3.24	0.009
	0	1014	37896	0.07	74.75±1.563	0.41±0.004	61.60±43.403	-0.039	0.43	4	1.87	0.004
	1	462	18119	0.17	78.44±1.823	0.47±0.005	70.46±44.242	-0.040	0.35	4	2.05	0.004
No. 15	2	233	8732	0.32	74.95±1.802	0.56±0.006	77.63±45.368	-0.042	0.26	3	2.47	0.005
	3	128	4011	0.49	62.67±1.602	0.66±0.006	82.71±46.851	-0.047	0.18	3	2.98	0.007
	4	82	2035	0.61	49.63±1.501	0.75±0.007	83.78±48.511	-0.074	0.13	2	3.60	0.009
	0	1014	39589	0.08	78.08±1.617	0.43±0.004	60.62±43.139	-0.046	0.41	4	1.95	0.004
	1	462	18938	0.18	81.98±1.837	0.49±0.005	69.34±43.964	-0.051	0.34	3	2.11	0.004
No. 16	2	233	9018	0.33	77.41±1.792	0.57±0.006	76.09±44.730	-0.055	0.26	3	2.43	0.005
	3	128	4068	0.50	63.56±1.545	0.66±0.006	80.33±46.104	-0.066	0.19	3	2.80	0.006
	4	82	2008	0.60	48.98±1.383	0.74±0.007	79.31±47.395	-0.086	0.16	2	3.24	0.009
	0	1014	38009	0.07	74.97±1.591	0.44±0.004	53.98±38.401	-0.026	0.43	4	1.95	0.004
	1	462	17734	0.17	76.77±1.784	0.49±0.005	61.72±39.467	-0.020	0.35	4	2.21	0.005
No. 17	2	233	8280	0.31	71.07±1.758	0.57±0.006	67.56±40.191	-0.037	0.28	3	2.62	0.005
	3	128	3815	0.47	59.61±1.525	0.65±0.007	71.55±41.296	-0.052	0.20	3	3.07	0.007
	4	82	1910	0.58	46.59±1.443	0.73±0.009	72.47±43.781	-0.100	0.16	2	3.64	0.009
	0	1014	46070	0.09	90.87±1.707	0.41±0.003	62.24±43.523	-0.033	0.37	3	1.90	0.003
	1	462	21730	0.20	94.07±1.881	0.49±0.004	71.29±44.918	-0.021	0.30	3	2.09	0.004
No. 18	2	233	10019	0.37	86.00±1.759	0.58±0.005	79.50±46.687	-0.030	0.24	3	2.56	0.004
	3	128	4435	0.55	69.30±1.475	0.68±0.005	85.99±48.874	-0.052	0.18	2	3.15	0.006
	4	82	2155	0.65	52.56±1.385	0.76±0.007	86.68±51.335	-0.103	0.14	2	2.59	0.007

Subject	Layer	N	L	ρ_l	$\langle k \rangle \pm$ SEM	$\langle c \rangle \pm$ SEM	$f^{(l)} \pm$ SEM	r_c	Q	N_c	β	μ
No. 19	0	1014	41676	0.08	82.20±1.639	0.42±0.004	57.88±40.396	-0.035	0.39	3	1.87	0.004
	1	462	19773	0.19	85.60±1.871	0.48±0.004	65.85±40.966	-0.031	0.32	3	2.11	0.004
	2	233	9225	0.34	79.18±1.837	0.57±0.005	72.99±42.182	-0.042	0.24	3	2.29	0.005
	3	128	4226	0.52	66.03±1.615	0.68±0.006	78.64±43.673	-0.065	0.17	3	3.00	0.006
	4	82	2066	0.62	50.39±1.556	0.76±0.008	78.10±45.409	-0.112	0.12	2	3.42	0.009
No. 20	0	1013	41727	0.08	82.38±1.620	0.43±0.004	52.87±37.651	-0.039	0.40	4	1.95	0.004
	1	462	19757	0.19	85.53±1.800	0.48±0.005	60.55±38.512	-0.032	0.31	3	2.15	0.004
	2	233	9241	0.34	79.32±1.723	0.57±0.006	67.10±39.748	-0.034	0.26	3	2.55	0.005
	3	128	4076	0.50	63.69±1.549	0.67±0.006	71.76±41.387	-0.048	0.19	2	3.09	0.007
	4	82	1972	0.59	48.10±1.455	0.74±0.008	70.69±43.019	-0.087	0.15	2	3.58	0.009
No. 21	0	1014	36659	0.07	72.31±1.553	0.43±0.004	55.79±40.647	-0.041	0.43	4	1.89	0.004
	1	462	17485	0.16	75.69±1.793	0.48±0.005	63.86±41.672	-0.047	0.33	3	2.07	0.004
	2	233	8392	0.31	72.03±1.760	0.56±0.006	70.54±42.918	-0.058	0.26	3	2.35	0.005
	3	128	3884	0.48	60.69±1.557	0.65±0.006	75.36±44.246	-0.083	0.17	3	2.71	0.007
	4	82	1995	0.60	48.66±1.407	0.73±0.007	76.37±46.385	-0.103	0.13	2	2.72	0.008
No. 22	0	1014	38855	0.08	76.64±1.514	0.40±0.004	65.81±46.676	-0.034	0.41	4	1.78	0.004
	1	462	18783	0.18	81.31±1.746	0.46±0.004	75.07±47.732	-0.031	0.29	3	2.02	0.004
	2	233	9072	0.34	77.87±1.721	0.56±0.005	82.94±48.893	-0.048	0.23	3	2.31	0.005
	3	128	4037	0.50	63.08±1.590	0.67±0.006	87.39±50.584	-0.052	0.18	3	2.90	0.006
	4	82	1966	0.59	47.95±1.553	0.75±0.008	86.89±52.990	-0.091	0.12	3	2.79	0.008
No. 23	0	1014	37235	0.07	73.44±1.444	0.40±0.004	60.43±43.800	-0.039	0.42	4	1.87	0.004
	1	462	17532	0.16	75.90±1.645	0.46±0.004	68.93±44.649	-0.039	0.34	3	2.06	0.004
	2	233	8467	0.31	72.68±1.607	0.54±0.005	76.18±45.622	-0.049	0.27	3	2.39	0.005
	3	128	3906	0.48	61.03±1.388	0.64±0.005	80.67±46.705	-0.056	0.20	3	2.95	0.007
	4	82	1929	0.58	47.05±1.286	0.71±0.007	80.18±48.393	-0.091	0.17	2	3.66	0.009
No. 24	0	1014	38407	0.07	75.75±1.534	0.41±0.004	59.11±42.707	-0.040	0.39	3	1.90	0.004
	1	462	18295	0.17	79.20±1.749	0.47±0.004	67.13±43.616	-0.034	0.33	3	2.08	0.004
	2	233	8666	0.32	74.39±1.687	0.56±0.005	73.38±44.184	-0.042	0.26	3	2.48	0.005
	3	128	3926	0.48	61.34±1.465	0.65±0.006	78.14±46.105	-0.049	0.19	2	3.08	0.007
	4	82	1919	0.58	46.80±1.385	0.73±0.008	76.37±46.714	-0.096	0.16	2	3.57	0.009
No. 25	0	1014	43631	0.08	86.06±1.659	0.42±0.003	57.71±40.073	-0.033	0.42	4	1.90	0.004
	1	462	20366	0.19	88.16±1.833	0.49±0.004	65.79±41.023	-0.021	0.30	3	2.10	0.004
	2	233	9329	0.35	80.08±1.812	0.58±0.006	72.29±41.947	-0.027	0.25	3	2.56	0.005
	3	128	4144	0.51	64.75±1.651	0.69±0.007	77.46±43.752	-0.047	0.18	3	3.33	0.007
	4	82	2033	0.61	49.59±1.543	0.76±0.009	76.84±45.405	-0.100	0.14	2	3.76	0.009
No. 26	0	1014	42351	0.08	83.53±1.634	0.42±0.004	57.06±40.212	-0.021	0.40	4	1.90	0.004
	1	462	20154	0.19	87.25±1.843	0.48±0.004	65.47±41.238	-0.010	0.32	3	2.11	0.004
	2	233	9465	0.35	81.24±1.745	0.57±0.005	72.29±42.137	-0.011	0.23	3	2.50	0.005
	3	128	4203	0.52	65.67±1.511	0.67±0.005	77.28±43.793	-0.023	0.17	3	3.01	0.006
	4	82	2090	0.63	50.98±1.412	0.75±0.007	77.41±45.244	-0.095	0.14	2	2.82	0.008
No. 27	0	1014	37875	0.07	74.70±1.469	0.42±0.004	60.28±44.013	-0.025	0.43	4	1.91	0.004
	1	462	17836	0.17	77.21±1.660	0.47±0.004	69.29±45.337	-0.020	0.31	3	2.14	0.004
	2	233	8418	0.31	72.26±1.619	0.56±0.006	75.70±45.756	-0.035	0.28	3	2.53	0.005
	3	128	3834	0.47	59.91±1.434	0.65±0.007	80.85±47.362	-0.047	0.22	2	2.96	0.007
	4	82	1889	0.57	46.07±1.366	0.73±0.009	79.79±49.279	-0.086	0.18	2	3.25	0.009
No. 28	0	1014	35737	0.07	70.49±1.478	0.42±0.004	56.48±41.154	-0.040	0.43	4	1.86	0.004
	1	462	16984	0.16	73.52±1.708	0.47±0.005	64.04±42.062	-0.039	0.33	3	2.10	0.005
	2	233	8227	0.30	70.62±1.707	0.54±0.006	70.74±43.134	-0.042	0.26	3	2.36	0.005
	3	128	3714	0.46	58.03±1.579	0.65±0.007	74.93±44.203	-0.042	0.18	2	2.97	0.007
	4	82	1844	0.56	44.98±1.547	0.73±0.009	74.89±45.887	-0.077	0.14	3	3.37	0.010

Subject	Layer	N	L	ρ_l	$\langle k \rangle \pm$ SEM	$\langle c \rangle \pm$ SEM	$f^{(l)} \pm$ SEM	r_c	Q	N_c	β	μ
No. 29	0	1014	39125	0.08	77.17±1.492	0.42±0.004	53.54±38.013	-0.033	0.45	4	1.86	0.004
	1	462	18508	0.17	80.12±1.681	0.48±0.004	61.19±39.093	-0.030	0.34	3	2.19	0.004
	2	233	8648	0.32	74.23±1.640	0.57±0.006	67.30±40.065	-0.048	0.26	3	2.66	0.005
	3	128	3898	0.48	60.91±1.427	0.65±0.007	71.73±41.755	-0.054	0.21	2	3.02	0.007
	4	82	1934	0.58	47.17±1.354	0.72±0.008	71.67±43.399	-0.099	0.16	2	3.40	0.009
No. 30	0	1014	41041	0.08	80.95±1.596	0.43±0.004	55.82±40.595	-0.033	0.40	3	1.94	0.004
	1	462	19264	0.18	83.39±1.793	0.48±0.004	64.27±41.937	-0.030	0.34	3	2.11	0.004
	2	233	9012	0.33	77.36±1.736	0.57±0.006	71.01±43.245	-0.037	0.27	3	2.45	0.005
	3	128	4097	0.50	64.02±1.548	0.66±0.006	76.38±44.786	-0.059	0.20	2	3.09	0.007
	4	82	2034	0.61	49.61±1.457	0.75±0.008	76.21±46.418	-0.096	0.15	2	2.78	0.008
No. 31	0	1014	39813	0.08	78.53±1.582	0.42±0.004	61.38±43.914	-0.036	0.40	4	1.84	0.004
	1	462	18826	0.18	81.50±1.805	0.47±0.004	70.46±45.286	-0.022	0.32	3	2.06	0.004
	2	233	8861	0.33	76.06±1.811	0.57±0.006	77.90±46.474	-0.030	0.24	2	2.50	0.005
	3	128	3949	0.49	61.70±1.655	0.67±0.007	82.78±47.844	-0.051	0.19	2	3.16	0.007
	4	82	1914	0.58	46.68±1.539	0.75±0.009	81.71±50.231	-0.081	0.15	2	3.79	0.010
No. 32	0	1013	39161	0.08	77.32±1.574	0.43±0.004	61.96±43.540	-0.033	0.43	4	1.91	0.004
	1	462	18393	0.17	79.62±1.795	0.49±0.005	70.68±44.698	-0.027	0.30	3	2.20	0.004
	2	233	8649	0.32	74.24±1.768	0.57±0.006	78.46±46.346	-0.030	0.27	3	2.72	0.005
	3	128	3827	0.47	59.80±1.607	0.66±0.007	82.92±48.538	-0.058	0.20	2	2.99	0.007
	4	82	1931	0.58	47.10±1.472	0.74±0.008	84.74±52.183	-0.096	0.15	2	3.22	0.009
No. 33	0	1014	40400	0.08	79.68±1.602	0.41±0.004	60.92±43.352	-0.034	0.41	4	1.90	0.004
	1	462	19127	0.18	82.80±1.801	0.47±0.004	69.55±44.780	-0.026	0.29	3	2.04	0.004
	2	233	9119	0.34	78.27±1.754	0.56±0.005	77.32±46.285	-0.028	0.26	3	2.29	0.005
	3	128	4058	0.50	63.41±1.579	0.66±0.006	82.08±47.901	-0.041	0.18	3	2.74	0.006
	4	82	1988	0.60	48.49±1.507	0.75±0.008	82.25±49.821	-0.072	0.15	2	2.73	0.008
No. 34	0	1014	44274	0.09	87.33±1.689	0.42±0.003	57.56±39.889	-0.036	0.40	3	1.87	0.003
	1	462	20590	0.19	89.13±1.871	0.49±0.004	65.60±40.953	-0.025	0.33	3	2.11	0.004
	2	233	9377	0.35	80.49±1.811	0.58±0.005	72.08±41.786	-0.032	0.26	3	2.49	0.005
	3	128	4226	0.52	66.03±1.547	0.68±0.006	77.22±43.408	-0.037	0.18	3	3.22	0.006
	4	82	2073	0.62	50.56±1.417	0.76±0.008	76.60±45.167	-0.084	0.14	2	3.78	0.009
No. 35	0	1014	46025	0.09	90.78±1.718	0.42±0.004	59.63±41.389	-0.039	0.42	4	1.92	0.003
	1	462	21758	0.20	94.19±1.866	0.49±0.005	67.87±42.403	-0.028	0.32	4	2.19	0.004
	2	233	10004	0.37	85.87±1.779	0.58±0.005	75.13±43.948	-0.026	0.23	3	2.32	0.004
	3	128	4407	0.54	68.86±1.552	0.68±0.005	80.19±45.905	-0.030	0.15	4	2.85	0.006
	4	82	2082	0.63	50.78±1.475	0.76±0.007	78.59±47.181	-0.079	0.14	2	3.11	0.008
No. 36	0	1014	37237	0.07	73.45±1.452	0.40±0.004	66.00±47.148	-0.034	0.42	4	1.84	0.004
	1	462	18008	0.17	77.96±1.669	0.46±0.004	74.83±47.827	-0.032	0.33	3	2.06	0.004
	2	233	8643	0.32	74.19±1.670	0.55±0.006	81.89±48.483	-0.037	0.24	3	2.34	0.005
	3	128	3839	0.47	59.98±1.594	0.66±0.007	85.54±49.436	-0.059	0.18	3	3.25	0.007
	4	82	1882	0.57	45.90±1.575	0.74±0.010	84.52±50.913	-0.105	0.14	2	3.89	0.010
No. 37	0	1014	45512	0.09	89.77±1.754	0.43±0.003	62.17±43.255	-0.034	0.37	3	1.90	0.003
	1	462	21300	0.20	92.21±1.907	0.49±0.004	71.61±44.528	-0.021	0.33	3	2.14	0.004
	2	233	9778	0.36	83.93±1.777	0.59±0.005	79.40±46.037	-0.030	0.26	3	2.49	0.005
	3	128	4329	0.53	67.64±1.522	0.68±0.005	84.30±47.821	-0.045	0.19	2	2.97	0.006
	4	82	2081	0.63	50.76±1.403	0.76±0.007	82.28±48.698	-0.083	0.15	2	4.09	0.009
No. 38	0	1014	40209	0.08	79.31±1.606	0.41±0.004	62.03±44.458	-0.034	0.39	3	1.86	0.004
	1	462	19094	0.18	82.66±1.810	0.47±0.004	71.12±45.812	-0.029	0.33	3	2.05	0.004
	2	233	9038	0.33	77.58±1.724	0.55±0.005	79.05±47.440	-0.029	0.22	2	2.39	0.005
	3	128	4024	0.50	62.88±1.606	0.66±0.006	84.41±49.498	-0.039	0.16	3	2.81	0.006
	4	82	1970	0.59	48.05±1.523	0.75±0.008	84.05±51.966	-0.052	0.14	2	2.87	0.008

Subject	Layer	N	L	ρ_l	$\langle k \rangle \pm$ SEM	$\langle c \rangle \pm$ SEM	$f^{(l)} \pm$ SEM	r_c	Q	N_c	β	μ
No. 39	0	1014	34947	0.07	68.93±1.521	0.43±0.004	56.48±40.483	-0.047	0.44	4	1.89	0.004
	1	462	16844	0.16	72.92±1.755	0.48±0.005	64.16±41.220	-0.041	0.36	4	2.09	0.005
	2	233	8121	0.30	69.71±1.767	0.56±0.006	70.91±42.134	-0.051	0.25	3	2.33	0.005
	3	128	3703	0.46	57.86±1.619	0.65±0.008	74.79±43.341	-0.062	0.18	3	2.87	0.007
	4	82	1877	0.57	45.78±1.542	0.73±0.009	73.59±44.114	-0.090	0.13	3	3.23	0.009
No. 40	0	1014	38384	0.07	75.71±1.547	0.41±0.004	55.33±40.100	-0.037	0.41	4	1.85	0.004
	1	462	18201	0.17	78.79±1.786	0.47±0.005	63.53±41.379	-0.032	0.29	3	2.02	0.004
	2	233	8652	0.32	74.27±1.753	0.56±0.005	70.13±42.407	-0.032	0.26	3	2.42	0.005
	3	128	3892	0.48	60.81±1.611	0.66±0.007	73.98±43.283	-0.040	0.19	2	2.95	0.007
	4	82	1916	0.58	46.73±1.541	0.74±0.009	72.01±43.377	-0.079	0.15	2	3.00	0.009
No. 41	0	1014	35161	0.07	69.35±1.455	0.42±0.004	56.84±41.915	-0.037	0.42	4	1.90	0.004
	1	462	16812	0.16	72.78±1.695	0.46±0.005	64.84±43.044	-0.036	0.30	4	1.96	0.004
	2	233	8086	0.30	69.41±1.727	0.55±0.006	71.68±44.498	-0.050	0.26	3	2.32	0.005
	3	128	3751	0.46	58.61±1.603	0.65±0.007	75.60±45.089	-0.058	0.19	3	2.77	0.007
	4	82	1886	0.57	46.00±1.542	0.74±0.009	75.09±46.191	-0.100	0.13	3	2.98	0.009
No. 42	0	1014	40731	0.08	80.34±1.544	0.42±0.004	58.24±42.013	-0.037	0.42	4	1.90	0.004
	1	462	19399	0.18	83.98±1.731	0.47±0.005	66.42±43.086	-0.033	0.34	3	2.13	0.004
	2	233	9190	0.34	78.88±1.677	0.56±0.006	73.32±43.902	-0.035	0.27	3	2.53	0.005
	3	128	4147	0.51	64.80±1.537	0.67±0.006	79.48±46.699	-0.052	0.19	3	3.08	0.006
	4	82	2057	0.62	50.17±1.447	0.76±0.008	80.02±49.576	-0.070	0.15	2	4.14	0.009
No. 43	0	1014	37845	0.07	74.64±1.535	0.43±0.004	56.27±40.721	-0.034	0.44	4	1.95	0.004
	1	462	17927	0.17	77.61±1.744	0.49±0.005	64.87±42.105	-0.034	0.32	3	2.19	0.004
	2	233	8449	0.31	72.52±1.728	0.57±0.006	71.61±43.110	-0.047	0.27	4	2.64	0.005
	3	128	3869	0.48	60.45±1.536	0.66±0.007	77.54±44.988	-0.057	0.16	3	2.81	0.007
	4	82	1898	0.57	46.29±1.416	0.73±0.008	76.80±46.405	-0.088	0.12	2	3.39	0.009

TABLE S3. The dispersion between empirical subjects for degrees, number of triangles of nodes, and sum of the degrees of neighbors in layer 0 for UL dataset. For each brain region, we calculate the mean and standard deviation σ of the three quantites over all subjects. Then we obtain the pearson correlation coefficient ρ and the χ^2 test ($\chi^2 = \sum_i^N (\frac{value_{real} - value_{group}}{\sigma_{group}})^2$) between specific subject and the average in the cohort. The quantity ζ corresponds to the fraction of nodes for which the value measured on the specific network lies outside the 2σ confidence interval around the average.

Subject	degree			number of triangles			sum degree of neighbors		
	ρ	χ^2/N	ζ	ρ	χ^2/N	ζ	ρ	χ^2/N	ζ
0	0.812	1.034	0.056	0.817	1.117	0.067	0.789	0.865	0.037
1	0.826	1.018	0.050	0.847	1.075	0.062	0.787	1.170	0.066
2	0.795	0.959	0.037	0.825	0.916	0.044	0.773	0.835	0.026
3	0.823	0.862	0.028	0.853	0.692	0.015	0.820	0.716	0.007
4	0.852	1.031	0.060	0.891	1.084	0.064	0.841	1.352	0.088
5	0.859	0.850	0.032	0.890	0.719	0.025	0.831	0.823	0.037
6	0.818	0.916	0.032	0.835	0.841	0.034	0.763	0.864	0.024
7	0.853	0.909	0.033	0.874	0.849	0.033	0.815	0.870	0.035
8	0.770	1.121	0.061	0.799	1.080	0.055	0.756	1.033	0.051
9	0.845	0.737	0.024	0.856	0.676	0.019	0.822	0.659	0.011
10	0.813	0.983	0.055	0.817	1.106	0.066	0.789	0.926	0.043
11	0.784	1.154	0.056	0.810	1.181	0.057	0.735	1.175	0.060
12	0.780	1.044	0.049	0.804	1.079	0.057	0.756	0.977	0.045
13	0.812	1.118	0.055	0.840	1.228	0.067	0.783	1.240	0.070
14	0.830	1.057	0.052	0.846	1.194	0.076	0.815	1.080	0.062
15	0.818	1.271	0.077	0.844	1.726	0.121	0.787	1.499	0.106
16	0.849	0.895	0.036	0.878	0.891	0.040	0.818	0.994	0.049
17	0.831	0.907	0.036	0.844	0.850	0.038	0.795	0.844	0.032
18	0.834	0.906	0.026	0.850	0.762	0.026	0.792	0.806	0.021
19	0.805	1.153	0.067	0.837	1.119	0.072	0.779	1.202	0.071
20	0.759	1.181	0.058	0.784	1.043	0.047	0.724	1.002	0.036
21	0.757	1.229	0.051	0.761	1.060	0.043	0.695	1.025	0.026
22	0.834	0.798	0.028	0.849	0.698	0.023	0.814	0.699	0.019
23	0.793	1.116	0.058	0.784	1.362	0.081	0.744	1.125	0.062
24	0.825	0.910	0.041	0.841	0.823	0.038	0.797	0.850	0.030
25	0.838	0.982	0.045	0.847	1.152	0.068	0.801	1.293	0.077
26	0.796	1.163	0.058	0.791	1.137	0.045	0.717	1.118	0.043
27	0.808	0.848	0.026	0.830	0.718	0.016	0.777	0.768	0.014
28	0.822	1.079	0.055	0.831	1.268	0.073	0.775	1.391	0.084
29	0.814	0.912	0.028	0.839	0.837	0.036	0.785	0.790	0.022
30	0.848	0.875	0.035	0.879	0.891	0.051	0.816	0.912	0.043
31	0.815	1.231	0.074	0.842	1.474	0.090	0.778	1.580	0.114
32	0.807	0.958	0.033	0.811	0.874	0.027	0.751	0.942	0.032
33	0.821	1.075	0.055	0.847	1.169	0.062	0.813	1.037	0.049
34	0.815	1.088	0.057	0.831	1.055	0.054	0.789	1.104	0.058
35	0.851	0.809	0.025	0.863	0.706	0.018	0.816	0.785	0.013
36	0.832	0.958	0.043	0.837	0.988	0.058	0.814	0.924	0.044
37	0.834	0.908	0.035	0.852	0.812	0.037	0.808	0.899	0.038
38	0.804	1.021	0.048	0.838	0.983	0.049	0.792	0.968	0.033
39	0.848	0.937	0.029	0.881	0.773	0.022	0.806	0.860	0.026

TABLE S4. The dispersion between empirical subjects for degrees, number of triangles of nodes, and sum of the degrees of neighbors in layer 0 for HCP dataset. For each brain region, we calculate the mean and standard deviation σ of the three quantites over all subjects. Then we obtain the pearson correlation coefficient ρ and the χ^2 test ($\chi^2 = \sum_i^N (\frac{value_{real} - value_{group}}{\sigma_{group}})^2$) between specific subject and the average in the cohort. The quantity ζ corresponds to the fraction of nodes for which the value measured on the specific network lies outside the 2σ confidence interval around the average.

Subject	degree			number of triangles			sum degree of neighbors		
	ρ	χ^2/N	ζ	ρ	χ^2/N	ζ	ρ	χ^2/N	ζ
0	0.875	0.937	0.035	0.913	0.805	0.017	0.873	0.858	0.022
1	0.909	0.859	0.027	0.938	0.779	0.025	0.899	0.796	0.029
2	0.904	0.802	0.023	0.942	0.713	0.019	0.897	0.712	0.016
3	0.894	1.037	0.044	0.929	1.017	0.050	0.888	0.988	0.044
4	0.888	1.180	0.068	0.932	1.240	0.079	0.875	1.353	0.084
5	0.869	1.093	0.059	0.922	1.047	0.053	0.853	0.981	0.051
6	0.897	0.864	0.028	0.936	0.803	0.022	0.881	0.763	0.026
7	0.899	1.131	0.065	0.942	1.421	0.105	0.892	1.388	0.088
8	0.888	1.064	0.034	0.918	0.952	0.030	0.870	0.934	0.026
9	0.866	1.208	0.060	0.905	1.097	0.047	0.840	1.075	0.049
10	0.889	0.880	0.026	0.935	0.771	0.022	0.882	0.737	0.017
11	0.886	0.933	0.027	0.927	0.841	0.010	0.881	1.159	0.034
12	0.888	0.969	0.039	0.932	0.886	0.037	0.883	0.829	0.024
13	0.895	1.005	0.043	0.928	1.033	0.049	0.882	0.967	0.046
14	0.873	1.052	0.058	0.910	1.086	0.062	0.855	0.948	0.045
15	0.888	0.975	0.044	0.932	0.846	0.025	0.870	0.842	0.022
16	0.899	0.882	0.029	0.934	0.820	0.029	0.876	0.799	0.019
17	0.889	0.976	0.039	0.913	0.965	0.037	0.877	0.916	0.030
18	0.860	1.616	0.116	0.906	2.177	0.170	0.858	2.041	0.175
19	0.884	1.060	0.056	0.929	1.083	0.064	0.872	1.069	0.061
20	0.881	1.032	0.052	0.924	1.094	0.054	0.870	0.995	0.050
21	0.884	1.024	0.039	0.922	0.888	0.025	0.865	0.923	0.025
22	0.893	0.851	0.023	0.934	0.747	0.020	0.880	0.724	0.011
23	0.891	0.829	0.018	0.931	0.719	0.009	0.874	0.797	0.019
24	0.897	0.837	0.024	0.932	0.744	0.020	0.884	0.732	0.020
25	0.896	1.082	0.062	0.940	1.242	0.085	0.886	1.224	0.076
26	0.884	1.077	0.052	0.926	1.151	0.069	0.885	1.124	0.061
27	0.894	0.832	0.023	0.928	0.731	0.014	0.884	0.773	0.012
28	0.892	0.913	0.019	0.929	0.804	0.009	0.878	0.914	0.020
29	0.883	0.885	0.034	0.928	0.773	0.019	0.875	0.725	0.017
30	0.891	0.956	0.038	0.928	0.974	0.055	0.872	0.927	0.031
31	0.895	0.852	0.026	0.934	0.772	0.023	0.886	0.734	0.019
32	0.894	0.903	0.028	0.934	0.815	0.029	0.884	0.788	0.021
33	0.894	0.943	0.036	0.936	0.860	0.037	0.880	0.858	0.027
34	0.901	1.144	0.061	0.944	1.353	0.088	0.893	1.382	0.084
35	0.884	1.494	0.095	0.925	2.074	0.167	0.870	2.204	0.185
36	0.872	0.942	0.029	0.915	0.851	0.016	0.852	0.889	0.022
37	0.885	1.383	0.095	0.926	2.008	0.141	0.878	1.977	0.159
38	0.893	0.951	0.042	0.932	0.948	0.048	0.880	0.887	0.032
39	0.915	0.885	0.020	0.946	0.782	0.013	0.899	0.874	0.013
40	0.890	0.866	0.029	0.932	0.744	0.019	0.877	0.749	0.016
41	0.894	0.938	0.025	0.929	0.839	0.010	0.879	0.981	0.015
42	0.880	0.963	0.042	0.918	0.940	0.042	0.860	0.875	0.036
43	0.888	0.897	0.028	0.924	0.764	0.019	0.882	0.789	0.017

TABLE S5. The goodness of fit between the predictions of our model and real values for degrees, number of triangles of nodes, and sum of the degrees of neighbors in layer 0 for UL dataset. The Pearson correlation coefficient ρ, the χ^2 test ($\chi^2 = \sum_i^N (\frac{x_{original} - x_{inferred}}{\sigma})^2$), the quantity ζ corresponds to the fraction of nodes for which the value measured on the original network lies outside the 2σ confidence interval.

Subject	degree			number of triangles			sum degree of neighbors		
	ρ	χ^2/N	ζ	ρ	χ^2/N	ζ	ρ	χ^2/N	ζ
0	1.000	0.011	0.000	0.977	0.944	0.049	0.963	1.419	0.082
1	1.000	0.010	0.000	0.979	0.932	0.053	0.963	1.728	0.127
2	1.000	0.010	0.000	0.981	0.824	0.034	0.964	1.465	0.096
3	1.000	0.010	0.000	0.985	0.769	0.033	0.955	1.721	0.116
4	1.000	0.010	0.000	0.980	0.888	0.034	0.968	1.736	0.123
5	1.000	0.011	0.000	0.983	0.832	0.038	0.959	1.545	0.088
6	1.000	0.011	0.000	0.983	0.751	0.029	0.956	1.647	0.110
7	1.000	0.010	0.000	0.983	0.843	0.041	0.956	1.662	0.116
8	1.000	0.010	0.000	0.980	0.877	0.040	0.964	1.547	0.089
9	1.000	0.011	0.000	0.976	0.713	0.022	0.960	1.545	0.076
10	1.000	0.010	0.000	0.973	1.092	0.064	0.966	1.328	0.073
11	1.000	0.010	0.000	0.979	1.094	0.067	0.965	1.352	0.087
12	1.000	0.010	0.000	0.974	1.016	0.052	0.968	1.496	0.104
13	1.000	0.010	0.000	0.989	0.833	0.045	0.969	1.562	0.105
14	1.000	0.010	0.000	0.982	0.787	0.035	0.967	1.461	0.089
15	1.000	0.009	0.000	0.983	0.823	0.034	0.968	1.416	0.080
16	1.000	0.009	0.000	0.985	0.894	0.041	0.966	1.482	0.104
17	1.000	0.010	0.000	0.983	0.749	0.032	0.970	1.265	0.074
18	1.000	0.010	0.000	0.986	0.653	0.024	0.960	1.387	0.086
19	1.000	0.010	0.000	0.983	0.811	0.036	0.962	1.723	0.114
20	1.000	0.011	0.000	0.987	0.584	0.013	0.965	1.299	0.072
21	1.000	0.010	0.000	0.985	0.665	0.017	0.950	1.865	0.120
22	1.000	0.010	0.000	0.978	0.898	0.040	0.958	1.508	0.091
23	1.000	0.010	0.000	0.987	0.731	0.025	0.967	1.526	0.091
24	1.000	0.011	0.000	0.981	0.698	0.030	0.964	1.351	0.081
25	1.000	0.010	0.000	0.989	0.656	0.028	0.969	1.649	0.103
26	1.000	0.010	0.000	0.986	0.712	0.022	0.963	1.360	0.089
27	1.000	0.010	0.000	0.983	0.669	0.022	0.958	1.439	0.091
28	1.000	0.010	0.000	0.982	1.038	0.059	0.968	1.603	0.113
29	1.000	0.011	0.000	0.979	0.762	0.033	0.960	1.621	0.102
30	1.000	0.011	0.000	0.982	0.732	0.028	0.963	1.540	0.103
31	1.000	0.010	0.000	0.986	0.948	0.057	0.970	1.625	0.103
32	1.000	0.011	0.000	0.984	0.980	0.053	0.963	1.582	0.104
33	1.000	0.011	0.000	0.984	0.912	0.047	0.961	1.629	0.109
34	1.000	0.010	0.000	0.982	0.892	0.044	0.964	1.581	0.102
35	1.000	0.010	0.000	0.987	0.710	0.032	0.956	1.704	0.135
36	1.000	0.010	0.000	0.977	0.939	0.051	0.961	1.623	0.106
37	1.000	0.010	0.000	0.980	0.946	0.048	0.962	1.430	0.084
38	1.000	0.010	0.000	0.986	0.738	0.033	0.966	1.791	0.110
39	1.000	0.010	0.000	0.985	0.862	0.044	0.941	1.916	0.145

TABLE S6. The goodness of fit between the predictions of our model and real values for degrees, number of triangles of nodes, and sum of the degrees of neighbors in layer 0 for HCP dataset. The Pearson correlation coefficient ρ, the χ^2 test ($\chi^2 = \sum_i^N (\frac{x_{original} - x_{inferred}}{\sigma})^2$), the quantity ζ corresponds to the fraction of nodes for which the value measured on the original network lies outside the 2σ confidence interval.

Subject	degree			number of triangles			sum degree of neighbors		
	ρ	χ^2/N	ζ	ρ	χ^2/N	ζ	ρ	χ^2/N	ζ
0	1.000	0.010	0.000	0.987	1.396	0.079	0.983	1.476	0.100
1	1.000	0.010	0.000	0.991	1.205	0.055	0.988	1.200	0.069
2	1.000	0.011	0.000	0.989	1.252	0.066	0.986	1.232	0.067
3	1.000	0.011	0.000	0.991	1.232	0.071	0.988	1.145	0.061
4	1.000	0.011	0.000	0.988	1.498	0.104	0.989	1.047	0.047
5	1.000	0.010	0.000	0.990	1.212	0.064	0.986	1.158	0.066
6	1.000	0.010	0.000	0.991	1.105	0.049	0.987	1.073	0.055
7	1.000	0.010	0.000	0.991	1.240	0.073	0.989	1.077	0.053
8	1.000	0.011	0.000	0.991	1.280	0.078	0.989	1.152	0.052
9	1.000	0.010	0.000	0.989	1.217	0.071	0.987	1.136	0.058
10	1.000	0.011	0.000	0.987	1.583	0.093	0.985	1.260	0.066
11	1.000	0.010	0.000	0.986	1.117	0.052	0.981	1.341	0.084
12	1.000	0.010	0.000	0.988	1.368	0.085	0.984	1.330	0.076
13	1.000	0.011	0.000	0.992	0.955	0.035	0.991	0.931	0.037
14	1.000	0.010	0.000	0.990	1.417	0.084	0.990	0.934	0.038
15	1.000	0.010	0.000	0.990	1.103	0.060	0.983	1.480	0.099
16	1.000	0.010	0.000	0.993	0.985	0.045	0.987	1.129	0.061
17	1.000	0.010	0.000	0.981	1.949	0.094	0.987	1.265	0.074
18	1.000	0.010	0.000	0.988	1.479	0.107	0.988	1.097	0.053
19	1.000	0.010	0.000	0.990	1.229	0.069	0.987	1.107	0.060
20	1.000	0.010	0.000	0.992	1.037	0.047	0.989	0.991	0.040
21	1.000	0.010	0.000	0.992	1.156	0.061	0.988	1.026	0.050
22	1.000	0.011	0.000	0.992	1.020	0.036	0.987	1.051	0.058
23	1.000	0.010	0.000	0.989	1.238	0.074	0.981	1.425	0.084
24	1.000	0.011	0.000	0.989	1.189	0.072	0.981	1.470	0.100
25	1.000	0.011	0.000	0.992	1.114	0.066	0.989	0.971	0.047
26	1.000	0.011	0.000	0.991	1.061	0.054	0.990	1.016	0.046
27	1.000	0.010	0.000	0.987	1.294	0.076	0.984	1.327	0.087
28	1.000	0.010	0.000	0.992	1.088	0.060	0.986	1.058	0.049
29	1.000	0.010	0.000	0.991	1.231	0.077	0.990	0.834	0.030
30	1.000	0.010	0.000	0.990	1.063	0.058	0.988	1.045	0.055
31	1.000	0.011	0.000	0.992	1.224	0.068	0.987	1.067	0.053
32	1.000	0.011	0.000	0.988	1.788	0.142	0.984	1.437	0.095
33	1.000	0.010	0.000	0.991	1.176	0.057	0.983	1.536	0.110
34	1.000	0.010	0.000	0.991	1.178	0.065	0.989	0.986	0.035
35	1.000	0.010	0.000	0.986	1.548	0.100	0.988	1.122	0.053
36	1.000	0.010	0.000	0.990	0.998	0.047	0.988	0.970	0.042
37	1.000	0.010	0.000	0.988	1.647	0.119	0.988	1.182	0.062
38	1.000	0.011	0.000	0.994	0.930	0.036	0.986	1.204	0.060
39	1.000	0.010	0.000	0.991	1.144	0.060	0.986	1.064	0.051
40	1.000	0.011	0.000	0.987	1.494	0.077	0.984	1.282	0.076
41	1.000	0.010	0.000	0.990	1.183	0.066	0.985	1.172	0.065
42	1.000	0.010	0.000	0.991	1.008	0.046	0.988	0.998	0.041
43	1.000	0.010	0.000	0.990	1.385	0.088	0.985	1.409	0.097

[1] G. García-Pérez, M. Boguñá, and M. Á. Serrano, "Multiscale unfolding of real networks by geometric renormalization," Nature Physics **14**, 583 (2018).

[2] G. García-Pérez, A. Allard, M. Á Serrano, and M. Boguñá, "Mercator: uncovering faithful hyperbolic embeddings of complex networks," New Journal of Physics **21**, 123033 (2019).

[3] Richard F Betzel, Andrea Avena-Koenigsberger, Joaquín Goñi, Ye He, Marcel A De Reus, Alessandra Griffa, Petra E Vértes, Bratislav Mišic, Jean-Philippe Thiran, Patric Hagmann, *et al.*, "Generative models of the human connectome," Neuroimage **124**, 1054–1064 (2016).